uOttawa

L'Université canadienne
Canada's university

FACULTÉ DES ÉTUDES SUPÉRIEURES ET POSTOCTORALES

uOttawa

L'Université canadienne
Canada's university

FACULTY OF GRADUATE AND POSDOCTORAL STUDIES

Laura Isabel Renart

AUTEUR DE LA THÈSE / AUTHOR OF THESIS

M.Sc. (Cellular and Molecular Medicine)

GRADE / DEGREE

Department of Cellular and Molecular Medicine

FACULTÉ, ÉCOLE, DÉPARTEMENT / FACULTY, SCHOOL, DEPARTMENT

Cell cycle regulation of the nuclear receptor coactivator SRC-3/AIB1 and impact of overexpression

TITRE DE LA THÈSE / TITLE OF THESIS

C. Pratt

DIRECTEUR (DIRECTRICE) DE LA THÈSE / THESIS SUPERVISOR

CO-DIRECTEUR (CO-DIRECTRICE) DE LA THÈSE / THESIS CO-SUPERVISOR

EXAMINATEURS (EXAMINATRICES) DE LA THÈSE / THESIS EXAMINERS

D. Gray

J. Lee

D. Lohnes

Gary W. Slater

LE DOYEN DE LA FACULTÉ DES ÉTUDES SUPÉRIEURES ET POSTDOCTORALES /
DEAN OF THE FACULTY OF GRADUATE AND POSTDOCORAL STUDIES

Cell cycle regulation of the nuclear receptor coactivator SRC-3/AIB1 and impact of overexpression

Laura Isabel Renart

This thesis is submitted as a partial fulfillment of the M.Sc. program in Cellular and Molecular Medicine.

May 13, 2005

University of Ottawa

Ottawa, ON, Canada

Your file Votre référence
ISBN: 0-494-11391-X
Our file Notre référence
ISBN: 0-494-11391-X

ABSTRACT

SRC-3 is a nuclear receptor coactivator which is amplified and overexpressed in many breast cancers. Although the importance of this protein in a plethora of cellular functions has been established, little is understood about how it is regulated. In this study, we have investigated the regulation of SRC-3 throughout the cell cycle and the effects of aberrant SRC-3 expression. We have found that SRC-3 is regulated throughout the cell cycle via changes in compartmentalization, post-translational modification and degradation, in a Cdk1-, MAPK- and proteasome-dependent manner. Deregulation of SRC-3 expression has substantial effects on cellular growth rate, cell cycle progression, cell morphology and DNA content. Collectively, these findings suggest that disruption of SRC-3 activity gives rise to cells with aberrant cell cycles, resulting in genetic instability and potential aneuploidy. Although in most cells this disruption results in cell cycle arrest and possible apoptosis, it might also set the stage for SRC-3-mediated oncogenesis.

TABLE OF CONTENTS

LIST OF FIGURES

CHAPTER I - INTRODUCTION

CHAPTER III - RESULTS

LIST OF ABBREVIATIONS

>2N<4N	greater than 2N but less than 4N
4EBP1	initiation factor 4E binding protein
AD1/AD2	activation domain 1/2
AF-1/AF-2	activation function 1/2
AIB1	amplified in breast cancer 1
APC	anaphase-promoting factor
bHLH-PAS	basic-helix-loop-helix-Per/ARNT/Sim
BL-I	butyrolactone-I
CARM1	coactivator-associated arginine methyltransferase-1
Cdk	cyclin-dependent kinase
CRS	cytoplasmic retention sequence
DMEM	Dulbecco's minimal essential medium
DTT	dithiothreitol
DUB	deubiquitinating enzyme
E1	ubiquitin-activating enzyme
E_2	17-ß-estradiol
E2	ubiquitin-conjugating enzyme / carrier enzyme
E3	ubiquitin protein ligase enzyme
EGF	epidermal growth factor
ER	estrogen receptor
ERE	estrogen response element
FBS	fetal bovine serum

G1	gap 1
G2	gap 2
GAPDH	glyceraldehyde phosphate dehydrogenase
GSK3	glycogen synthase kinase 3
GST	glutathione-S-transferase
HA	hemagglutinin
HAT	histone acetyl transferase
HRE	hormone response element
IGF-1	insulin-like growth factor-1
IGF-1R	insulin-like growth factor-1 receptor
IKK	IκB kinase
IP	immunoprecipitation
KCl	potassium chloride
M	mitosis
mAb	monoclonal antibody
MAPK	mitogen activated protein kinase
MEF	mouse embryonic fibroblasts
MPF	maturation-promoting factor
mTOR	mammalian target of rapamycin
NaCl	sodium chloride
NaOAC	sodium acetate
NE	nuclear envelope
OA	okadaic acid

PBS	phosphate buffered saline
p/CIP	p300/CBP interacting protein
PI3K	phosphatidylinositol 3 kinase
pRb	retinoblastoma protein
PP2A	protein phosphatase 2A
RAC-3	receptor associated coactivator 3
RIPA	radioimmunoprecipitation assay buffer
RNAi	interfering RNA
RPM	rotations per minute
S	DNA synthesis phase
S6K1	40S ribosomal S6 kinase 1
SA-ß-gal	senescence-associated-ß-gal
SDS	sodium dodecyl sulfate
SDS-PAGE	sodium dodecyl sulfate- polyacrylamide gel electrophoresis
SERM	selective estrogen receptor modulator
siRNA	small interfering RNA
SPF	S phase-promoting factor
SRC	steroid receptor coactivator
TBS-T	tris-buffered saline- tween
TNFα	tumour necrosis factor α
UBC	ubiquitin conjugating enzyme
UPS	ubiquitin-proteasome pathway

ACKNOWLEDGEMENTS

First and foremost, I would like to thank Dr. Christine Pratt for challenging me to think, encouraging me to persevere and supporting me when I truly needed it. I would like to thank Minying Niu, whose constant help and input were integral to the success of this project. I would also like to thank Drs. Doug Gray and Bruce McKay for their insight and suggestions. Finally, I would like to thank Casey McGowan, whose patience, understanding and unconditional support carried me along the way.

I dedicate this thesis to my mami, who not only taught me the true meaning of strength, but showed me that death is not synonymous with being conquered.

INTRODUCTION

BREAST CANCER AND THE ESTROGEN RECEPTOR

Breast cancer is the most common malignancy among women in Canada. It is estimated that 1 in every 9.5 Canadian women will contract this disease during her lifetime; it will be fatal in approximately one third of these cases (reviewed in Vahabi, 2003). Several risk factors have been associated with this disease, including mutations in the breast cancer genes BRCA1/2, reproductive history and environmental elements. Approximately 60–65% of primary breast cancers are initially estrogen receptor (ER) positive and are generally responsive to anti-estrogen treatment by selective ER modulators (SERMs) (Putti *et al*, 2004). These tumours also tend to be more differentiated and are associated with a relatively better prognosis. In contrast, ER negative tumours represent a more malignant group of tumours that tend to be poorly differentiated and associated with a worse prognosis. It has been postulated that over time, ER positive cancers lose ER expression in their progression towards a more malignant phenotype.

Breast cancer cell lines are commonly used model systems for the investigation of the molecular pathogenesis and disease progression of breast cancers. MCF-7 is the prototypic cell line used for the study of ER positive breast adenocarcinoma. It was originally established from a malignant pleural effusion of a 69-year old female patient (Soule *et al*, 1973). ZR-75-1 is a similar ER positive breast carcinoma cell line also established from a malignant pleural effusion (Engel *et al*, 1978). Both of these cell lines

express high levels of SRC-3 protein (see below). Conversely, several cell lines lacking the ER and having a more aggressive tumour phenotype have also been established. These include the breast adenocarcinoma cell lines MDA-MB-231 (Cailleau *et al*, 1974) and SK-Br-3. These cell lines express low SRC-3 protein levels.

The ER is a member of the nuclear/steroid hormone receptor superfamily, a group of ligand-dependent transcription factors involved in growth, differentiation and development (reviewed in MacGregor and Jordan, 1998; Kong *et al*, 2003). The ER is responsible for mediating the biological and physiological effects of its ligand 17-ß-estradiol (E_2), including normal development and differentiation of mammary tissues. Consequently, deregulation of ER activity has been implicated as a major player in breast cancer onset and progression.

There are two known homologues of the ER: ERα and ERβ. The ERα (henceforth referred to as the ER), is much more widely studied than the ERβ, and its relevance in breast cancer is well established. The structural and functional domains of the ER include an amino-terminal activation function domain (AF-1) which is ligand-independent and constitutively active; a DNA-binding domain and hinge region which mediate response element binding and receptor dimerization; and a carboxy-terminal ligand-binding domain containing the second activation function (AF-2), which mediates ligand-specific activation (figure 1.1). Upon ligand-binding, the ER undergoes a conformational change that promotes dimerization and binding to the estrogen response element (ERE), a 13-base pair palindromic sequence in or upstream of the promoter region of ER target genes. The ER then mediates transcriptional activation by recruiting transcription factors and coregulatory molecules that affect target gene expression.

Figure 1.1. Schematic illustration of the structural and functional domains of the ER.

Structural and functional domains are depicted by highlighted boxes and solid bars. The ER contains an amino-terminal, ligand-independent and constitutively active activation function domain (AF-1); a DNA-binding domain and hinge region; and a carboxy-terminal ligand-binding domain containing the second activation function (AF-2).

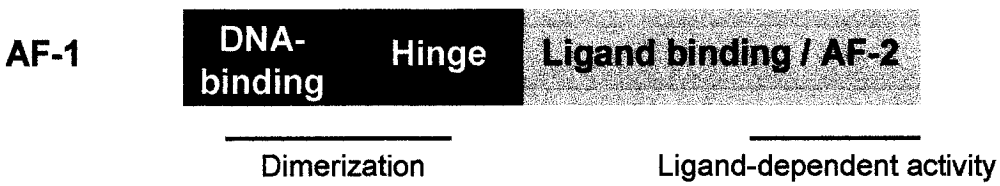
AF-1
DNA-binding
Hinge
Ligand binding / AF-2
Dimerization
Ligand-dependent activity

THE NUCLEAR RECEPTOR COACTIVATOR SRC-3

Nuclear/steroid receptor coactivators are proteins that are recruited by nuclear receptors to promote their transcriptional activation in response to endocrine signals (McKenna and O'Malley, 2002). Coactivators enhance transcription using several modes of action including stabilization of the transcription factor complex, recruitment of general transcription factors or chromatin modifiers, or mediation of chromatin remodelling using intrinsic enzymatic activity. The most well characterized group of coactivators is the p160 family of nuclear/steroid receptor coactivators (SRC), which includes SRC-1 (NCoA-1), SRC-2 (GRIP1, TIF2, or NCoA-2) and SRC-3 (p/CIP, RAC3, ACTR, AIB1, or TRAM-1). This gene family encodes proteins of approximately 160 kDa in size that are relatively well conserved: SRC-3 has 45% amino acid identity with TIF2 and 33% with SRC-1 (Anzick *et al*, 1997).

The newest member of this family, SRC-3, was originally identified by several groups as a protein that interacts with, and activates, nuclear receptors in a ligand-dependent manner (Anzick *et al*, 1997; Chen *et al*, 1997; Li *et al*, 1997; Suen *et al*, 1998; Torchia *et al*, 1997; Tan *et al*, 2000). SRC-3 enhances transcription in several ways, including recruitment of the histone acetyl transferases (HATs) CBP/p300, p/CAF and GCN5 to hormone response elements (HREs) in the presence of ligand (Chen *et al*, 1997; Brown *et al*, 2003). It also contains intrinsic HAT enzymatic activity that may aid in the modification of histones H3 and H4, as well as other unidentified proteins (Chen *et al*, 1997). Additionally, SRC-3 facilitates recruitment of RNA polymerase II to the androgen

receptor enhancer in response to ligand, suggesting that SRC-3 itself can mediate the recruitment of general transcription factors (Louie *et al*, 2003).

Structural and functional characterization

Characterization of the structural and functional domains of SRC-3 has identified several regions that help mediate its biological activity (figure 1.2). At the amino terminus, SRC-3 has a basic-helix-loop-helix-Per/ARNT/Sim (bHLH-PAS) domain, which was originally identified in *Drosophila* as a DNA-binding and heterodimerization domain (Huang *et al*, 1993). However, its function in SRC-3 has yet to be described. Downstream is a Ser/Thr rich region followed by multiple LXXLL motifs (where L is leucine and X is any amino acid). Using mutational studies, several groups have shown that these motifs are required for interaction with, and transactivation of, ligand-bound nuclear receptors in an AF-2 dependent manner (Chen *et al*, 1997; Li *et al*, 1997; Torchia *et al*, 1997; Li and Chen, 1998). This region also contains a potential PEST site (Yan *et al* 2003), a polypeptide sequence associated with promotion of protein turnover (Rechsteiner, 1990). Toward the carboxy-terminus, SRC-3 has a glutamine rich domain that contains three more LXXLL motifs, followed by a glutamine tract. This region contains the first SRC-3 activation domain (AD1), which activates transcription via recruitment of CBP/p300, p/CAF and GCN5 (Chen *et al*, 1997; Brown *et al*, 2003). Finally, at the extreme carboxy-terminus, SRC-3 harbours a second activation domain (AD2). AD2 interacts with coactivator-associated arginine methyltransferase-1 (CARM1) and protein-arginine methyltransferase-1, leading to an increase in the activating potential of SRC-3 (Chen *et al*, 1999). *In vitro* studies have also shown that SRC-3 has intrinsic

Figure 1.2. Schematic illustration of the structural and functional domains of SRC-3.

Structural domains are indicated in the highlighted boxes and interaction sites are indicated by bars. The six bonafide phosphorylation sites are designated by the amino acid residue and location in the SRC-3 sequence. The nuclear receptor interaction domain (NRID) is located amongst the LXXLL motifs. See text for details.

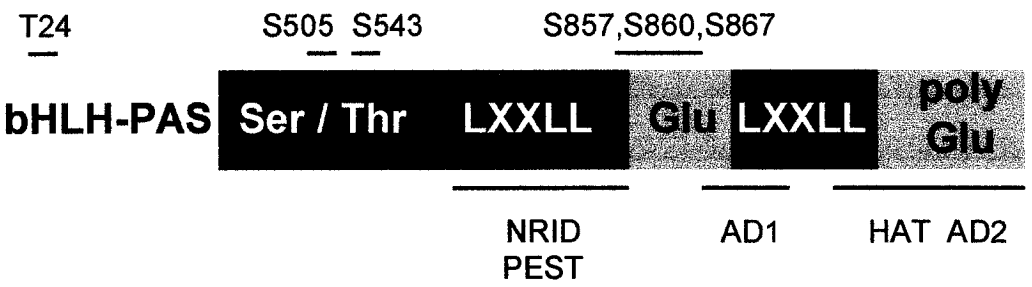
T24
S505
S543
S857,S860,S867
bHLH-PAS
Ser / Thr
LXXLL
Glu
LXXLL
poly Glu
NRID
PEST
AD1
HAT
AD2

HAT activity in this domain, with substrate preference for histones H3 and H4 (Chen *et al*, 1997). These results suggest that SRC-3 may play a role in chromatin remodelling in response to recruitment by nuclear receptors. However, Brown *et al* (2003) found that p/CIP, the mouse homologue of SRC-3, only has HAT activity in the presence of CBP or GCN5. Thus, it appears that either species differences in SRC-3 function exist, or SRC-3 mediates acetylation of histones in an indirect manner via recruitment of other HAT proteins.

Other protein interactions and role in growth and proliferation

Several studies have found that SRC-3 acts as a coactivator for proteins other than nuclear receptors. Werbajh *et al* (2000) demonstrated that SRC-3 interacts with the Rel-A heterocomplex and enhances NFκB transcriptional activity in response to tumour necrosis factor α (TNFα). Goel and Janknecht (2004) showed that the amino-terminus of SRC-3 directly interacts with ER81, a member of the PEA3 group of transcription factors, which are downstream targets of the receptor tyrosine kinase HER2/neu. Additionally, they found that p300, SRC-3 and HER2/neu synergistically activate ER81. These associations suggest that SRC-3 plays a role in cell proliferation.

One of the principle signalling molecules involved in regulating cell growth and proliferation is the Ser/Thr kinase mammalian target of rapamycin (mTOR) (reviewed in Fingar and Blenis, 2004). mTOR integrates signals from nutrients and growth factors and uses this information to control cell growth, at least in part by regulating protein biosynthesis. mTOR has two main downstream targets, 40S ribosomal protein S6 kinase 1 (S6K1) and initiation factor 4E binding protein 1 (4EBP1) (figure 1.3). 4EBP1

Figure 1.3. The IGF-1/PI3K/Akt/mTOR pathway.

Signalling begins when IGF-1 interacts with its cognate receptor tyrosine kinase IGF-1R, triggering a cascade that ultimately results in increased protein translation and cell growth (see text for details). Red and green lines represent inhibitory and stimulatory signals, respectively.

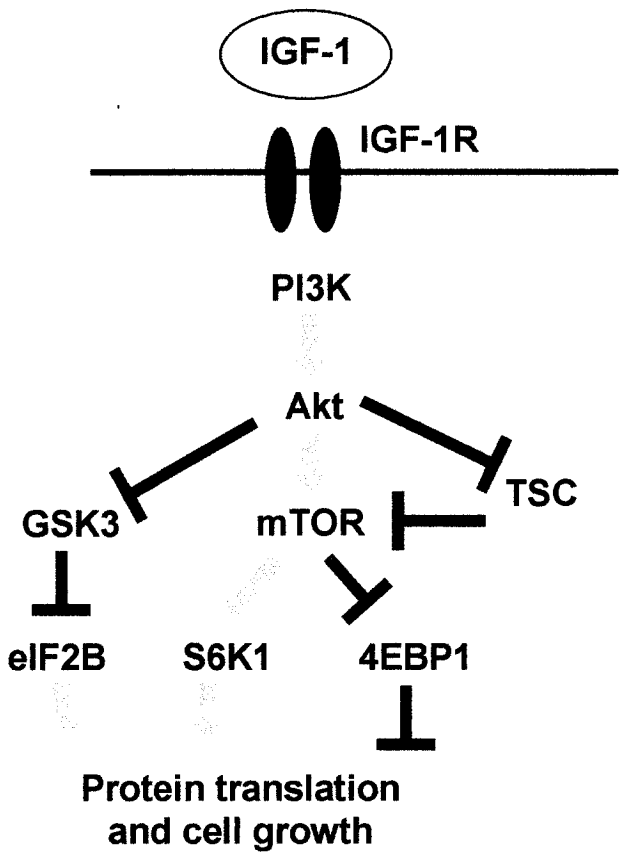
IGF-1
IGF-1R
PI3K
Akt
GSK3
mTOR
TSC
eIF2B
S6K1
4EBP1
Protein translation
and cell growth

phosphorylation triggers release of its binding partner, the initiation factor 4E, leading to increased protein translation and cell growth. Activation of S6K1 by mTOR also increases protein translation and cell growth. One of the key upstream growth factors regulating mTOR activity is insulin-like growth factor 1 (IGF-1), a highly mitogenic molecule that stimulates the activity of the PI3K/Akt/mTOR pathway. Signalling via this pathway begins when IGF-1 interacts with its cognate receptor tyrosine kinase IGF-1R. Interaction stimulates receptor dimerization and activation, triggering a cascade via phosphatidylinositol 3 kinase (PI3K), Akt (protein kinase B) and finally mTOR. Additionally, Akt can increase translation and cell growth by inhibiting the activity of glycogen synthase kinase 3 (GSK3).

To seek further insight into the physiological role of SRC-3, Xu *et al* (2000) generated SRC-3 knock-out mice using homologous recombination in embryonic stem cells. The mice had a diverse phenotype of dwarfism, delayed puberty, abnormal reproductive function and mammary gland growth retardation. Interestingly, they had normal growth hormone levels but lower circulating IGF-1 levels than their wild type counterparts. Thus, the Xu group postulated that growth retardation in SRC-3 knock-out mice was most likely due to decreases in IGF-1 levels. Wang *et al* (2000) studied this further in a SRC-3 knockout mouse line lacking a different region of the SRC-3 gene. They also observed the small-sized phenotype and a 30-50% decrease in serum and liver IGF-1 levels, as well as a defective response to IGF-1 hormone signalling. However, the authors postulated that decreased IGF-1 levels did not account for the growth defect since mice with liver-specific inactivation of the IGF-1 gene, which reduces systemic IGF-1

concentrations by 75%, still displayed normal postnatal body growth (Sjogren *et al*, 1999). Additionally, using mouse embryonic fibroblasts (MEF) and primary hepatocyte cultures prepared from the knockout mice, they showed that cells lacking the SRC-3 gene failed to proliferate following IGF-1 treatment, even though they had no discernable difference in the expression levels of IGF-1R or other targets such as the insulin receptor. Thus, the observed phenotypes were at least partially caused by signalling pathways downstream of IGF-1.

Anzick *et al* (2003) sought to elucidate the effect of SRC-3 overexpression by stably transfecting MDA-MB-436 breast cancer cells with this gene. The cells displayed a giant size cell phenotype with abundant cytoplasm. Similarly, Zhou *et al* (2003) found that transient overexpression of SRC-3 resulted in an increased cell size phenotype in several prostate cancer cell lines, in part by mediating the activity of Akt, mTOR and S6K1. Importantly, the growth effect was steroid independent and cell-autonomous. They also found that down-regulation of SRC-3 using RNAi decreased cell size. Since IGF-1 signalling is decreased in SRC-3 knock-out mice, they examined the possibility that SRC-3 knockout mice also had decreased Akt expression or activity. Indeed, they found that knockout mice had lower levels of both phosphorylated and total Akt protein, suggesting that SRC-3 helps mediate growth through the PI3K/Akt/mTOR pathway.

More recently, Louie *et al* (2004) showed that SRC-3 mediates hormone-independent proliferation by functioning as an E2F coactivator in T-47D breast cancer cells. They showed that SRC-3 overexpression results in the upregulation of the cell cycle regulators E2F1, E2F3, cyclin E, cyclin A, cyclin B1 and Cdk2 (see "The mammalian cell cycle" below). This upregulation was due to the ability of SRC-3 to coactivate the

E2F1 transcription factor. They also found that SRC-3 overexpression increases the proportion of proliferating cells and abolishes cell cycle arrest caused by treatment with the SERM tamoxifen and with pure anti-estrogens. Thus, SRC-3 plays an important role in cell growth and proliferation independent of its steroid receptor coactivator function.

Links to tumourigenesis

Several studies have suggested that there is a link between SRC-3 and cancer. SRC-3 was originally identified as a gene that is amplified and overexpressed in many breast and ovarian cancer (AIB1) cell lines, as well as breast cancer tumours (Anzick *et al*, 1997). Subsequently, it was found that the SRC-3 gene was amplified and/or overexpressed in several other cancers including pancreatic, ovarian, gastric, prostate, hepatocellular carcinoma and oral squamous cell carcinoma (Ghadimi *et al*, 1999; Tanner *et al*, 2000; Sakakura *et al*, 2000; Gnanapragasam, 2001; Wang *et al*, 2002; Chen *et al*, 2004). Moreover, overexpression and amplification of this gene were often associated with more extensive metastases and a poorer prognosis (Sakakura *et al*, 2000; Gnanapragasam *et al*, 2001; Wang *et al*, 2002; Zhao *et al*, 2003; Chen *et al*, 2004; Henke *et al*, 2004). These results suggest that aberrant SRC-3 activity plays a role in tumourigenesis in a variety of tissues.

Because of the role SRC-3 plays in coactivating the ER, many groups have focused on the association of SRC-3 with breast tumourigenesis. Multiple lines of evidence implicate SRC-3 overexpression and overactivity with breast cancer onset and progression. Firstly, several groups have found that SRC-3 mRNA and protein are increased in breast cancer tissue compared to normal breast tissue (Bautista *et al*, 1998;

Murphy *et al*, 2000; List *et al*, 2001b). Secondly, SRC-3 is a rate-limiting factor for the estrogen-dependent growth of human MCF-7 breast cancer cells (List *et al*, 2001a). SRC-3 reduction using ribozyme targeting decreases the ability of cells to form colonies in agar in response to estradiol and limits growth of tumours following sub-cutaneous injection of MCF-7 cells. Thirdly, SRC-3 enhances the functional interaction between the ER and the cyclin D1 promoter, and enhances estrogen-dependent induction of cyclin D1 expression, suggesting a role in promotion of cell cycle progression (Planas-Silva *et al*, 2001). Fourthly, SRC-3 interacts with the tumour suppressor p53 and represses its transactivational potential in gene reporter assays (Lee *et al*, 1999).

Notably, SRC-3 expression in tumours has been associated with positivity for p53, which is commonly associated with mutation and subsequent stabilization of this protein in an inactive form (Bouras *et al*, 2001). SRC-3 overexpression has also been associated with positivity for the epidermal growth factor receptor HER2/neu/erbB, a proto-oncogene that encodes a transmembrane tyrosine kinase receptor acting upstream of ras (Bouras *et al*, 2001; Osborne *et al*, 2003). Ras activation leads to increased mitogen activated protein kinase (MAPK) activity. Significantly, SRC-3 can be phosphorylated by MAPK, which results in its increased interaction with, and activation of, the ER (see "Regulation of function" below). Thus, tumours expressing high levels of HER2 may have increased SRC-3 activity, which further promotes cell proliferation and growth via the ER.

In a recent pivotal study using transgenic mice expressing a human SRC-3 cDNA gene under the transcriptional control of the mammary tumour virus long terminal repeat promoter/enhancer, Torres-Arzayus *et al* (2004) showed that increased SRC-3 expression

results in abnormal mammary gland development, including increased gland size due to hyperplasia, hypertrophy and decreased apoptosis. They detected a large number of mammary gland adenocarcinomas (mostly ER positive), pituitary adenomas, uterine leiomyosarcomas and lung carcinomas in the transgenic mice. Specifically, 76 of 100 SRC-3 transgenic mice carried 1 or more tumours (for a total of 145 tumours) while only 5 of 105 control mice carried tumours (for a total of 5 tumours). They also demonstrated that ectopic expression of SRC-3 leads to activation of the IGF-1/PI3K/Akt/mTOR and GSK3 pathways, at least in part due to increased IGF-1 levels. Taken together, they demonstrated that SRC-3 can function as an oncogene, suggesting that overexpression or amplification of the SRC-3 gene may lead to the development and progression of breast cancers and possibly other cancers.

Regulation of function

Although significant progress has been made in elucidating the functions of SRC-3 within the cell, little is yet understood about how SRC-3 is itself regulated. Font de Mora and Brown (2000) were amongst the first to address this issue by showing that SRC-3 is phosphorylated by p42 MAPK/Erk2 both *in vitro* and *in vivo*, leading to the enhancement of the transactivational potential of SRC-3. Similarly, Wu *et al* (2002) found that IκB kinase (IKK) phosphorylates SRC-3. This phosphorylation is increased by addition of TNFα, and is important for SRC-3-enhanced NFκB gene activation. Moreover, SRC-3 is translocated to the nucleus following TNFα treatment, and phosphorylated SRC-3 is predominantly localized in the nucleus, suggesting that SRC-3 phosphorylation may signal its translocation to the nucleus.

In a recent study, Wu *et al* (2004) identified six functional *in vivo* SRC-3 phosphorylation sites that increase its coactivating capacity (figure 1.2). They found that different signals such as steroids and TNFα triggered the phosphorylations via the activity of kinases including IKK and p38 MAPK. Importantly, SRC-3 phosphorylation enhanced its ability to interact with transcriptional activators and other coactivators, suggesting that the increase in its coactivating capability resulted from increased interaction with its binding partners.

Qutob *et al* (2002) studied the regulation of SRC-3 localization by observing that p/CIP is differentially compartmentalized in proliferating and non-proliferating cells in a CRM-1 export receptor-dependent manner. Firstly, p/CIP is localized in the cytoplasm of differentiated cells whereas it is predominantly in the nucleus of undifferentiated cells. In cell lines, p/CIP is detected in varying amounts in both the cytoplasm and the nucleus. Secondly, in mouse embryonic fibroblasts, serum starvation results in the translocation of p/CIP to the cytoplasm, while epidermal growth factor (EGF), insulin and the tumour-promoting phorbol ester PMA result in the translocation of p/CIP back to the nucleus. Thirdly, p/CIP localization changes throughout the cell cycle: in G1, p/CIP is predominantly but not exclusively cytoplasmic as it can be detected in the nucleus; in S, p/CIP is completely excluded from the nucleus; in G2/M, and prior to nuclear membrane breakdown, there is rapid nuclear accumulation of this protein; and in late M, p/CIP is once again cytoplasmic.

In addition to regulation by phosphorylation and subcellular localization, SRC-3 is also regulated by degradation. SRC-3 is ubiquitinated and degraded by the proteasome in association with the ubiquitin-conjugating enzymes (E2s) UBC2, UBC3, UBC4 or

UBC5 (Yan *et al*, 2003). The SRC-3 mRNA transcript has a half life of approximately 3 hours, while the SRC-3 protein is even less stable (Lonard *et al*, 2004). Interestingly, tamoxifen increases steady state levels of SRC-3 protein in MCF-7 cells, but not T47-D or ZR-75-1 breast cancer cells, suggesting that SRC-3 is differentially regulated in different cell types or tissues. Conversely, estradiol decreases SRC-3 mRNA and protein levels (Lauritsen *et al*, 2002).

THE UBIQUITIN-PROTEASOME SYSTEM

The ubiquitin-proteasome system (UPS) is the primary mechanism used by the cell for catabolism of proteins. It plays a crucial role in the regulation of many cellular functions including cell cycle progression, apoptosis and cell transformation (reviewed in Wilkinson, 2000; Adams, 2003). The UPS consists of the 26S proteasome, a multicatalytic enzyme complex whose primary function is protein degradation; ubiquitin, a 7.6 kDa protein that is covalently attached to the target molecule for recognition by the proteasome; and E1, E2 and E3, a group of enzymes that function in a cascade to catalyze the activation and transfer of ubiquitin molecules to the target protein. The ubiquitin-activating enzyme (E1) activates ubiquitin in an ATP-dependent manner by forming a thioester bond between a glycine residue on the ubiquitin molecule and a cysteine residue on itself. It then transfers the ubiquitin molecule to E2 (figure 1.4). The carrier or ubiquitin-conjugating enzyme (E2) then presents ubiquitin to the ubiquitin-protein ligase E3, which covalently links ubiquitin to the target protein. After several cycles, the proteasome recognizes and degrades the poly-ubiquitinated molecule.

Figure 1.4. Schematic illustration of the ubiquitin-proteasome system.

Protein ubiquitination proceeds via the activity of E1, E2 and E3 (see text for details). The process repeats itself until the target protein is polyubiquitinated and is targeted to the 26S proteasome for degradation. Alternatively, proteins can be deubiquitinated by DUBs that can salvage proteins from degradation.

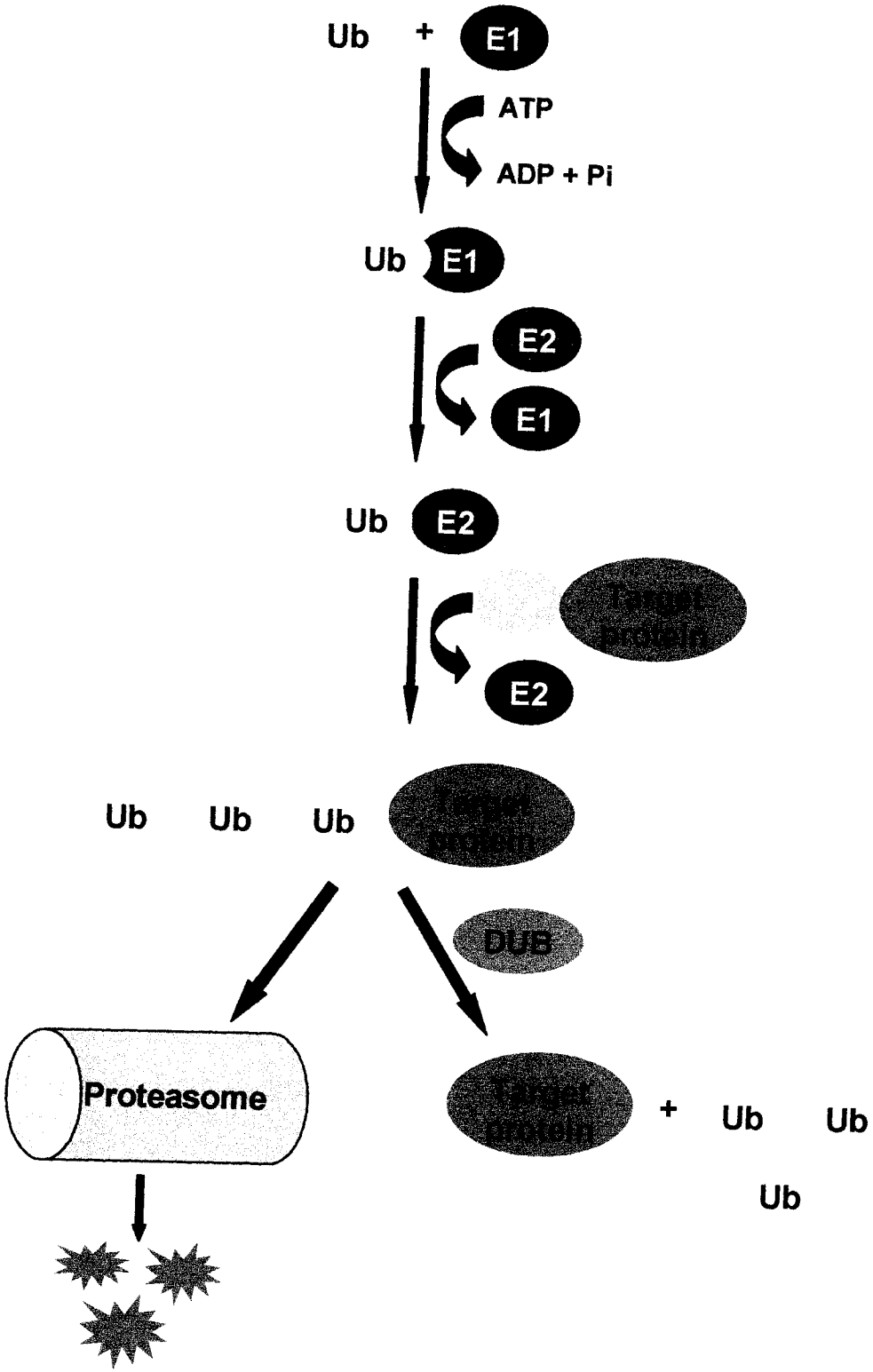
Ub
+
E1
ATP
ADP + Pi
Ub
E1
E2
E1
Ub
E2
Target protein
E2
Ub
Ub
Ub
Target protein
DUB
Proteasome
Target protein
+
Ub
Ub
Ub

In addition to being degraded by the proteasome, ubiquitinated proteins can be salvaged by deubiquitinating enzymes (DUBs), which remove the ubiquitin tag prior to degradation (figure 1.4) (reviewed in Hegde and DiAntonio, 2002). This process can either prevent destruction of the target protein or ease the potentially rate-limiting step of poly-ubiquitin chain disassembly prior to protein entry into the proteasome.

Protein ubiquitination is triggered by several different types of signals. These include genetically programmed sequences within the target protein, binding of adaptor proteins, post-translational modifications and protein damage such as oxidation, fragmentation or aging (reviewed in Wilkinson, 2000). Phosphorylation acts as the signal for ubiquitination of many cellular regulators such as cyclins, checkpoint proteins, signal transduction components and transcription factors (King *et al*, 1996).

Study of the UPS has been simplified by the identification of several proteasome inhibitors that inhibit the degradative function of the proteasome (reviewed in Lee and Goldberg, 1998). One of the most commonly used inhibitors is the peptide aldehyde MG132 (z-Leu-Leu-Leu-CHO), a substrate analogue that acts as a transition state inhibitor of the chymotrypsin-like activity of the proteasome. An increase in protein levels or prevention of protein disappearance following MG132 treatment is generally a good indicator of proteasome-mediated degradation.

THE MAMMALIAN CELL CYCLE

The mammalian cell cycle is comprised of a set of highly regulated events that culminate in the division of a parent cell into two identical daughter cells (reviewed in

King *et al*, 1996; Ford and Pardee, 1999). It is divided into interphase, which includes gap 1 (G1), synthesis (S) and gap 2 (G2), and mitosis (M) (figure 1.5). Progression through the cell cycle is dependent on the activity of cyclin-dependent kinases (Cdks), which are only active when bound to their related cyclins at specific points in the cell cycle. These cyclin/Cdk complexes initiate signalling cascades necessary for cell cycle progression. Cdk activities are primarily regulated by the expression of their cognate cyclins, which are targeted by ubiquitin-mediated proteolysis at specific points in the cell cycle. Additionally, Cdks are regulated by their phosphorylation status and compartmentalization within the cell.

In vivo, normal mammalian cells are in G0, a quiescent stage characteristic of non-dividing, differentiated cells (Ford and Pardee, 1999). Some quiescent cells can be stimulated by growth factors to enter G1, the first stage of the cell cycle characterized by DNA transcription, protein synthesis and growth. Growth factor stimulation results in the upregulation of cyclin D1, which forms a complex with Cdk4/6 and phosphorylates the retinoblastoma protein (pRb). Phospho-pRb then releases its binding partner E2F, which mediates the transcription of multiple genes involved in the S phase. The cyclin D1/Cdk4/6 complex also stimulates cyclin E/Cdk2 activity, promoting G1 to S transition.

DNA replication occurs in the S phase. Early in this phase, cyclins D and E are targeted for proteolysis, while cyclin A levels rise. Cyclin A binds Cdk2, forming the S-phase promoting factor (SPF), which translocates to the nucleus and initiates a cascade that signals chromosome replication. Accurate DNA replication is absolutely crucial for cell survival. Consequently, cells have developed cell cycle checkpoints to deal with problems such as damaged or incompletely replicated DNA (reviewed in McGowan,

Figure 1.5. Schematic illustration of the mammalian cell cycle.

The mammalian cell cycle is divided into interphase, which includes G1, S and G2, and mitosis. Non-dividing, differentiated cells exit the cycle and become quiescent in G0. Cyclin/Cdk complexes responsible for progression through specific phases are indicated (see text for details).

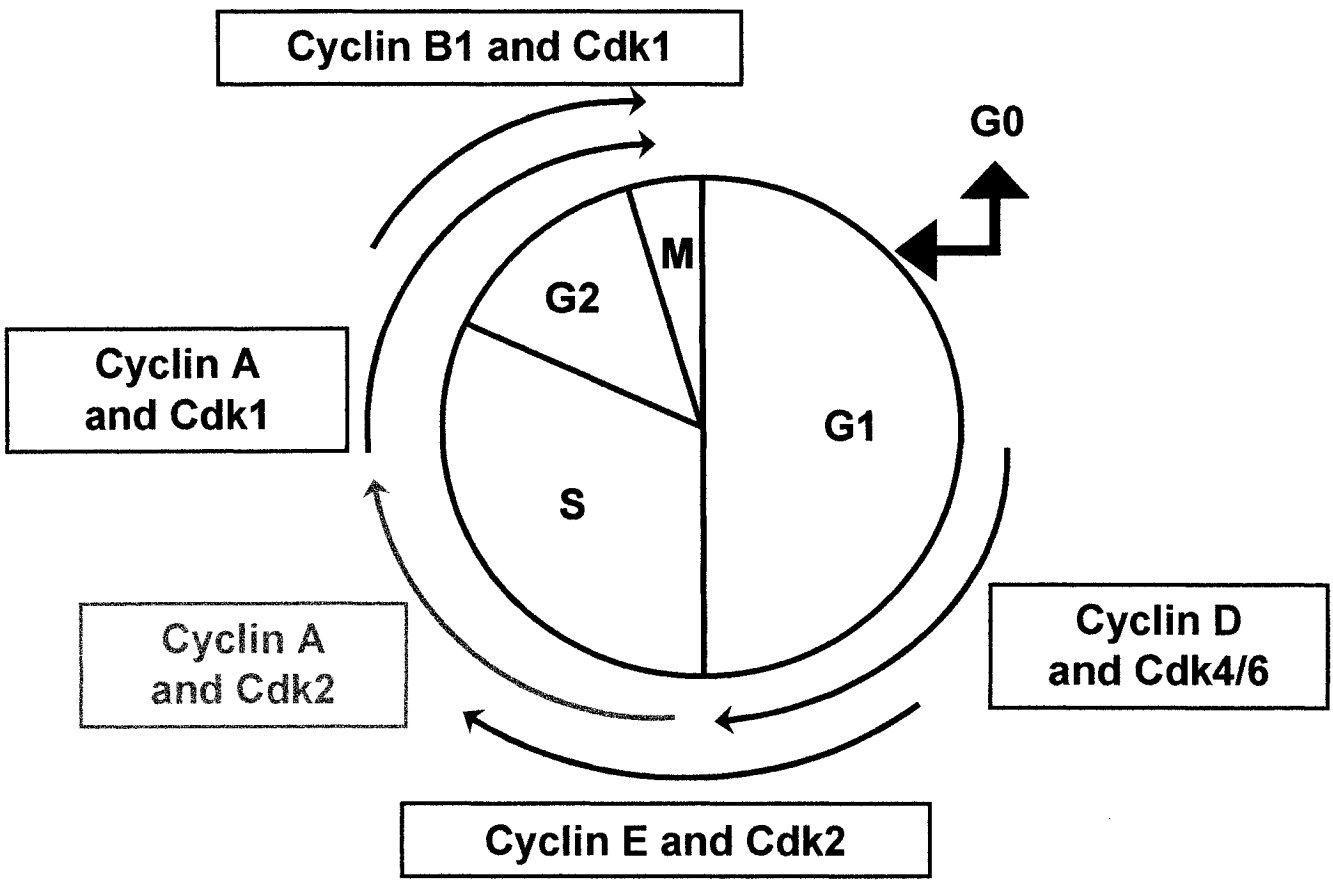
Cyclin B1 and Cdk1
G0
M
G2
Cyclin A
and Cdk1
G1
S
Cyclin A
and Cdk2
Cyclin D
and Cdk4/6
Cyclin E and Cdk2

2002; Eastman, 2004). Checkpoints afford cells the opportunity to repair damage prior to progression through the cell cycle, which would otherwise lead to propagation of damaged genomes. The first checkpoint, which occurs in late G1, prevents damaged cells from entering the S phase and often leads to apoptosis. The intra-S-phase checkpoint does not block S phase completely, but rather slows down progression in response to DNA damage. In contrast, the G2-M checkpoint arrests cells to allow proper repair of damaged chromatids prior to mitosis. Both the S and G2-M checkpoints are dependent on the inactivation of their respective Cdc25 homologues by Chk1 and Chk2. p53 also plays an essential role in initiating cell cycle arrest and/or apoptosis in response to DNA damage (reviewed in Ford and Pardee, 1999). Cell cycle checkpoints in p53-defective cells are severely compromised. Consequently, these cells are unable to arrest or sustain an arrest in response to DNA damage.

In late S and throughout G2, cells begin to prepare for mitosis. Cyclin B1, the key mitotic cyclin, is synthesized during these phases (reviewed in Smits and Medema, 2001; Porter and Donoghue, 2003; Murray, 2004). When threshold levels of cyclin B1 are attained, it binds Cdk1, initiating a conformational change that ultimately leads to phosphorylation and activation of the Cdk1 catalytic subunit. Cyclin B1 is also phosphorylated in the cytoplasmic retention sequence (CRS), which prevents its export from the nucleus, thus promoting cyclin B1/Cdk1 accumulation in the nucleus. Additionally, inhibitory phosphorylations on Cdk1 are removed at the onset of mitosis by the protein phosphatase Cdc25C.

Prophase, the first stage of mitosis characterized by chromosome condensation, is initiated by the active cyclin B1/Cdk1 complex, which is traditionally known as the

maturation promoting factor (MPF) (reviewed in Murray, 2004; Takizawa and Morgan, 2000; Hutchins and Clarke, 2004). During this phase, MPF phosphorylates several cytoskeletal proteins, promoting formation of the mitotic spindle from the centrioles. It also initiates nuclear envelope (NE) disassembly by phosphorylating and consequently depolymerizing the nuclear lamina, key components of the NE. Premetaphase, the next phase of mitosis, is characterized by microtubule-driven NE fragmentation (Georgatos *et al*, 1997; reviewed in Gönczy, 2002). Additionally during this phase and subsequent metaphase, elongating and contracting microtubules emanating from the centrioles attach to the two kinetochores of sister chromatid pairs, aligning them at the centre of the cell, called the metaphase plate.

Anaphase, the fourth phase of mitosis, involves the segregation of chromosomes to opposite ends of the cell (reviewed in Bharadwaj and Yu, 2004). This process depends on the proteasome-dependent degradation of cyclin B1, which results in MPF deactivation. Cyclin B1 degradation is stimulated by the activity of the anaphase-promoting complex (APC), the key mitotic ubiquitin protein ligase that is activated at the onset of anaphase by phosphorylation of several of its subunits and association with its activating partner Cdc20 (reviewed in Peters, 2002). Additionally, prior to the commencement of anaphase, the spindle checkpoint ensures that all sister chromatids are lined up at the metaphase plate and attached to the mitotic spindle. Once this requirement is satisfied, a signalling cascade initiated by APC activation leads to the separation and segregation of sister chromatids to opposite ends of the cell via the activity of microtubules.

Telophase and cytokinesis mark the last phases of mitosis, and are characterized by reformation of the NE, chromosome decondensation and cytoplasmic division. At the end of mitosis, two identical daughter cells re-enter G1.

Mitosis and aneuploidy

Most somatic eukaryotic cells contain a diploid (2N) complement of chromosomes. Deviation from this number results in polyploidy, an increase in the chromosome number by a whole-number multiple of the original chromosome complement (reviewed in Storchova and Pelman, 2004; Bharadwaj and Yu, 2004). Polyploidy can occur naturally in the development of specific cell types, such as skeletal muscle cells and megakaryocytes. In contrast, aneuploidy, an aberrant chromosome number associated with genetic instability, is a consequence of pathological situations. Aneuploidy can result from gross chromosomal changes such as non-reciprocal translocations, amplifications and deletions or from abortive cell cycles, often caused by defects in the spindle checkpoint. Aneuploidy and chromosomal instability are commonly observed in malignancy. Consequently, aberrant expression of genes involved in cell cycle progression, such as Aurora A (Meraldi *et al*, 2002) and cyclin B1 (Sarafan-Vasseur *et al*, 2002), has been implicated in the development of aneuploid cells.

Cell cycle arrest and synchronization

Study of the cell cycle has been simplified by the establishment of several synchronization methods that allow researchers to arrest cells in a specific phase of the cell cycle with an inhibiting agent. When cells are released from the inhibiting block, the

entire population proceeds through the cell cycle in a synchronous manner. The most widely used inhibiting agent for late G1/early S arrest is thymidine (Spector *et al*, 1998). In order for DNA replication to occur, the enzyme ribonucleoside diphosphate reductase must convert ribonucleotide diphosphate (NDP) into deoxyribonucleotide diphosphate (dNDP). However, addition of thymidine increases the intracellular pool of deoxythymidine triphosphate (dTTP), which inhibits the conversion of cytidine diphosphate (CDP) to dCDP. Consequently, DNA replication is inhibited and cells accumulate in late G1/S. Mitotic inhibition can be achieved by incubation with nocodazole, a microtubule depolymerizing agent that causes selective loss of non-kinetochore microtubules (Zieve *et al*, 1980). Nocodazole treatment arrests cells in metaphase. Similarly, taxol treatment causes a metaphase block by stabilizing microtubules, thus preventing proper microtubule dynamics during cell division (Abal *et al*, 2003).

STATEMENT OF PROBLEM

Significant progress has been made in elucidating the functions of SRC-3 as a nuclear and non-nuclear receptor coactivator. There is a growing line of evidence linking SRC-3 activity with signalling pathways in proliferation and cell size control. Although recent studies show its overexpression is associated with cancer, and transgenic expression results in cancer, little is known about the regulation of SRC-3 or the direct impact it has on cell cycle progression. In our initial studies, we found that SRC-3 is stabilized throughout interphase, post-translationally modified in mitosis, and degraded

as MCF-7 exit mitosis. These data led us to hypothesize that SRC-3 may play a role in normal cell cycle events, and that its activity must be attenuated during mitosis. Consequently, aberrant SRC-3 expression could lead to abnormal cell cycle progression and division, resulting in catastrophic cellular damage. The present study was undertaken to further investigate this cell cycle-dependent regulation of SRC-3, and to determine the consequences of deregulated SRC-3 expression.

MATERIALS AND METHODS

Cell culture

MCF-7, MCF-10A, ZR-75-1, COS-7 and HeLa cells were maintained in high glucose Dulbecco's minimal essential media (DMEM) (Gibco) containing phenol red, supplemented with 5% fetal bovine serum (FBS), 1% non-essential amino acids and 10 μg/ml gentamicin (Gibco). MDA-MB-231 cells were maintained in low glucose DMEM supplemented as above. Cells were incubated at 37°C under 5% CO_2. Cells were washed with phosphate buffered saline (PBS) (137 mM sodium chloride [NaCl], 2.7 mM potassium chloride [KCl], 10 mM disodium hydrogen orthophosphate, 1.76 mM potassium dihydrogen orthophosphate, pH 7.0 - 7.4) prior to isolation. PBS was removed by aspiration and 1 ml trypsinizing solution (0.25% trypsin [Invitrogen], 1 mM EDTA in PBS) was added per 100 mm plate. The cells were incubated for 3 minutes at 37°C, and subsequently resuspended in the trypsinizing solution, which was inactivated by addition of fresh media containing serum. At this point, the cells were plated at the desired density or isolated via centrifugation.

Clonogenic assays

5 x 10^3 MCF-7 cells were seeded in triplicate on 60 mm dishes and grown for a period of 8 days. Cells were washed twice with PBS and fixed in 2 ml of a 3:1 methanol:acetone solution for 30 minutes at room temperature. Following 3 more washes in PBS, cells were air dried for 2 days. For staining, cells were incubated in 2 ml of a 2% cresyl violet solution for 25 minutes at room temperature. Cells were then washed

repeatedly with distilled water and air dried overnight. Foci were counted to determine the number of colonies formed.

Cresyl violet staining solution was prepared by heating 1 g of cresyl violet in 50 ml water for 1 hour at 40°C, then filtering through double filter paper. In separate preparations, 6 ml of glacial acetic acid were diluted in 1000 ml of distilled water, and 1.36 g sodium acetate (NaOAC) were dissolved in 100 ml distilled water. The final staining solution was prepared by mixing 5 ml cresyl violet solution with 8 ml of NaOAC solution and 92 ml of acetic acid.

Enumeration of viable cells

Cells were isolated by trypsinization and centrifugation (described above). Floating cells present in the media and PBS used for washing were also isolated and added to the sample. Cells were stained with 0.2% trypan blue (Gibco) and enumerated using a hemocytometer according to their viability as assessed by their ability to exclude trypan blue.

Cell cycle synchronization

Cells were synchronized in mitosis by incubation in 250 ng/ml nocodazole (Sigma) for 16 hours. Cells were synchronized in G1 by performing a double thymidine block, which consisted of a 12-hour incubation in 2 mM thymidine (Sigma), followed by a 10- to 12-hour incubation in untreated media, followed by a final 12- to 14-hour incubation in 2 mM thymidine. During and after treatments, cells were washed twice with PBS in order to remove the drug and release the cells from cell cycle arrest.

Flow cytometry

Cells to be analyzed for cell cycle phase distribution were harvested by trypsinization and collected by centrifugation for 5 minutes at 1,800 RPM, 4°C. The pellet was washed one time with PBS and resuspended in 1 ml cold PBS plus 1 mM EDTA. Cells were then fixed in 3 ml of 70% ethanol at -20°C. Immediately prior to analysis, cells were spun down, washed and resuspended as above, and treated with 100 μg/ml RNase A (Sigma) at room temperature for 20 minutes to eliminate all free RNA. Finally, propidium iodide (Sigma) was added to a final concentration of 50 μg/ml. DNA content was assessed with a Beckman-Coulter EPICS Altra flow cytometer, using a 675 nm Band Pass Filter in PMT3, with all events being mirrored into PMT3. Events were acquired with EXPO version 2 Software from Beckman-Coulter, and then re-analyzed using WinCycle Version 3.0.

Plasmid isolation

Plasmid DNA was routinely propagated in DH5α competent bacterial strains. Cultures were transformed with plasmid DNA by incubation on ice for 45 minutes, followed by a 2-minute heat shock period at 42°C and a 1-hour incubation period at 37°C with mixing at intervals of 15 minutes. Colonies were grown overnight on Luria-Bertani (LB) agar plates containing 50 μg/ml ampicillin (VWR). Single colonies were picked with a sterile pipette tip and grown overnight in LB plus 50 μg/ml ampicillin. Plasmid DNA was isolated using the QIAGEN Plasmid Maxi Kit (10) as per the manufacturer's protocol.

Transfections

Transient transfections

For transient or stable transfections, cells were seeded at 2.5-3.0 x 10^6 cells/60 mm plate or 7.5 x 10^6 cells/100mm plate (approximately 50–60% confluence). The following day, cells were transfected with the desired plasmid using Fugene 6 Transfection Reagent (Roche Molecular Biochemicals) as per the manufacturer's protocol. Cells were grown for a minimum of 10 hours prior to further treatment.

Generation of SRC-3 stable MCF-7 cells

To generate stable clones, MCF-7 cells were cotransfected with pCMX.F.RAC3 (SRC-3) and CMV-puromycin. The pCMX.F.RAC3 expression plasmid, a gift of Dr. Don Chen (Massachusetts Medical School), consists of full-length RAC3 containing a FLAG and a hemagglutinin (HA) epitope linked to the amino-terminus (Li *et al.*, 1997). Empty vector control cells were transfected with pcDNA3 and CMV-puromycin. 48 hours post-transfection, cells were grown in the appropriate selection antibiotic (4 μg/ml puromycin [Sigma]) for 2-4 weeks. Colonies were isolated individually, categorized according to phenotype and expanded, generally for an additional 2-4 weeks, prior to assaying for protein expression by Western blot analysis. Typically, clones were seeded 3-4 times before experimental analyses were conducted. Established clones were maintained in 2 μg/ml puromycin.

Generation of SRC-3 deficient MCF-7 cells using RNAi

For interfering RNA (RNAi), crude, annealed, double stranded small interfering RNA (siRNA) was prepared by Xeragon Oligoribonucleotides (Qiagen-Xeragon) with the SRC-3 target sequence AAG GTG AAT CGA GAC GGA AAC (kindly provided by Dr. Anna Tate Riegel, Georgetown University). Prior to the first use, lyophilized siRNA was dissolved in 1 ml of the provided sterile buffer (100 mM potassium acetate, 30 mM HEPES-KOH, 2 mM magnesium acetate, pH 7.4), heated to 90°C for 1 minute and then incubated at 37°C for 1 hour. This procedure disrupted higher order aggregates which may have formed during the lyophilization process.

To deplete SRC-3, MCF-7 cells were seeded at 5 x 10^4 cells/35 mm plate (approximately 30% confluence) in 1 ml DMEM supplemented with 10% FBS without antibiotics. The following day, 5 μl of a 40 μM siRNA solution were dissolved in 175 μl of Opti-MEM (Invitrogen) (200 pmol siRNA final). In a separate tube, a solution containing 3 μl Oligofectamine (Invitrogen) and 12 μl Opti-MEM was incubated for 7 minutes. The two solutions were combined, incubated for an additional 20-25 minutes and added to the cultured cells. 5-12 hours later, 500 μl of DMEM supplemented with 30% serum were added to the cells. Typically, protein expression was assayed 24-96 hours post-transfection by Western blotting.

Antibodies

The following primary antibodies were used for western blot analysis and immunoprecipitations: anti-AIB1 (clone 34) mouse IgG1 (Transduction Laboratories); anti-GST-AIB1 rabbit serum (kind gift of Dr. Myles Brown); anti-FLAG M2 monoclonal

antibody (mAb) (Sigma); anti-phospho p44/42 MAPK (Thr 202/Tyr 204) E10 mAb (Cell Signaling Technology); anti-actin rabbit antibody (Sigma); anti-ß-tubulin clone TUB2.1 (Sigma); anti-p70 S6 kinase (Thr 389) (Cell Signaling); anti-cdc2 p34/Cdk1 mouse IgG_{2A} (Santa Cruz Biotechnology Inc.); anti-His_6 mAb (Roche); anti-ubiquitin (kind gift of Dr. Doug Gray). For immunocytochemistry, anti-AIB1 (AIB1-AC3) mAb (Novus Biologicals) was utilized.

The following secondary antibodies were used for western blot analysis and immunocytochemistry: peroxidase-conjugated AffiniPuro goat anti-rabbit IgG (H+L) (Jackson Research Laboratories Inc.); peroxidase-conjugated AffiniPuro goat anti-mouse IgG (H+L) (Jackson Research Laboratories Inc.); CY3-conjugated AffiniPuro goat anti-mouse IgG (H+L) (Jackson Research Laboratories Inc.)

SDS-polyacrylamide gel electrophoresis, immunoblotting and immunoprecipitations

Whole cell lysates were prepared from cell cultures washed twice with PBS and scraped in radioimmunoprecipitation assay buffer (RIPA) (1% NP40, 0.5% deoxycholate, 0.1% sodium dodecyl sulfate (SDS) in PBS plus 10 μl/ml phenylmethylsulfonyl fluoride [PMSF] [Sigma], 1 mM sodium orthovanadate [Sigma], 30 μl/ml aprotinin [Sigma A-6279]). The cell solution was incubated on ice for a minimum of 10 minutes, vortexed at maximum speed to maximize cell rupturing and centrifuged for 20 minutes at 15,000 RPM, 4°C to remove insoluble material. Lysate protein concentrations were determined using the Biorad D_C Protein Assay kit. Typically, 20 μg of protein were denatured in sample buffer (50 mM Tris-HCl, pH 6.8, 0.1 M dithiothreiotol [DTT], 2% SDS, 0.1% bromophenol blue, 10% glycerol) for 5 minutes at 100°C and resolved in a 5-12.5% SDS

polyacrylamide gel by electrophoresis (SDS-PAGE). A modified, highly porous, discontinuous minigel system was used unless otherwise indicated (separating gel: 25% acrylamide/0.25% bisacrylamide, diluted with water to desired concentration, 78 mM Tris/0.23 M glycine pH 8.8, 4% glycerol, 0.32% SDS, 0.12% APS, 0.8% TEMED; stacking gel: 5% acrylamide/0.05% bisacrylamide, 78 mM Tris pH 6.8, 5.3% glycerol, 4.4 mM EDTA, 0.44% SDS, 0.31% APS, 1.1% TEMED) (Doucet *et al*, 1990). This gel system helped maintain the secondary and tertiary structure of proteins. Consequently, our proteins ran at slightly higher molecular weights than predicted. On occasion, and when indicated, Laemmli gels were used (Laemmli, 1970). Gels were transferred to PVDF membranes (Perlin Elmer) at 50 V for 2.5 hours or at 20 V overnight. The membrane blots were blocked for one hour in 5% Carnation skim milk powder dissolved in Tris-buffered saline (20 mM Tris-HCl pH 7.6, 137 mM NaCl) containing 0.1% Tween-20 (TBS-T), and then incubated with the appropriate primary antibody dissolved in blocking solution plus 0.02% sodium azide for 1 hour at room temperature. The blots were washed for 15 minutes once and 5 minutes twice in TBS-T prior to a one-hour incubation with horseradish peroxidase-conjugated goat anti-mouse or anti-rabbit secondary antibody, diluted 1:5000 in blocking solution. Finally, the blots were washed in TBS-T as above, and the bands were detected using the Enhanced Chemiluminescence Analysis System (Amersham Biosciences) according to the manufacturer's protocol.

For immunoprecipitations (IPs), 20-70 μl protein A Sepharose beads (Sigma) were washed with PBS and isolated by centrifugation at 2,500 RPM for 2 minutes. Typically, 0.35-1 mg protein was precleared by rotating with the washed beads for 1-2 hours at 4°C. Preclearing the samples removed proteins that non-specifically bound the

sepharose beads, thus decreasing background signals. The supernatants were isolated and rotated overnight in the presence of the appropriate antibody. The following day, 40-70μl of beads were added to the supernatant and rotated for 4 hours at 4°C. The bead-antibody-protein complexes were isolated by centrifugation at 2,500 RPM at 4°C for 3 minutes and washed 3-4 times with PBS. Immune complexes were dissolved and denatured in 2x sample buffer by heating to 100°C for 5 minutes. Proteins were separated by SDS-PAGE, transferred to PVDF and analyzed by immunoblotting as above.

***In vitro* Cdk1 assay**

MCF-7 cells were harvested in a buffer containing 20 mM HEPES (pH 7.5), 150 mM NaCl, 10 mM EGTA, 40 mM ß-glycerophosphate, 1% NP40, 2.5 mM $MgCl_2$, 2 mM orthovanadate, 1 mM DTT, 1 mM PMSF, 10 µg/ml aprotinin and 10 µg/ml leupeptin. Whole cell lysates containing 1.5 mg of total protein were immunoprecipitated with 7 μl anti-GST-AIB1 rabbit serum (Font de Mora and Brown, 2000) or control rabbit IgG. Immune complexes were isolated with protein A sepharose beads as described above. Immunoprecipitates were washed 4 times with PBS and then dephosphorylated with 500 U of λ-protein phosphatase (New England Biolabs) in 20 µl total volume for 30 minutes as outlined in the manufacturer's protocol. Following dephosphorylation, immunoprecipitates were washed five times and incubated in lysis buffer for 30 minutes, and then washed one time with distilled water. Finally, immunoprecipitates were phosphorylated in Cdc2 (Cdk1) protein kinase buffer containing 15 µCi γ-^{32}P[ATP], 100 µM cold ATP and 20 U cdc2 (New England Biolabs) for 1 hour as outlined in the manufacturer's protocol. The reaction was stopped by a 5-minute incubation at 100°C in

5x loading buffer. Immunoprecipitates were resolved in an 8% Laemmli gel overnight and exposed to film for various time periods.

Immunocytochemistry

Cell cultures were seeded on coverslips at the desired confluence. When treatments were complete, cells were washed twice with PBS, fixed with 4% para-formaldehyde in PBS for 30 minutes at room temperature and washed again 3-4 times with PBS. Fixed cells were stored in PBS at 4°C. For staining, cells were permeabilized with a 1:1 100% methanol:100% acetone solution for 5 minutes and washed 3 times with PBS. Each subsequent 1-hour incubation was performed at room temperature and was followed by 3 consecutive washes with PBS. Coverslips were transferred to a wet filter paper contained in a Petri dish and incubated with blocking solution (5% normal goat serum, 0.5% bovine serum albumin [BSA], 0.1% triton-X 100 in PBS). Cells were then incubated with primary antibody (diluted in 3% BSA in PBS) followed by incubation with the appropriate secondary antibody (CY3-conjugated anti-mouse or anti-rabbit IgG, diluted as above). DNA was stained for 1 minute with Hoechst (1 μg/ml in water) (Sigma). Coverslips were mounted on slides with anti-fade (50 mg *p*-phenylenediamine in 5 ml PBS, 45 ml filtered glycerol; pH 8.0 with 0.5 M carbonate/bicarbonate buffer) and visualized using fluorescent microscopy.

RNA extraction and northern blot analysis

All steps were performed at 4°C with RNase-free materials. Total RNA was isolated using TRIZOL reagent (Gibco BRL) as outlined in the manufacturer's protocol

and subsequently dissolved in DEPC water. For Northen blot analysis, 30 μg of RNA were heated in sample buffer (3% formaldehyde, 0.4% formamide, 1x MOPS [20 mM 3-[N-morpholino]propanesulfonic acid, 5 mM NaOAC, 1 mM EDTA, pH 7.0]) for 15 minutes at 65°C. After cooling, 0.02 μg/μl ethidium bromide and 6x loading buffer (0.25% bromophenol blue, 0.25% xylene cyanol FF in 30% glycerol) were added. RNA samples were resolved via electrophoresis on a 1% agarose gel containing 2% formaldehyde and 1x MOPS. The gel was washed for 30 minutes in DEPC water prior to RNA transfer to a nylon membrane (Amersham) via capillary action overnight in 10x SSC (1.5 M NaCl, 0.15 M sodium citrate, pH 7.0). RNA was immobilized by UV cross-linking (122 mJ for 30 seconds). The membrane was incubated for 4 hours at 42°C in pre-hybridization buffer (50% deionized formamide, 5x SSPE [0.75 M NaCl, 50 mM sodium orthophosphate, 5 mM EDTA, pH 7.0], 5x Denharts [0.5% polyvinylpyrrolidone, 0.5% bovine serum albumin, 0.5% Ficoll 400], 0.1% SDS, 250 μg/ml denatured, sonicated herring sperm DNA). Following pre-hybridization, radiolabelled probe was added to the buffer and incubated overnight at 42°C for hybridization. Membranes were washed at room temperature in low stringency buffer (2X SSC, 0.1% SDS) for 20 minutes, medium stringency buffer (0.5X SSC, 0.1% SDS) for 10 minutes and high stringency buffer (0.2X SSC, 0.1% SDS) for 5 minutes. Membranes were exposed to film for several days at -70°C, as determined by the intensity of the signal. An 800 base pair probe from glyceraldehyde phosphate dehydrogenase (GAPDH) was used as a loading control.

For probe labelling, CMV-RAC3 was digested with BamH1 and Xba1 and resolved in a 1% agarose gel using electrophoresis. The 2400 base pair fragment was excised and purified using the QIAquick Gel Extraction Kit (50) (Qiagen), and

radiolabelled with 50 μCi [α-^{32}P]-dCTP (Amersham) using the DecaLabel DNA Labeling Kit (Fermentas).

Senescence-associated (SA)-ß-gal staining

Staining was performed as described previously to detect senescent cells (Dimri *et al*, 1995). Briefly, washed cells were fixed for 5 minutes in 2% formaldehyde at room temperature and incubated at 37°C for 12-16 hours in fresh SA-ß-gal staining solution (1 mg/ml X-gal [MBI Fermentas] [20 mg/ml stock in dimethylformamide], 40 mM citric acid, 5 mM potassium ferrocyanide, 5 mM potassium ferricyanide, 150 mM NaCl, 2 mM magnesium chloride, sodium phosphate buffer, pH 6.0). Cells were visualized under a phase contrast microscope.

Additional reagents

The following reagents were purchased from Sigma unless otherwise stated: taxol, okadaic acid (OA), MG132, 4-hydroxy tamoxifen, butyrolactone-I (BL-I) (BIOMOL Research Labs), Faslodex/ICI 182,780 (Tocris), Z-VAD (BD Biosciences), UO126 (Promega). These reagents were utilized as described in the results.

RESULTS

SRC-3 protein expression is regulated throughout the cell cycle

As a first step towards investigating the regulation of SRC-3, we examined the effects of G1 and mitotic arrest on SRC-3 protein expression. To this end, immunocytochemical analysis was performed on MCF-7 cells arrested in mitosis with nocodazole or in late G1 with a double thymidine block. Following treatment, cells were fixed on coverslips and stained with a SRC-3 monoclonal antibody and Hoechst DNA stain. Strikingly, nocodazole-blocked cells expressed significantly higher levels of SRC-3 protein than thymidine-blocked cells (compare figure 3.1A and B). As an internal control, cells that were not blocked in mitosis in the nocodazole sample did not express high levels of SRC-3 protein (figure 3.1B, arrow). This result suggests that SRC-3 protein is stabilized in G2/M.

In order to examine SRC-3 protein expression throughout the cell cycle, western blot analysis was performed on cycling MCF-7 cells following synchronization in mitosis with nocodazole. Total protein was harvested every 3 hours for 15 hours following release from nocodazole block and resolved in a porous glycerol gel system, which conserved more secondary and tertiary structure in proteins. Cell cycle phase distribution was also determined every 3 hours by measuring DNA content using flow cytometry. Immediately following nocodazole treatment, a second SRC-3 species with an increased molecular weight appeared, coincident with a maximal proportion of cells in G2/M (figure 3.2A and B). As the cells ended and/or exited mitosis, this larger species disappeared.

Figure 3.1. SRC-3 protein is stabilized in G2/M of the cell cycle.

Immunocytochemical analysis of MCF-7 cells. Blue indicates Hoechst-stained DNA, red indicates SRC-3 protein. **(A)** SRC-3 protein expression in cells arrested in late G1 with a double thymidine block. **(B)** SRC-3 protein expression in cells arrested in metaphase with nocodazole. Cells that were not successfully blocked in mitosis following nocodazole treatment acted as an internal control (white arrow).

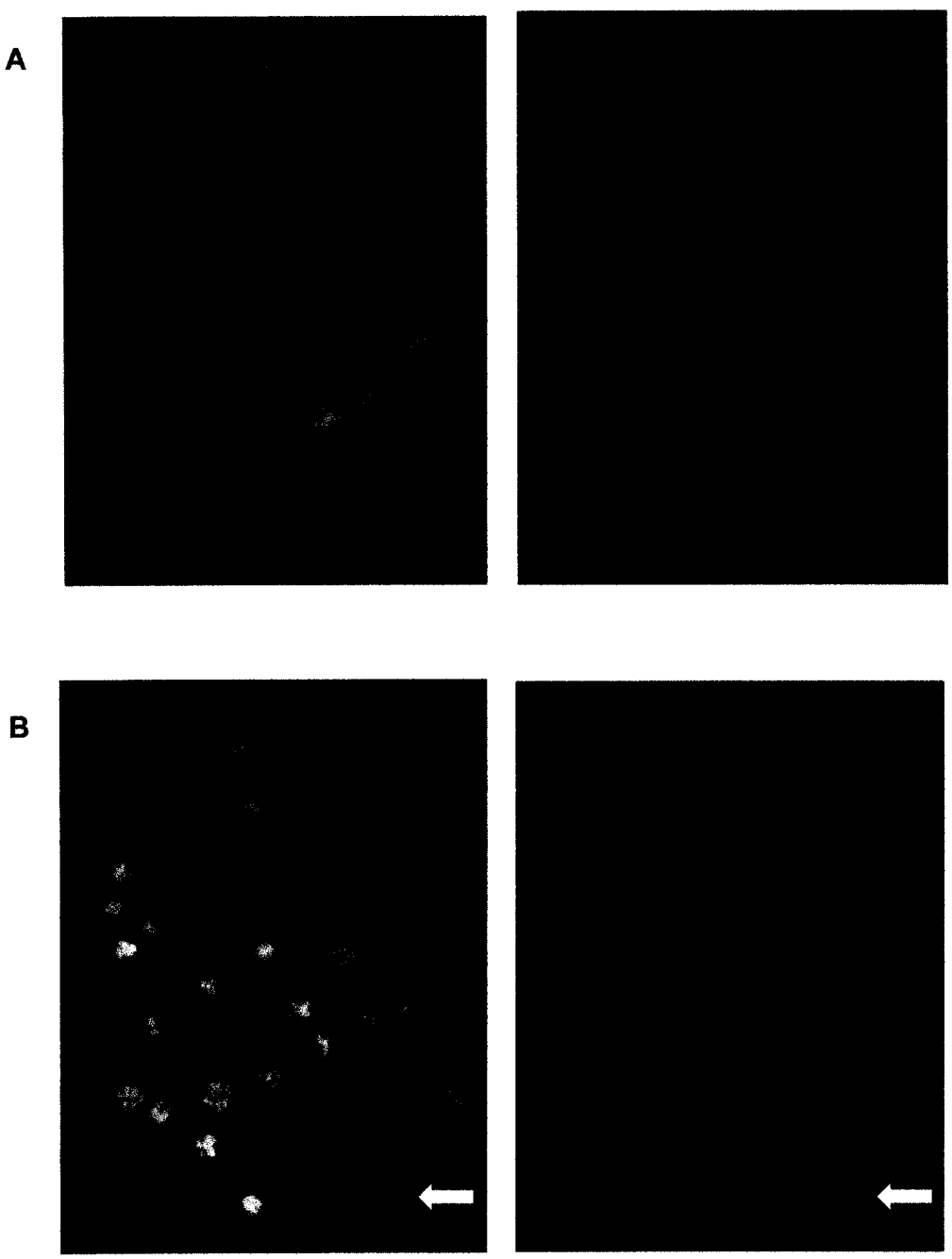
A
B

Figure 3.2. SRC-3 is modified during mitosis then rapidly degraded.

(A) Western blot analysis showing SRC-3 protein expression in nocodazole-synchronized (noco) cells. **(B)** Cell cycle phase distribution in nocodazole-synchronized cells as determined by flow cytometry. **(C)** Western blot analysis showing SRC-3 protein expression in thymidine-synchronized (thy) cells. **(D)** Cell cycle phase distribution in thymidine-synchronized cells as determined by flow cytometry. **(E)** Western blot analysis showing SRC-3 protein expression in taxol-synchronized cells (100 nM, 18h).

Actin protein expression was used as a loading control.

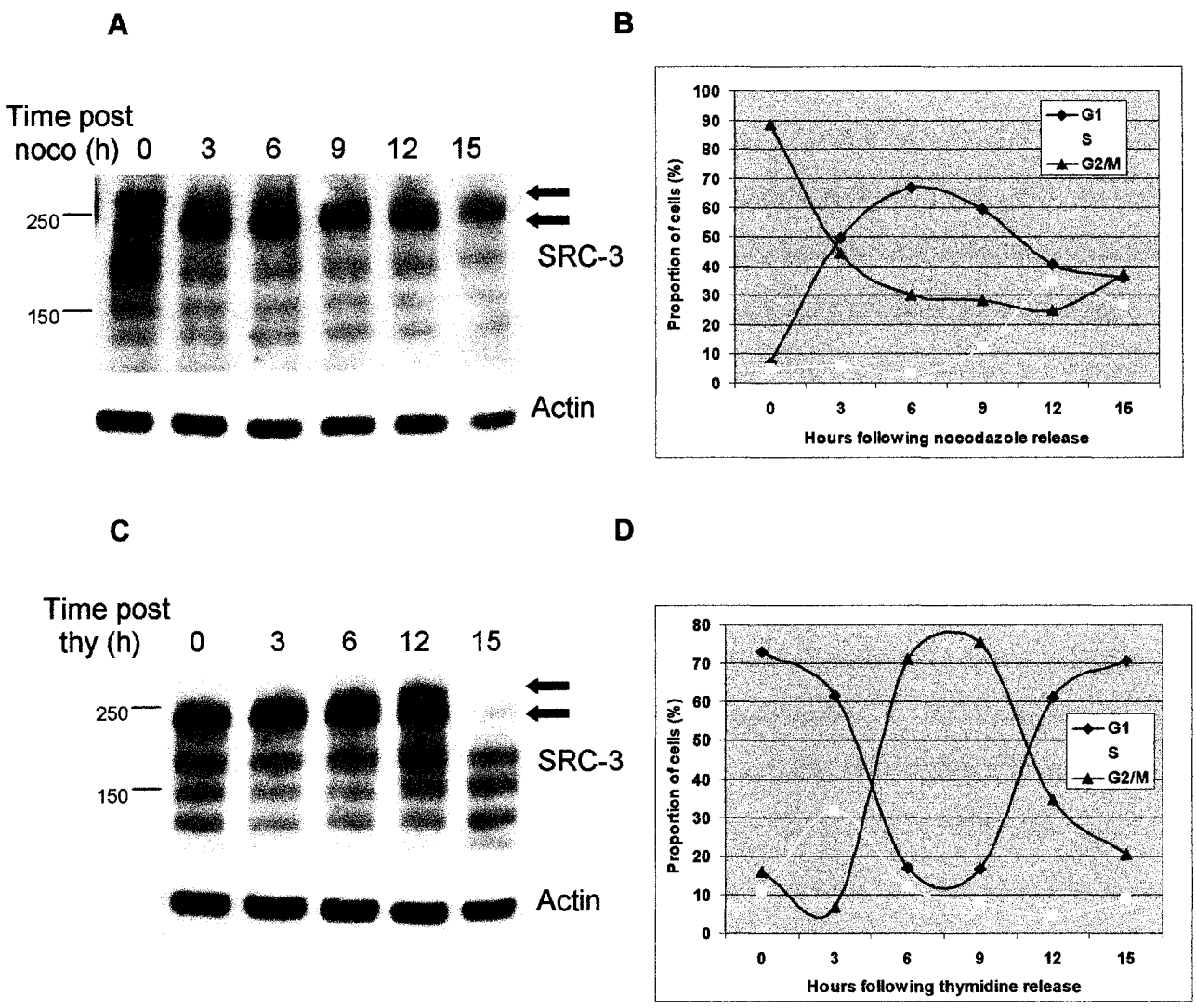
A
Time post noco (h) 0 3 6 9 12 15
250
150
SRC-3
Actin
B
Proportion of cells (%)
100
90
80
70
60
50
40
30
20
10
0
G1
S
G2/M
0 3 6 9 12 15
Hours following nocodazole release
C
Time post thy (h) 0 3 6 12 15
250
150
SRC-3
Actin
D
Proportion of cells (%)
80
70
60
50
40
30
20
10
0
G1
S
G2/M
0 3 6 9 12 15
Hours following thymidine release
E
Time post taxol (h) 0 1 3 6 9 12 15 18 21 24
250
150
75
50
SRC-3
Actin

To confirm that the increase in molecular weight was indeed a cell cycle effect and was not due to nocodazole treatment, SRC-3 protein expression and cell cycle phase distribution were examined in cycling MCF-7 cells synchronized in late G1 using a double thymidine block. Immediately following treatment, when the greatest proportion of cells was in G1, only the lower molecular weight form of SRC-3 was present. This species became increasingly diffuse as the cells progressed through S and entered G2/M. When the cells were subsequently exiting G2/M and/or entering G1 (12 hours following release), the larger species of SRC-3 re-appeared. The occurrence of this form was transient, as it disappeared by 15 hours following release, coincident with an overall decrease in SRC-3 expression. This experiment was repeated three times with similar results.

SRC-3 protein expression was also examined in cycling MCF-7 cells synchronized in G2/M with 100 nM taxol for 18 hours. As in the nocodazole-treated cells, immediately following taxol treatment, the larger species of SRC-3 appeared (figure 3.2E). This form disappeared by 12 hours and was again present by 18 hours following release. The appearance of the larger form of SRC-3 was coincident with a decrease in the number of immunoreactive lower molecular weight species. Interestingly, the lower molecular weight species reappeared as SRC-3 expression levels decreased, suggesting that they might be SRC-3 degradation products.

Transient increases in the molecular weight of a protein are usually attributed to post-translational modifications such as phosphorylation, acetylation or ubiquitination. Thus, we hypothesized that the increased molecular weight form of SRC-3 was a post-translationally modified species. The modified form was more readily identifiable in the

porous glycerol gel system than the regular Laemmli gel system (data not shown), suggesting that the apparent increase in molecular weight was at least partially due to a conformational change only detected when the secondary and tertiary structures of the protein were partially conserved.

Since it appeared that SRC-3 protein was regulated in a cell cycle-dependent manner, we questioned whether it might also be cyclically regulated at the transcriptional level. In order to examine this possibility, MCF-7 cells were synchronized with thymidine and nocodazole. Total RNA was harvested at various time points following release and northern blot analysis was performed to examine any changes in SRC-3 mRNA expression. SRC-3 mRNA levels did not fluctuate as cells progressed through the cell cycle (figure 3.3A and B). This result suggests that the cell cycle-dependent regulation of SRC-3 occurs exclusively at the protein level.

SRC-3 localization is dynamically regulated throughout the cell cycle

Protein compartmentalization is a mechanism commonly used by cells to regulate protein activity. Many cell cycle proteins including cyclin B1 are differentially compartmentalized during different phases of the cell cycle. In order to determine if SRC-3 compartmentalization was also regulated in the cell cycle, we examined its localization using immunocytochemistry as cells progressed through interphase and mitosis. MCF-7 cells synchronized in late G1 with a double thymidine block were fixed every 2 hours following release and stained with SRC-3 monoclonal antibody and Hoechst DNA counterstain. Immediately after thymidine treatment, when cells were in late G1, SRC-3 protein was predominantly localized in the nucleus, with minimal

Figure 3.3. SRC-3 is not transcriptionally regulated in a cell-cycle dependent manner.

(A) Northern blot analysis showing SRC-3 mRNA expression in MCF-7 cells progressing through the cell cycle following synchronization with nocodazole or thymidine. **(B)** Cell cycle phase distribution in nocodazole and thymidine synchronized MCF-7 cells.

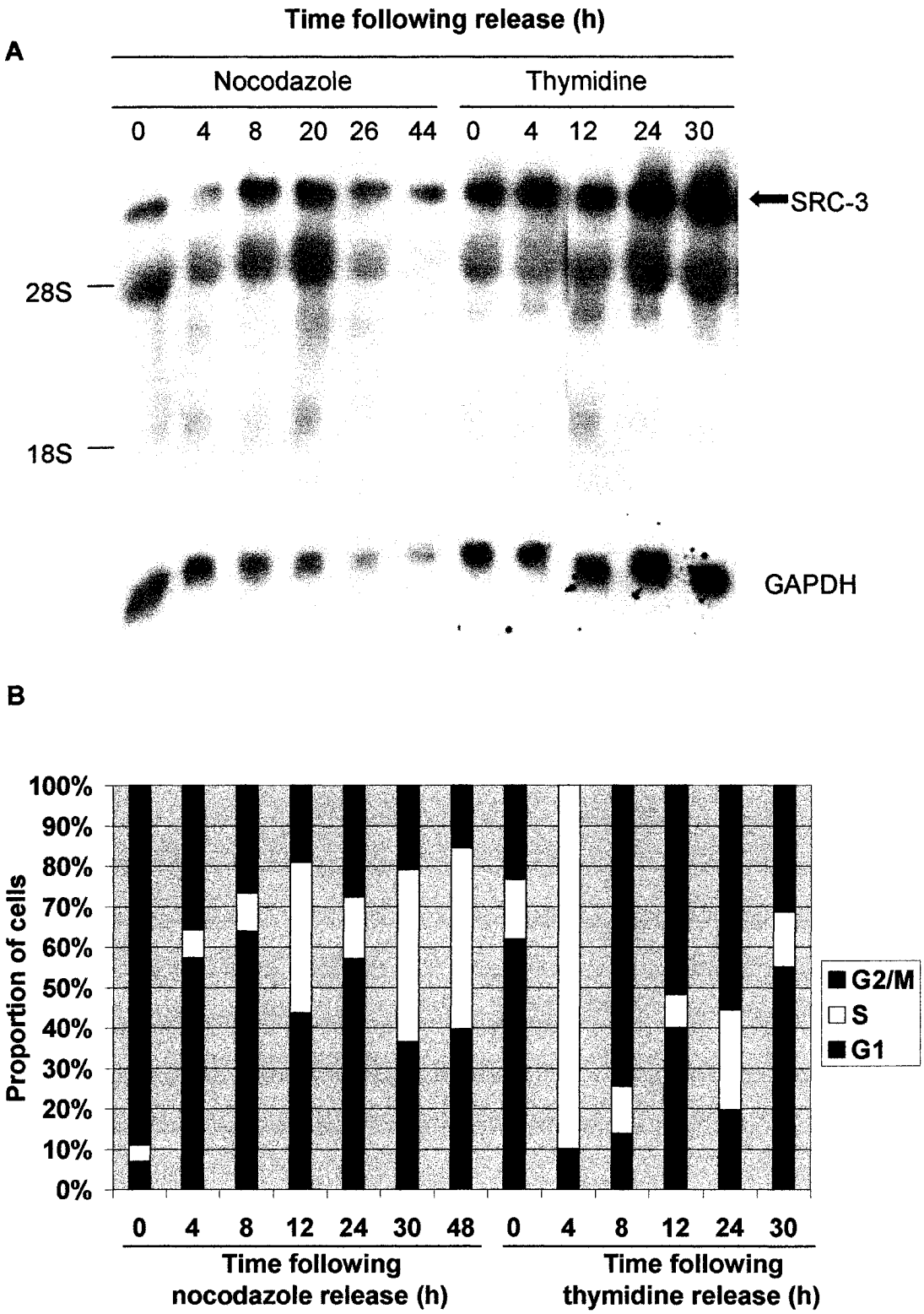
A
Time following release (h)
Nocodazole
Thymidine
0 4 8 20 26 44 0 4 12 24 30
SRC-3
28S
18S
GAPDH
B
100%
90%
80%
70%
60%
50%
40%
30%
20%
10%
0%
Proportion of cells
G2/M
S
G1
0 4 8 12 24 30 48 0 4 8 12 24 30
Time following nocodazole release (h)
Time following thymidine release (h)

punctate expression in the cytoplasm (figure 3.4A). Additionally, SRC-3 was completely excluded from the nucleoli. As cells continued through S and G2, SRC-3 protein levels increased and became more punctate in nature (figure 3.4B, bottom arrow). This expression pattern was more pronounced by early prophase, when chromosomes had begun to condense (figure 3.4B, top arrow). Cytoplasmic SRC-3 protein levels also increased at this point. Later in prophase, when the chromosomes had completely condensed, SRC-3 protein was almost exclusively localized in the cytoplasm (figure 3.4C, top arrow). Notably, the expression was extremely punctate and formed a circular pattern around the nucleus, suggesting that SRC-3 might be associating with another unknown protein, possibly in the NE. By prometaphase, when the NE had disintegrated and chromosomes had begun to move to the metaphase plate, SRC-3 remained punctate and excluded from the DNA, but was no longer present in the circular configuration (figure 3.4C, bottom arrow). This expression and localization pattern continued through metaphase (figure 3.4D), anaphase (figure 3.4E) and telophase (figure 3.4F). By late telophase/cytokinesis, when the NE had begun to reform, the separation between SRC-3 and DNA localization was less distinct (figure 3.4G). Finally, when the daughter cells had finished dividing yet DNA was still decondensing, SRC-3 was once again predominantly a nuclear protein. Interestingly, SRC-3 localization was similarly regulated in ZR-75-1 (ER positive) and SK-Br-3 (ER negative) breast cancer cells, as well as COS-7 fibroblast-like African green monkey kidney cells (Gluzman, 1981) (data not shown), suggesting that the SRC-3 localization patterns observed in MCF-7 cells were not strictly related to the ER status of breast cancer cells or even to breast malignancies. These complex localization and expression patterns suggest that SRC-3

Figure 3.4. SRC-3 protein localization is regulated during the cell cycle.

Immunocytochemical analysis of MCF-7 cells as they progressed through the cell cycle following release from late G1 arrest with a double thymidine block. Blue indicates Hoechst-stained DNA, red indicates SRC-3 protein. **(A)** In late G1, SRC-3 protein was predominantly localized in the nucleus with minimal punctate expression in the cytoplasm. **(B)** In G2 (bottom arrow) and early prophase (top arrow), SRC-3 protein levels progressively increased and became more punctate in nature. **(C)** When the chromosomes had condensed in prophase (top arrow), SRC-3 protein was almost exclusively localized in the cytoplasm. There was also a punctate, circular pattern around the nucleus. In prometaphase (bottom arrow), SRC-3 remained punctate and excluded from DNA. In metaphase **(D)**, anaphase **(E)** and telophase **(F)**, SRC-3 remained punctate and excluded from the DNA. **(G)** In late telophase/ cytokinesis, SRC-3 was no longer distinctly excluded from DNA. **(H)** When DNA was still decondensing but the daughter cells had divided, SRC-3 was again predominantly localized in the nucleus.

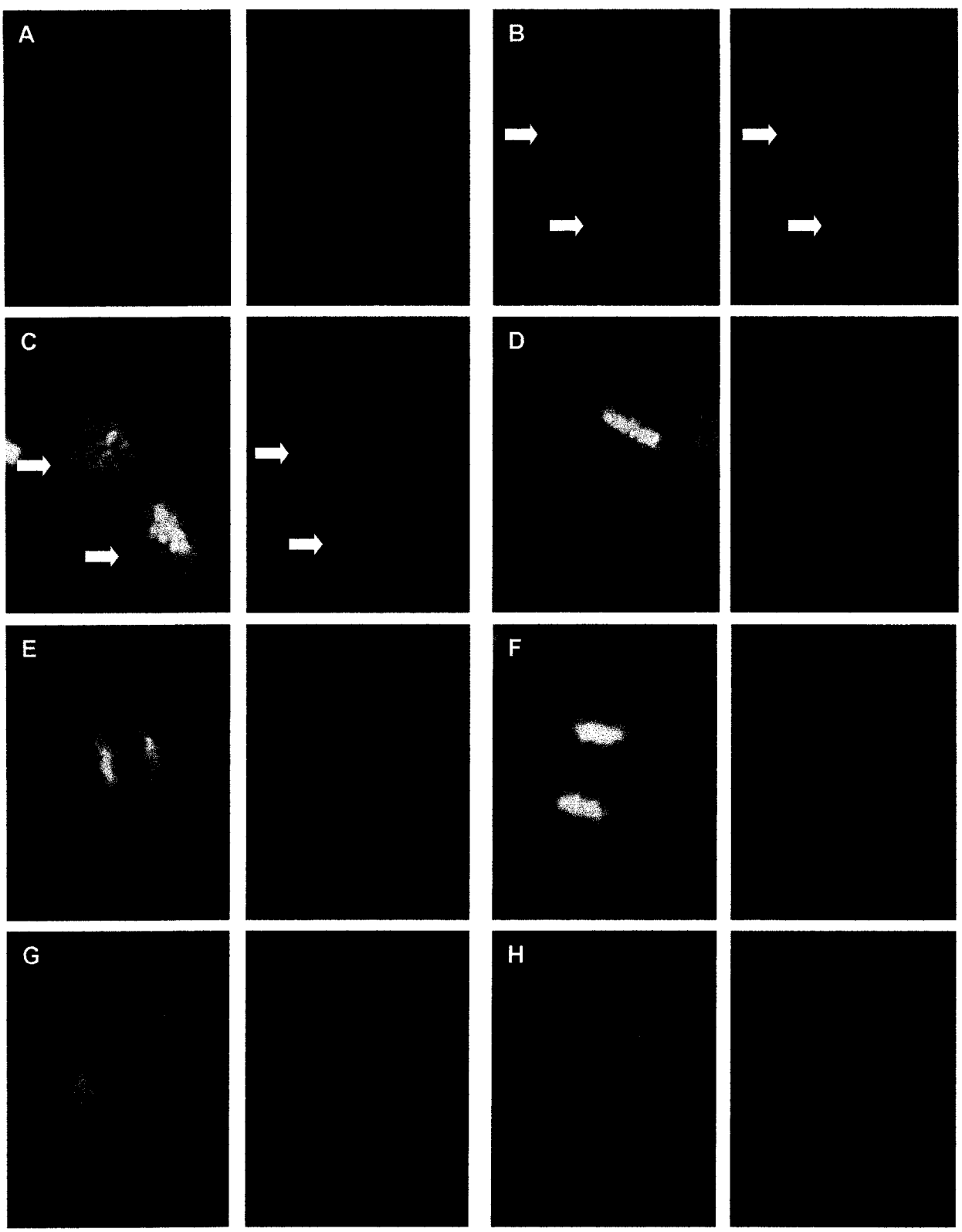
A
B
C
D
E
F
G
H

activity is highly regulated throughout the cell cycle.

SRC-3 is degraded in a proteasome-dependent, caspase-independent manner

Because we detected changes in SRC-3 protein expression throughout the cell cycle (figures 3.1 and 3.2), we hypothesized that the modified form of SRC-3 might act as a signal for ubiquitination and subsequent degradation by the proteasome as cells exit mitosis. In order to examine this possibility, we synchronized MCF-7 cells in mitosis and subsequently released the cells from block for 4 hours in the presence or absence of the proteasome inhibitor MG132 (56 μM). In MCF-7 cells released from nocodazole, SRC-3 was predominantly present as the regular molecular weight form (figure 3.5A, lane 1). Moreover, there were many putative degradation products also present in this sample. In contrast, in MCF-7 cells released in the presence of MG132, both the regular and modified forms of SRC-3 were present (figure 3.5A, lane 2). There was also an overall increase in the level of SRC-3 protein present in the sample and fewer degradation products, suggesting that MG132 was stabilizing both forms of SRC-3. In support of the results observed in MCF-7 cells, SRC-3 was also stabilized in MCF-10A spontaneously immortalized normal human mammary epithelial cells (Tait *et al*, 1990) treated with nocodazole and MG132 as above (figure 3.5A, lanes 3-4), suggesting that stabilization and degradation of SRC-3 are normal events not limited to malignancy. Furthermore, both SRC-3 species were stabilized in MCF-7 cells released from taxol arrest in the presence of MG132 (figure 3.5A, lanes 5-6). These observations suggest that the modification of SRC-3 may lead to degradation by the proteasome as cells exit G2/M.

Figure 3.5. SRC-3 is ubiquitinated and degraded in a proteasome-dependent, caspase-independent manner.

(A) Western blot analysis showing SRC-3 protein expression in nocodazole-synchronized MCF-7 cells (lanes 1-2) and MCF-10A cells (lanes 3-4), and taxol-synchronized MCF-7 cells (lanes 5-6), released from block for 4 hours in the presence or absence of MG132 (56 μM). SRC-3 protein was stabilized in cells treated with MG132 (lanes 2, 4 and 6). **(B)** Ubiquitinated SRC-3 protein present in asynchronous and mitotic MCF-7 cells transfected with CMX-RAC3 (SRC-3) and a His_6-ubiquitin expression vector. SRC-3 protein was immunoprecipitated from whole cell lysates, isolated and resolved in an 8% Laemmli gel. The membrane was probed with anti-His_6. **(C)** Western blot analysis showing SRC-3 protein expression in nocodazole-synchronized MCF-7 cells released from block for 3 hours in the presence or absence of 50 μM Z-VAD. Z-VAD did not stabilize SRC-3 following release from block (compare lanes 2, 3 and 4). Actin protein expression was used as a loading control.

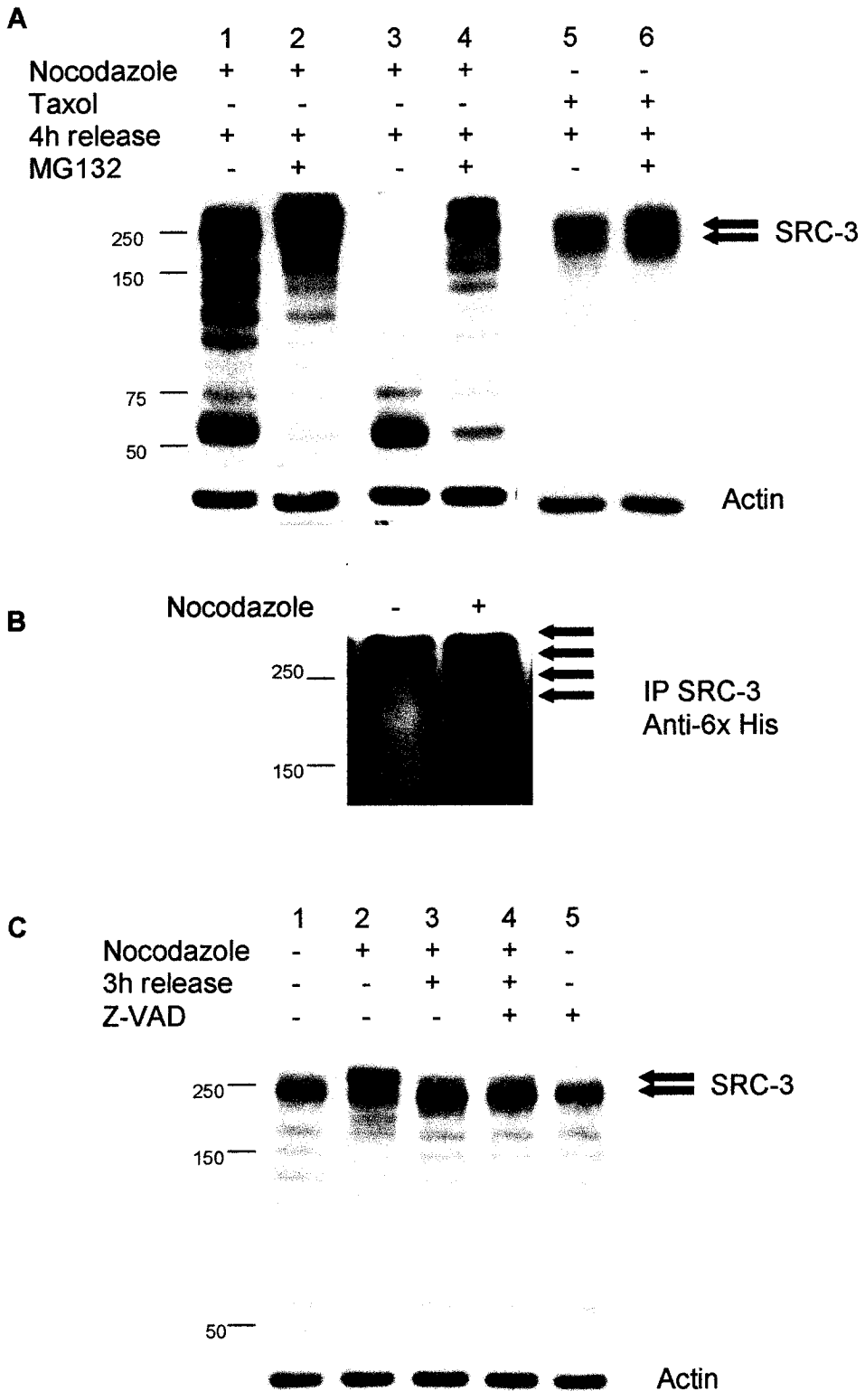
A
1 2 3 4 5 6
Nocodazole + + + + - -
Taxol - - - - + +
4h release + + + + + +
MG132 - + - + - +
250
150
75
50
SRC-3
Actin
B
Nocodazole - +
250
150
IP SRC-3
Anti-6x His
C
1 2 3 4 5
Nocodazole - + + + -
3h release - - + + -
Z-VAD - - - + +
250
150
50
SRC-3
Actin

In order to confirm that SRC-3 could be ubiquitinated, we transfected MCF-7 cells with CMX-RAC3 (SRC-3) and a histidine tagged- (His_6) ubiquitin expression plasmid. The following day, one plate of cells was blocked in mitosis with nocodazole and the other was left asynchronous. SRC-3 was immunoprecipitated from 1 mg of total protein using a SRC-3-specific monoclonal antibody. Immune complexes were resolved in an 8% Laemmli gel and visualized with an anti-His_6 antibody. The nocodazole-treated cells contained more ubiquitinated SRC-3 protein than the untreated cells (figure 3.5B). Additionally, several weak bands could be detected in the nocodazole-treated sample, which may represent differentially poly-ubiquitinated SRC-3 protein (red arrows). These results suggest that SRC-3 is preferentially ubiquitinated in G2/M of the cell cycle.

Caspases are cysteine proteases that cleave proteins at specific recognition sites, resulting in the formation of discrete low molecular weight protein fragments. This cleavage is different from proteasome-dependent proteolytic cleavage, which is generally associated with a smear-like appearance due to the formation of polyubiquitinated protein adducts, and the complete digestion of proteins. Based on the appearance of discrete low molecular weight species coincident with a reduction in SRC-3 protein expression levels, we questioned whether caspase(s) might also be involved in the degradation of SRC-3. In order to examine this possibility, MCF-7 cells were synchronized in mitosis as above and released from block for 3 hours in the presence or absence of 50 μM Z-VAD, a general caspase inhibitor that irreversibly binds the catalytic site of caspase proteases (Gregoli and Bondurant, 1999). Western blot analysis showed that there was no difference in SRC-3 expression levels between the Z-VAD-treated and control cells following mitotic release (figure 3.5C). Additionally, there was no difference in the number or amount of

low molecular weight immunoreactive species in these samples (figure 3.5C, compare lanes 3 and 4). Moreover, Z-VAD treatment alone did not affect SRC-3 stability or the presence of low molecular weight immunoreactive species (figure 3.5C lane 5). These results are in contrast to the stabilization observed in the MG132-treated cells, suggesting that SRC-3 degradation following mitosis is proteasome-dependent and caspase-independent.

SRC-3 is degraded as cells become quiescent

Since SRC-3 is degraded as cells exit mitosis, we questioned whether cells remain devoid of SRC-3 in quiescence. In order to examine this possibility, SRC-3 protein levels were monitored in MCF-7 cells deprived of serum for 24, 54 and 72 hours. SRC-3 protein levels progressively decreased as cells became quiescent, coincident with the appearance of lower molecular weight species (figure 3.6). This result demonstrates that SRC-3 is degraded and eventually depleted in quiescence.

SRC-3 is modified in G2/M in a MAPK- and Cdk1-dependent manner

Phosphorylation often acts as a signal for targeting proteins for shuttling, ubiquitination or degradation. Previous studies have shown that SRC-3 is phosphorylated by p42 MAPK/ERK1/2, resulting in increased transactivational potential and ability to recruit p300 (Font de Mora and Brown, 2000). We hypothesized that MAPK might also be involved in the modification of SRC-3 in G2/M. To examine this possibility, we treated MCF-7 cells with UO126, a MAPK inhibitor that functions by inhibiting

Figure 3.6. SRC-3 is progressively degraded as MCF-7 cells become quiescent.

Western blot analysis showing SRC-3 protein expression in MCF-7 cells deprived of serum for up to 72 hours. Actin protein expression was used as a loading control.

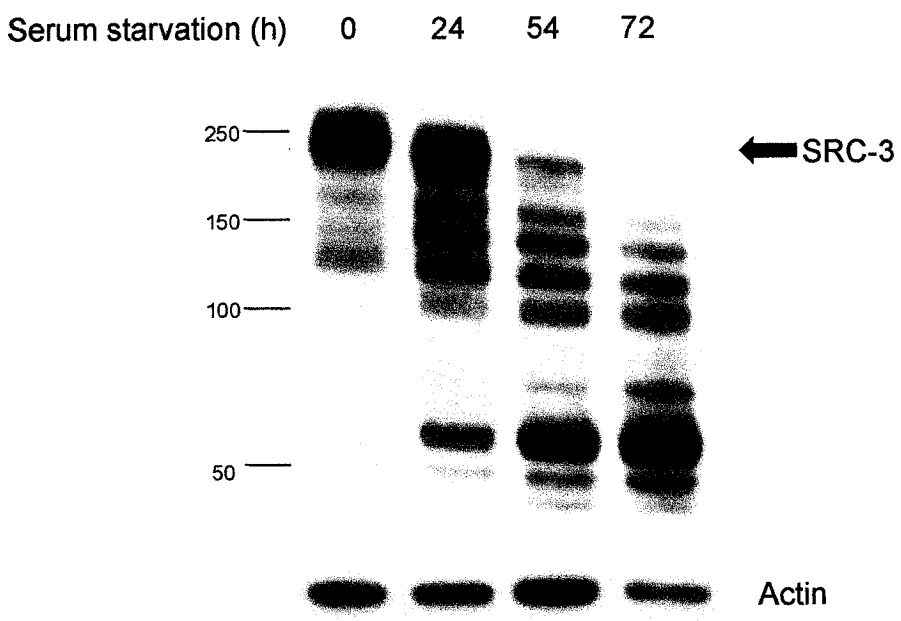
Serum starvation (h)
0
24
54
72
250
150
100
50
SRC-3
Actin

MEK1/2, the MAPK kinase responsible for MAPK activation, prior to and during nocodazole block in mitosis. MAPK activity was monitored using a phospho-MAPK antibody. We also examined cell cycle phase distribution using flow cytometry following UO126 treatment to ensure that the cells were able to progress through G2. Following a 16-hour treatment in nocodazole that blocked cells in G2/M, the modified SRC-3 species appeared (figure 3.7A, lane 1 and figure 3.7B). However, when cells were pretreated with 10 μM UO126 for 3 hours, and then co-treated with nocodazole for 16 hours, a decrease in the amount of modified SRC-3 was observed, coincident with the inactivation of MAPK (figure 3.7A, lane 2). This decrease occurred with minimal effect on the cell cycle, suggesting that the decrease was due to MAPK inhibition and not a reduction in mitotic cells. Thus, SRC-3 is modified in G2/M in a MAPK-dependent manner.

Since SRC-3 modification was only partially inhibited by UO126, we examined the possible involvement of another kinase in this process. Cdk1/cdc2 is a Ser/Thr kinase that is central in regulating mitotic entry and progression. Since Cdk1 activation occurs in late G2/early prophase, we examined its possible contribution to SRC-3 regulation by treating MCF-7 cells with okadaic acid (OA), an inhibitor of the Ser/Thr protein phosphatase 2A (PP2A) (Dinter and Berger, 1998) and activator of Cdk1 (Furukawa *et al*, 2000). Following treatment with 250 nM OA, there was an increase in the molecular weight of SRC-3, suggesting that Cdk1 may be involved in SRC-3 modification (figure 3.8A). OA did not significantly affect the cell cycle during the treatment time (figure 3.8B).

Since the modification of SRC-3 following OA treatment could be attributable to activation of MAPK by inhibition of PP2A (Millward *et al*, 1999), we examined the

Figure 3.7. SRC-3 modification in G2/M is partially MAPK-dependent.

(A) Western blot analysis showing SRC-3 protein expression in MCF-7 cells pretreated with 10 μM UO126 (UO) for 3 hours, and then cotreated with nocodazole (noco) and UO126 for 16 hours. Actin protein expression was used as a loading control. **(B)** Cell cycle phase distribution following nocodazole and UO126 treatments as determined by flow cytometry.

A

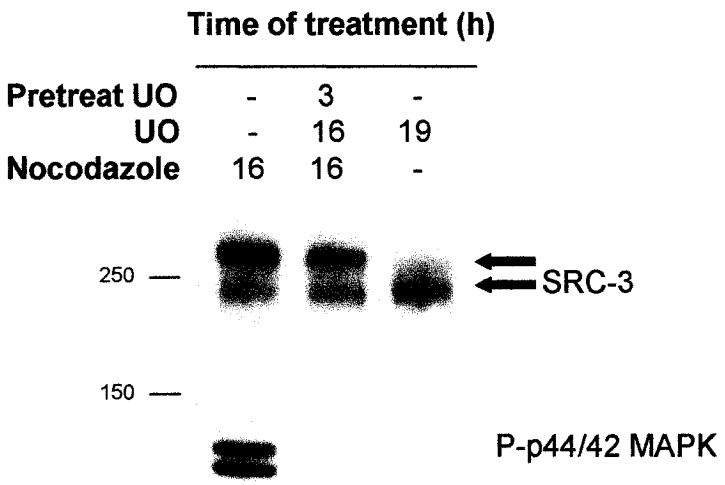
Time of treatment (h)
Pretreat UO - 3 -
UO - 16 19
Nocodazole 16 16 -
250
150
SRC-3
P-p44/42 MAPK

B

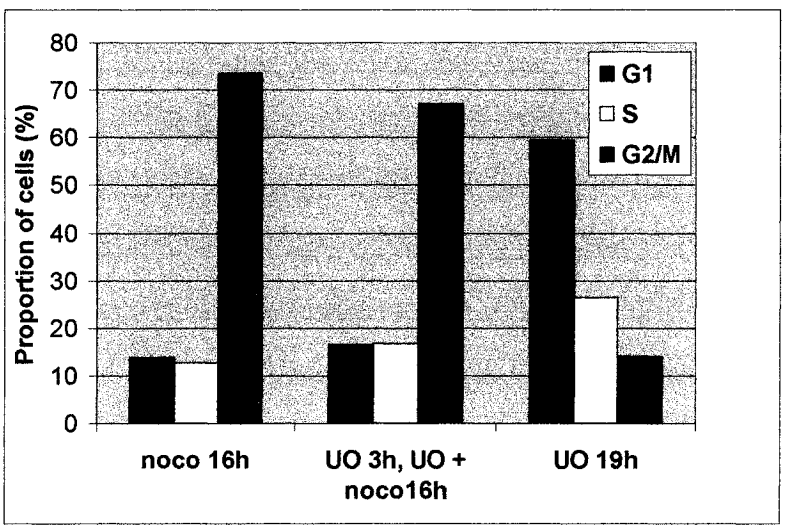
Proportion of cells (%)
80
70
60
50
40
30
20
10
0
G1
S
G2/M
noco 16h
UO 3h, UO + noco16h
UO 19h

Figure 3.8. SRC-3 modification in G2/M is partially Cdk1-dependent.

(A) Western blot analysis showing SRC-3 protein expression in MCF-7 cells treated with 250 nM okadaic acid (OA) for 4 or 16 hours. **(B)** Cell cycle phase distribution following okadaic acid treatment as determined by flow cytometry. **(C)** Western blot analysis showing SRC-3 protein expression in MCF-7 cells pretreated with 10 μM and 20 μM butyrolactone-I (BL-I) for 16h, and then co-treated with nocodazole and BL-I for 12h. Actin protein expression was used as a loading control.

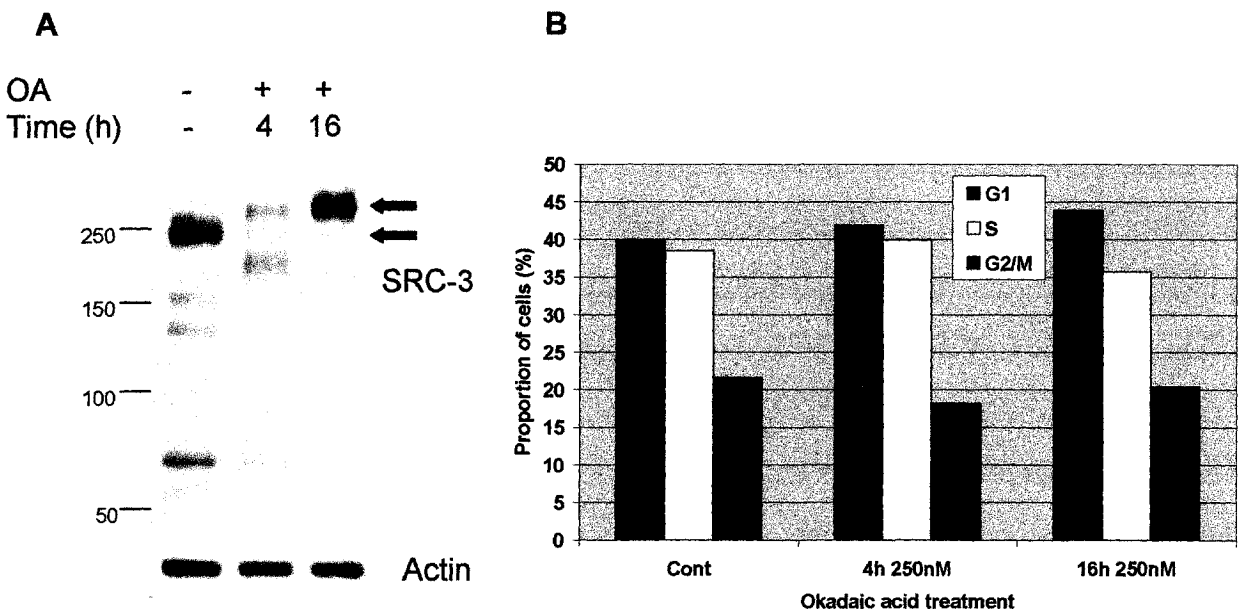
A
OA - + +
Time (h) - 4 16
250
150
100
50
SRC-3
Actin
B
Proportion of cells (%)
50
45
40
35
30
25
20
15
10
5
0
G1
S
G2/M
Cont
4h 250nM
16h 250nM
Okadaic acid treatment

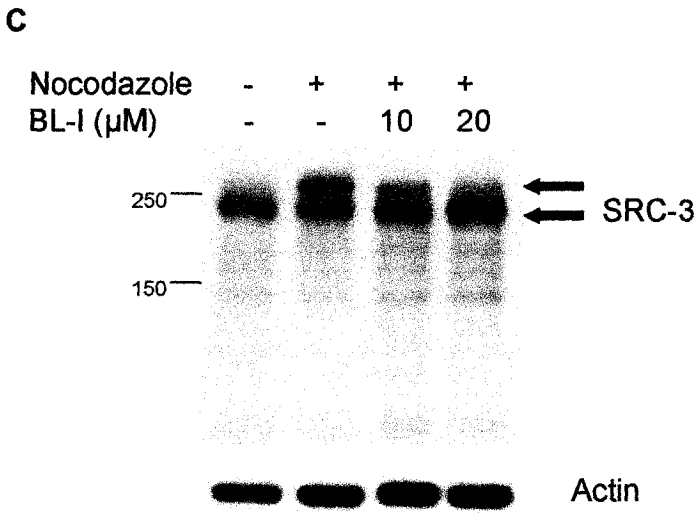
C
Nocodazole - + + +
BL-I (μM) - - 10 20
250
150
SRC-3
Actin

effect of butyrolactone-I (BL-I) treatment on SRC-3 during G2/M. BL-I specifically and potently inhibits Cdk1 activity both *in vivo* and *in vitro* by competing for its binding site (Kitagawa *et al*, 1993). MCF-7 cells were pretreated with increasing doses of BL-I for 16 hours to ensure complete Cdk1 inhibition. The cells were then blocked in mitosis with a 12-hour nocodazole treatment. BL-I prevented the shift in molecular weight of SRC-3 in a dose-dependent manner (figure 3.8C, compare lanes 2, 3 and 4), further implicating Cdk1 involvement in SRC-3 modification.

SRC-3 interacts with Cdk1

The results above suggest that Cdk1 may be directly involved in the modification of SRC-3. To assess whether SRC-3 and Cdk1 interact, we immunoprecipitated endogenous SRC-3 from 900 μg of total protein extracted from asynchronous, G1 (thymidine-blocked) and mitotic (nocodazole-blocked) MCF-7 cells using a polyclonal antibody against GST-AIB1 (SRC-3) (Font de Mora and Brown, 2000). Immunoprecipitates were resolved in an 8% Laemmli gel and visualized with an anti-Cdk1 antibody. Cdk1 interacted with SRC-3, either directly or in a protein complex, in a cell cycle-independent manner (figure 3.9).

In order to determine if Cdk1 could directly phosphorylate SRC-3, we performed a Cdk1 *in vitro* kinase assay using purified Cdk1 (New England Biolabs). SRC-3 was immunoprecipitated with anti-GST-AIB1, dephosphorylated with λ-phosphatase and then incubated in the presence of Cdk1, γ-^{32}P[ATP] and cold ATP. Rabbit serum was used as a control for all the reactions. Immune complexes were resolved in a glycerol gel, stained with coomassie and exposed to film. However, we were unable to detect

Figure 3.9. SRC-3 coimmunoprecipitates with Cdk1.

Immunoprecipitation of SRC-3 from 900 μg of total protein extracted from MCF-7 cells, synchronized in G1 and mitosis or left asynchronous (A/S). Immunoprecipitates were resolved in an 8% Laemmli gel. Membranes were probed with anti-Cdk1 and anti-AIB1 (Transduction Laboratories).

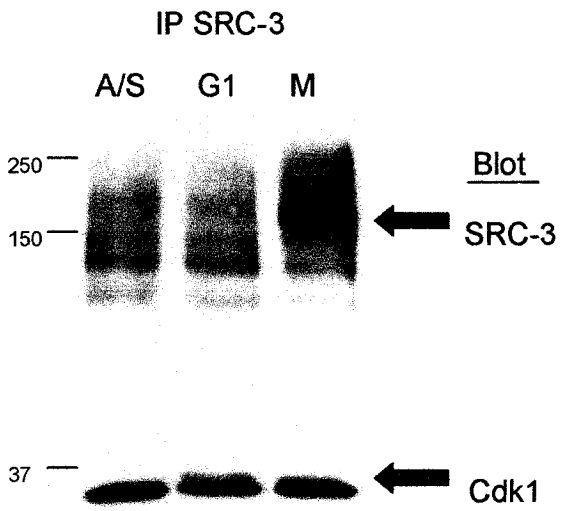
IP SRC-3
A/S
G1
M
250
150
Blot
SRC-3
37
Cdk1

immunoprecipitated SRC-3 (data not shown). In the future, we would like to repeat this experiment with *in vitro* translated SRC-3.

SRC-3 depletion results in shortened G2/M phases and a prolonged G1 phase but does not affect cell cycle arrest or re-entry

Based on the ability of SRC-3 to regulate the transcription factors E2F (Louie *et al*, 2004) and p53 (Lee *et al*, 1999), as well as influence translation through mTOR (Zhou *et al*, 2003), coupled to our own finding that SRC-3 is highly regulated in mitosis, we predicted that deregulation of SRC-3 expression would alter progression through the cell cycle. In order to address this issue, MCF-7 cells were treated with RNAi targeted to a specific sequence within the SRC-3 transcript. Cell cycle phase progression was analyzed by measuring DNA content 28, 50 and 74 hours following transfection, while protein expression levels were monitored to ensure effective depletion. As expected, SRC-3 protein expression was significantly reduced 28 hours after RNAi treatment (figure 3.10A). Depletion was coincident with a slightly prolonged G1 phase and shortened G2/M phases (figure 3.10B), which became increasingly pronounced by 74 hours post transfection. This result can be interpreted in two ways. Firstly, SRC-3 protein could be involved in promotion of G1 progression or G1/S phase transit; accordingly, SRC-3 depletion results in a prolonged G1 phase. Conversely, SRC-3 protein degradation may be involved in the signalling pathways triggering mitotic exit. Consequently, premature SRC-3 depletion may increase the rate of mitotic exit.

In order to determine if SRC-3 depletion also affects the ability of MCF-7 cells to arrest in or re-enter the cell cycle, we depleted SRC-3 as above, synchronized the cells in

Figure 3.10. SRC-3 depletion results in a shortened G2/M phase and prolonged G1 phase but does not affect cell cycle arrest or re-entry following block.

MCF-7 cells transfected with RNAi targeted to a specific sequence within SRC-3. Actin protein expression was used as a loading control. **(A)** Western blot analysis showing SRC-3 protein expression 28, 50 and 74 hours following transfection. **(B)** Cell cycle phase distribution following transfection as determined by flow cytometry. **(C)** Western blot analysis showing SRC-3 protein expression in thymidine-synchronized cells. **(D)** Cell cycle phase progression in thymidine-synchronized cells as determined by flow cytometry. **(E)** Western blot analysis showing SRC-3 protein expression in nocodazole-synchronized cells. Tubulin protein expression was used as a loading control. **(F)** Cell cycle phase distribution in nocodazole-synchronized cells as determined by flow cytometry.

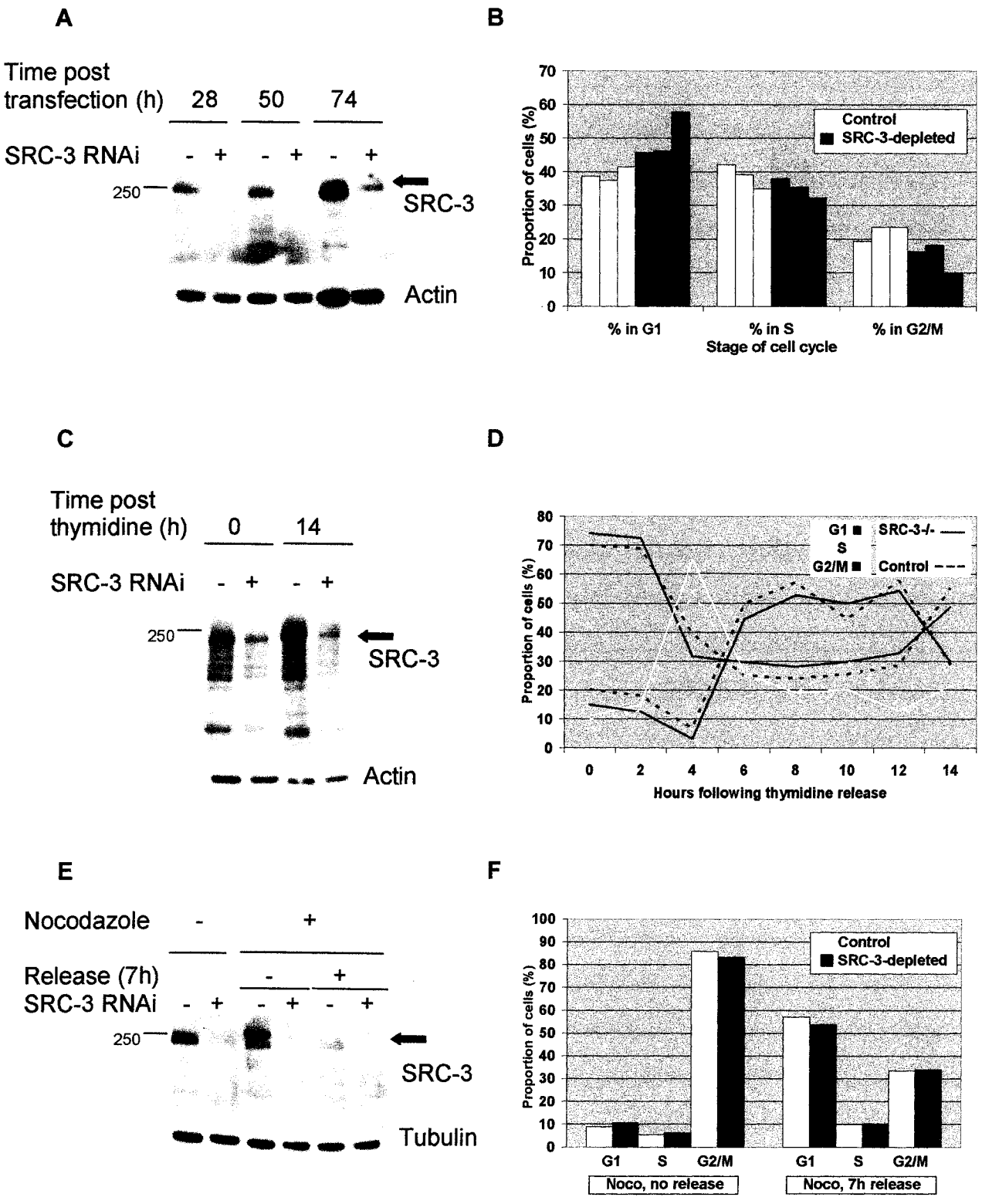
A
Time post transfection (h)
28
50
74
SRC-3 RNAi
- + - + - +
250
SRC-3
Actin
B
Proportion of cells (%)
Control
SRC-3-depleted
% in G1
% in S
% in G2/M
Stage of cell cycle
C
Time post thymidine (h)
0
14
SRC-3 RNAi
- + - +
250
SRC-3
Actin
D
Proportion of cells (%)
G1
S
G2/M
SRC-3-/-
Control
Hours following thymidine release
E
Nocodazole
-
+
Release (7h)
SRC-3 RNAi
- + - + - +
250
SRC-3
Tubulin
F
Proportion of cells (%)
Control
SRC-3-depleted
G1
S
G2/M
Noco, no release
Noco, 7h release

G1 with a double thymidine block and monitored cell cycle progression every two hours following release using flow cytometry. Downregulation of SRC-3 protein did not affect the proportion of cells arrested in G1, or re-entry into and progression through the cell cycle (figure 3.10C and D). Similarly, SRC-3 depletion did not affect mitotic arrest by nocodazole or subsequent re-entry into the cell cycle (figure 3.10E and F). These results suggest that acute SRC-3 depletion does not affect induced cell cycle arrest or re-entry into, and short-term progression, through the cell cycle following arrest.

SRC-3 overexpression decreases growth rate, disrupts cell morphology and cell cycle progression and leads to aneuploidy

In order to further examine the consequences of deregulated SRC-3 expression, we established cells stably overexpressing SRC-3. To this end, MCF-7 cells were co-transfected with FLAG-tagged full-length SRC-3 and a selection vector that confers puromycin resistance. Control cells were co-transfected with pcDNA3 and the same puromycin resistance vector. Cells were cultured in the presence of puromycin for the selection of stable clones. Resistant colonies were selected for expansion and passaged an average of 3-4 times prior to assaying for protein expression by immunoblotting. Four individual sets of clones that expressed high levels of SRC-3 protein (clones 2, 7, 13 and 14) were pooled for further analysis (figure 3.11A).

SRC-3 stable clones grew at a distinctly slower rate than their control counterparts. In order to quantify this observation, a clonogenic assay was performed. Control and stable cells were seeded in triplicate at a very low density ($5x10^3$ cells/ 60mm plate) and cultured for 8 days. Following the growth period, one plate from each

Figure 3.11. SRC-3 overexpression decreases the rate of MCF-7 cell proliferation.

(A) Western blot analysis of SRC-3 protein expression in MCF-7 cells transfected with pCMX-RAC3 (SRC-3) selected for puromycin resistance. Control cells were transfected with pcDNA3. Clones 2, 7, 13 and 14 (indicated with arrows) were pooled for further analysis. **(B)** Clonogenicity assay of SRC-3-overexpressing versus control cells. Cell population was determined by trypsinization and enumeration of viable cells. **(C)** Clonogenicity assay of SRC-3 versus control cells. Foci formation was measured following cresyl blue staining (n=2). **(D)** Western blot analysis of SRC-3 protein expression in stable clones after several passages. Tubulin protein expression was used as a loading control.

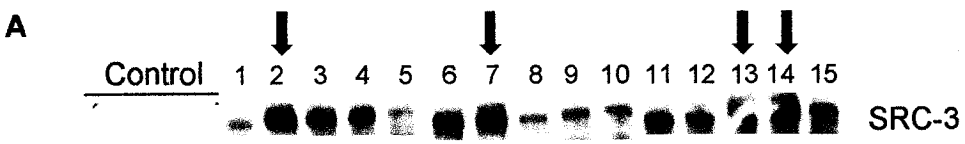
A
Control
1 2 3 4 5 6 7 8 9 10 11 12 13 14 15
SRC-3

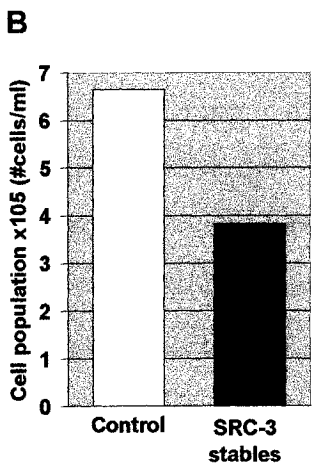
B
Cell population x105 (#cells/ml)
0 1 2 3 4 5 6 7
Control
SRC-3 stables

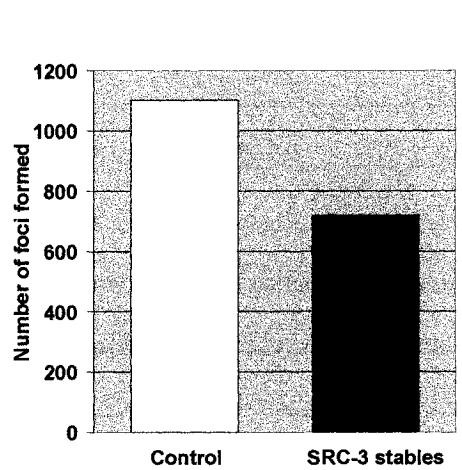
C
Number of foci formed
0 200 400 600 800 1000 1200
Control
SRC-3 stables

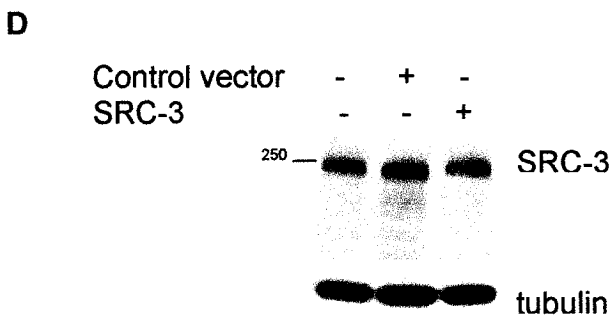
D
Control vector - + -
SRC-3 - - +
250
SRC-3
tubulin

triplicate was used to determine the cell population by trypsinization and enumeration of viable cells. The other 2 plates of cells were fixed and stained with 2% cresyl violet for enumeration of foci formation. The number of cells that failed to survive plating appeared to be similar between the control and SRC-3 clones (i.e. there were similar amounts of dead, floating cells in both sets of plates), suggesting that the plating efficiency of SRC-3 stable clones and control clones was similar. However, the number of viable cells was significantly reduced in the SRC-3 samples. Specifically, there were 42% fewer cells and 35% fewer foci on the SRC-3 plates than on the empty vector control plates (figures 3.11 B and C). These results suggest that SRC-3 overexpression decreases the growth rate of MCF-7 cells.

Although the stable clones originally expressed high levels of SRC-3, they lost their ability to overexpress this protein after five to six passages, even while maintained in puromycin-supplemented media (figure 3.11D). Additionally, HeLa and COS-7 cells transfected in the same manner as the MCF-7 cells failed to overexpress SRC-3 (data not shown). Furthermore, although numerous puromycin-resistant MCF-7 colonies were selected, many did not survive the expansion process. These results suggest that constitutive high levels of SRC-3 may prevent proliferation and/or be toxic to cells.

Colonies were originally picked when they reached the approximate size of the microscope field using a 10X magnification lens. We questioned whether this method was selecting against phenotypic changes present in the slower growing clones whose colonies did not reach the size of the microscope field, and consequently, were not picked. In order to address this issue, we repeated the cotransfection with a different method of colony selection. Previous reports have demonstrated that SRC-3 stable clones

have distinct morphological changes such as increased cell size with abundant cytoplasm (Anzick *et al*, 2003; Zhou *et al*, 2003). We therefore categorized the colonies according to the size of the average cell within the colony (small, medium or large) prior to selection and expansion. In addition, colonies of various sizes and densities were selected.

As in the first transfection, there was a substantial variety in the growth rates of the individual clones and although numerous colonies were selected, many failed to survive the selection process. Interestingly, the rate of proliferation was inversely proportional to the size of the clones; accordingly, cells categorized as large failed to survive passaging.

Resistant colonies were assayed for SRC-3 protein expression in an 8% Laemmli gel. S6K1 activity was also assessed using a phospho-S6K1 antibody since previous reports demonstrated that the Akt/PI3K/mTOR pathway is activated in SRC-3 overexpressing cells (Zhou *et al*, 2003). In agreement with previous studies (Dr. Don Chen, personal communication), exogenous SRC-3 was undetectable using a FLAG-specific antibody (data not shown), but SRC-3 was detectable using a SRC-3-specific antibody (figure 3.12). Additionally, several clones had increased Akt/PI3K/mTOR activity, as demonstrated by the phospho-S6K1 antibody. However, this activity was not strictly correlated with SRC-3 protein expression.

SRC-3 stable transfectants possessed a variety of phenotypic alterations in their morphology that were more noticeable in the large-sized cells; thus, clones categorized as small-sized appeared to be in a transitional state between control and medium-sized clones (compare figure 3.13 A, B and C). The most obvious change in morphology was

Figure 3.12. Establishment of SRC-3-overexpressing MCF-7 cells.

Western blot analysis showing SRC-3 protein expression in MCF-7 cells transfected with pCMX-RAC3 (SRC-3) or pcDNA3 and selected for puromycin resistance. SRC-3 stable cells were categorized according to the size of the average cell within a colony prior to expansion. Small and medium SRC-3 clones are labelled. Proteins were resolved in an 8% Laemmli gel. S6K1 activity was determined using a phospho-S6K1 (P-S6K1) antibody.

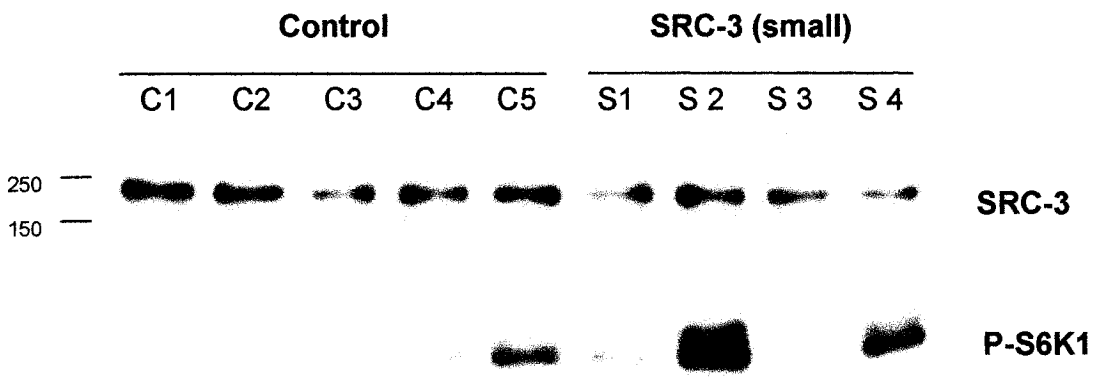
Control
SRC-3 (small)
C1
C2
C3
C4
C5
S1
S 2
S 3
S 4
250
150
SRC-3
P-S6K1

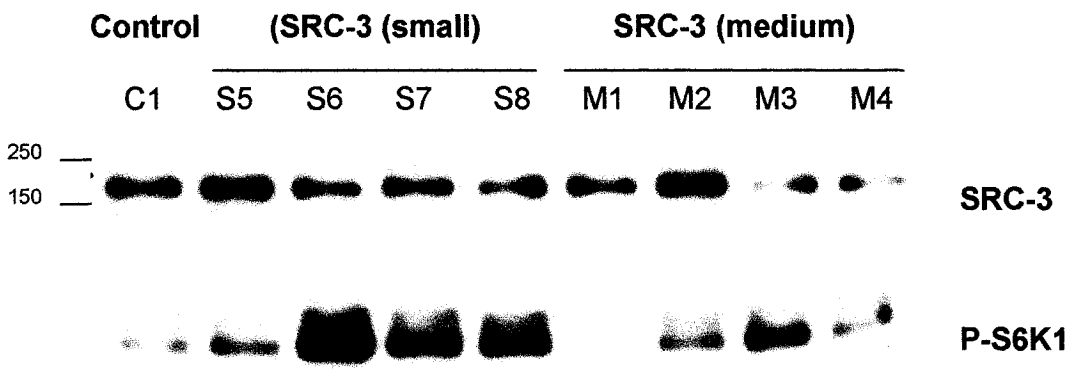
Control
(SRC-3 (small)
SRC-3 (medium)
C1
S5
S6
S7
S8
M1
M2
M3
M4
250
150
SRC-3
P-S6K1

Figure 3.13. SRC-3 overexpression disrupts cell morphology.

Phase contrast photographs of control pcDNA3- and pCMX-RAC3- (SRC-3) transfected MCF-7 cells. SRC-3 stable cells were categorized according to the size of the average cell within a colony prior to expansion. **(A)** Control clones. **(B)** Small SRC-3-overexpressing clones had a similar morphology to control cells. **(C)** Medium SRC-3-overexpressing clones were large and flat with abundant cytoplasm and multiple nuclei (red arrows) or large nuclei (panels i-iii); or spindly with reduced cell-cell contacts (panels iv-vi).

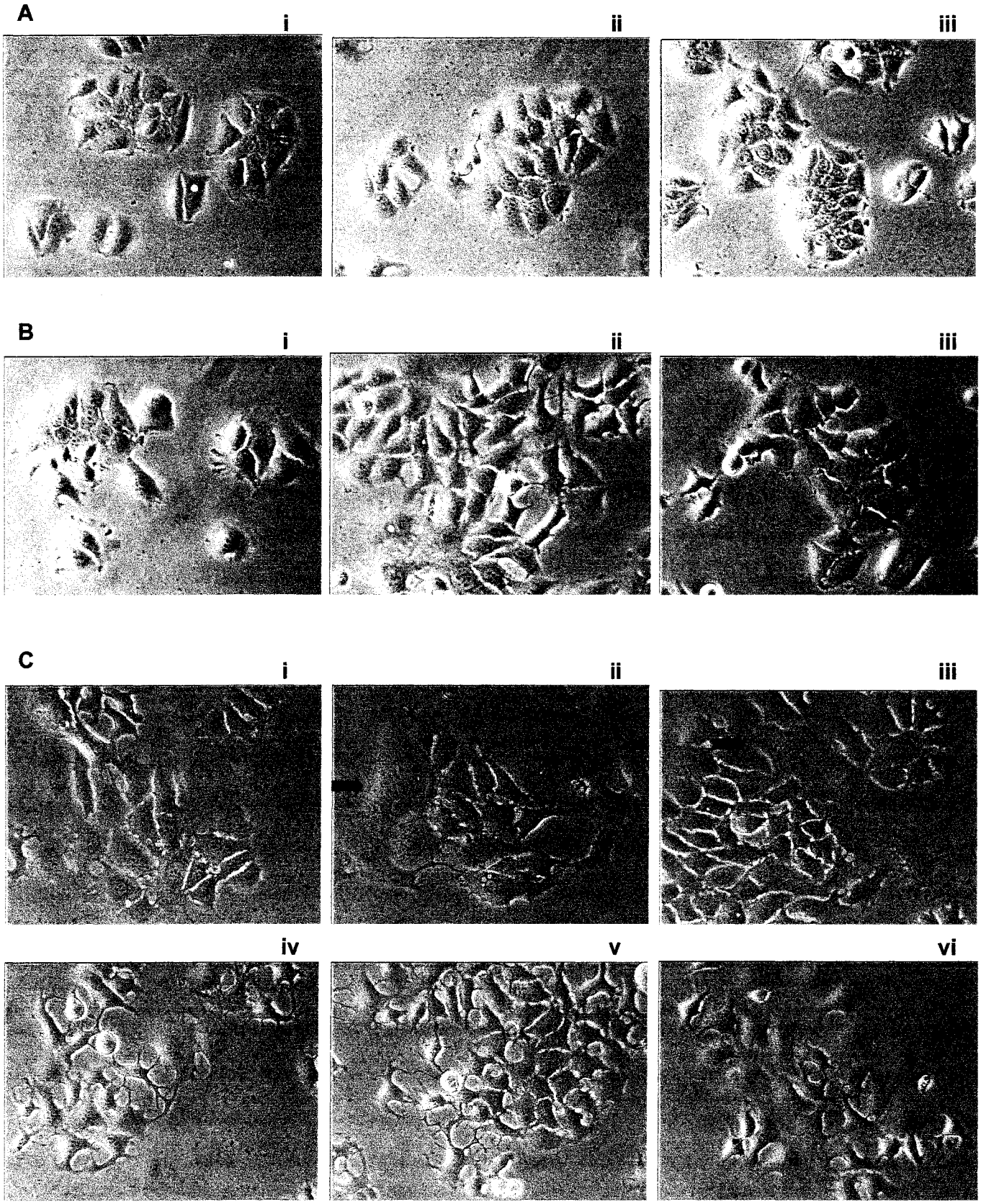
A
i
ii
iii
B
i
ii
iii
C
i
ii
iii
iv
v
vi

the prevalence of very large, flat cells with abundant cytoplasm and large nuclei (figure 3.13C i, ii and iii). Additionally, many of the SRC-3 clones were multinucleated. Another common morphological change was a spindly cell shape characterized by long, thin, dendrite-like processes and small cell bodies (figure 3.13C iv, v and vi). These cells also grew more loosely with fewer cell-cell contacts than control cells.

Replicative senescence is a state of irreversible arrested growth and proliferation. It is thought to occur as a protective mechanism against tumour growth (Dimri *et al*, 1995). One of the most easily distinguishable traits of senescent cells is an alteration in cellular morphology, usually involving a flattened shape and extensive cytoplasm. Since these characteristics were observed in our stable clones, we questioned whether SRC-3 overexpression could be inducing senescence in this population. In order to examine this possibility, we performed SA-ß-gal staining, which identifies senescent cells by their unique ability to express ß-galactosidase at a pH of 6.0 (Dimri *et al*, 1995). SRC-3 overexpressing cells and pcDNA3 control cells were fixed in formaldehyde and stained overnight in SA-ß-gal staining solution. Positive cells stained blue. However, we were unable to detect differences in the number of positive SRC-3 stable and pcDNA3 control cells (data not shown). This result suggests that SRC-3 overexpressing cells are not senescent.

Based on our depletion studies, we predicted that SRC-3 overexpression would also alter progression through the cell cycle. In order to address this issue, a number of SRC-3 stable clones were analyzed using flow cytometry. Predictably, some of the SRC-3 stable clones had dramatically altered S and G2/M phases (figure 3.14A). This trend was more pronounced in medium-sized clones than small-sized SRC-3 clones.

Figure 3.14. SRC-3 overexpressing cells display cell cycle deregulation and alteration of DNA contents.

Graphs of flow cytometry analysis from control pcDNA3- and pCMX-RAC3- (SRC-3) transfected MCF-7 cells. SRC-3 clones were categorized as small-sized or medium-sized prior to expansion. **(A)** Cell cycle phase distributions in control, SRC-3 small-sized and medium-sized clones. **(B)** Mean G1 (2N) and G2 (4N) DNA contents in control, SRC-3 small-sized and medium-sized clones. **(C)** Examples of DNA content graphs of several clones. Clones are identified by their clone number. **i)** Control pcDNA3 cells. **ii)** Small-sized SRC-3 transfected clones. S1 weakly expressed and S5 strongly expressed SRC-3. **iii)** Medium-sized SRC-3 clones. M3 weakly expressed and M2 strongly expressed SRC-3. *(SD of mean: (A) pcDNA control n = 4, SRC-3 small n = 15, SRC-3 medium n = 4; (B) pcDNA control n = 4, SRC-3 small n = 6, SRC-3 medium n = 3).*

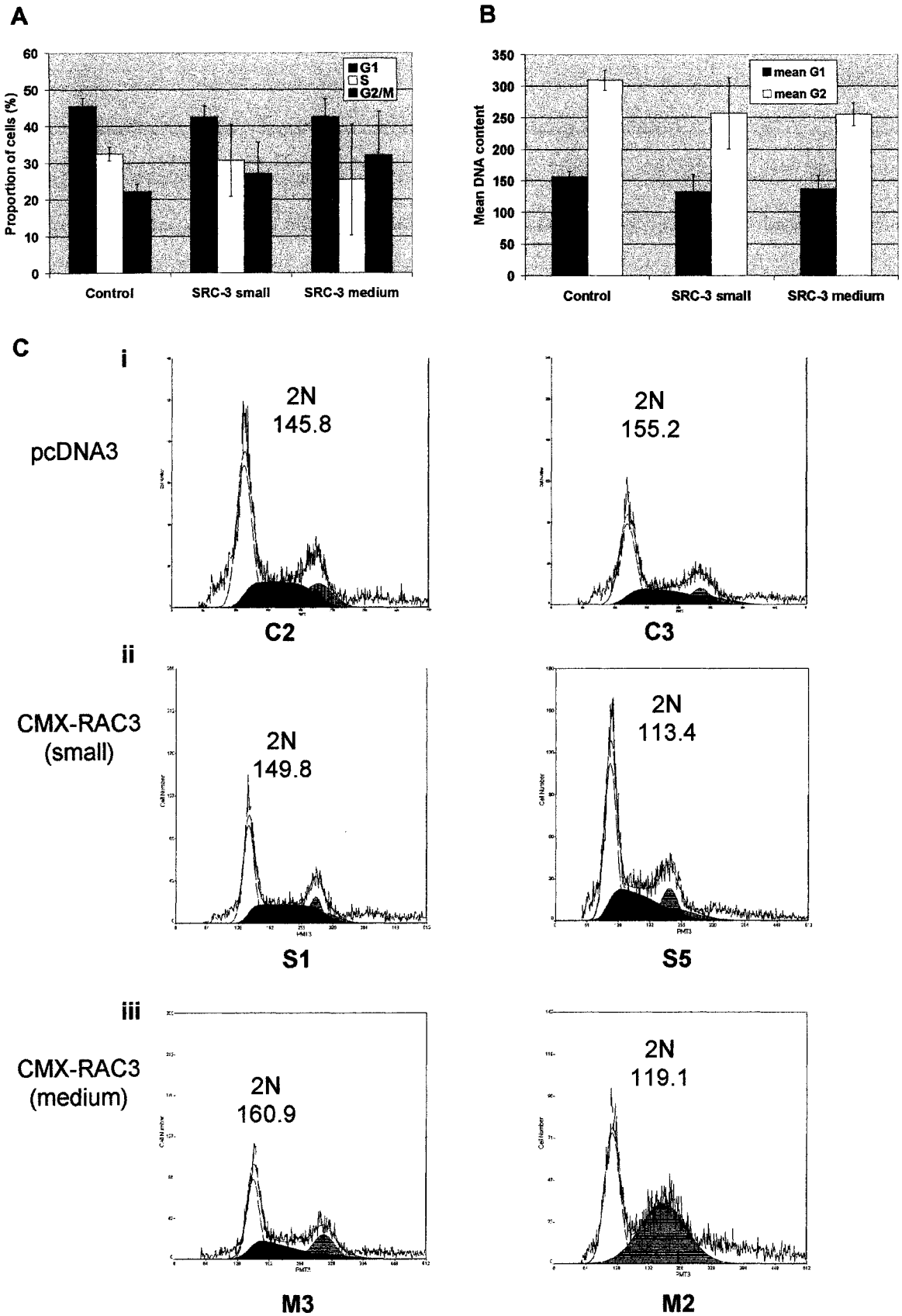
A
Proportion of cells (%)
60
50
40
30
20
10
0
G1
S
G2/M
Control
SRC-3 small
SRC-3 medium
B
Mean DNA content
350
300
250
200
150
100
50
0
mean G1
mean G2
Control
SRC-3 small
SRC-3 medium
C
i
pcDNA3
2N
145.8
C2
2N
155.2
C3
ii
CMX-RAC3
(small)
2N
149.8
S1
2N
113.4
S5
iii
CMX-RAC3
(medium)
2N
160.9
M3
2N
119.1
M2

Additionally, the mean G1/2N/diploid and G2/4N/replicated DNA contents were determined. These values indicate the total amount of DNA contained in the 46 chromosomes of a quiescent or G1 somatic cell, and the 92 replicated chromatids of a G2 or mitotic somatic cell, respectively. The mean 2N and 4N DNA contents of the small-sized and medium-sized clones were decreased compared to those of the control clones (figure 3.14B), suggesting that SRC-3 overexpression resulted in the loss of whole or parts of chromosomes. Loss of DNA might be due to aberrant mitosis, leading to aneuploidy.

Since DNA loss occurs in a random manner in a given clone, there was a significant variation in DNA content amongst the different clones. This variation accounts for the large standard deviations observed when the clones were grouped together (figure 3.14A and B). In order to avoid this variation in values, several clones were analyzed individually. pcDNA3 control cells had typical cell cycle phase distributions and similar mean 2N DNA contents (figure 3.14C i). In contrast, the small-sized SRC-3 clone S5, which overexpressed SRC-3, had a decreased 2N mean DNA content and an increased population of early S phase cells compared to clone S1, which only weakly expressed SRC-3 (figures 3.12 and 3.14C ii). Medium-sized SRC-3 clones had the most significant alterations in DNA content profiles. Clone M2, which overexpressed SRC-3, had a decreased mean 2N DNA content compared to clone M3, which only weakly expressed this protein. It also had a significantly altered cell cycle phase distribution, with a virtual merge of the S and G2/M phases. The decrease in mean 2N DNA content in the SRC-3 clones reflects a loss of DNA, which is likely due to aneuploidy. In contrast, the increase in the proportion of cells with greater than 2N but

less than 4N (>2N<4N) DNA contents may be due to an increase in proliferating (S phase) cells, an S phase block or nascent aneuploidy. Thus, it appears that cells that lose the ability to overexpress SRC-3 quickly, such as clones S1 and M3, are less prone to severe losses in DNA or cell cycle disruptions than cells that continue to overexpress this protein.

Cell cycle-dependent degradation of SRC-3 is independent of ER activity in MCF-7 cells

All our experiments were performed in estrogenic conditions, which resulted in SRC-3 degradation after G2/M release. Efforts to maintain high-levels of SRC-3 expression in stable transfectants were unsuccessful. We therefore hypothesized that estrogen may affect the turnover of SRC-3. Consequently, ER-antagonists may prevent SRC-3 degradation, resulting in stabilization of SRC-3 and subsequent cytotoxicity. In order to test this hypothesis, MCF-7 cells were synchronized in mitosis with nocodazole. During the last 8 hours of nocodazole treatment and throughout the release period, the ER antagonists tamoxifen (10^{-6} M), raloxifene (10^{-6} M) and ICI 182,780 (10^{-7} M) were added. SRC-3 protein levels were examined by immunoblotting. The results show that the higher molecular weight species of SRC-3 was not stabilized by addition of the ER antagonists (figure 3.15). This suggests that E2 signalling is not involved in the cell cycle-dependent degradation of SRC-3.

Figure 3.15. The modified form of SRC-3 is not stabilized by SERM treatment.

Western blot analysis showing SRC-3 protein expression in nocodazole-synchronized MCF-7 cells released from arrest in the presence or absence of the SERMs tamoxifen (TAM, 10^{-6} M), raloxifene (RAL, 10^{-6} M) or ICI 182,780 (ICI, 10^{-7} M). Cells were harvested 0, 2, 4 and 6 hours following nocodazole release.

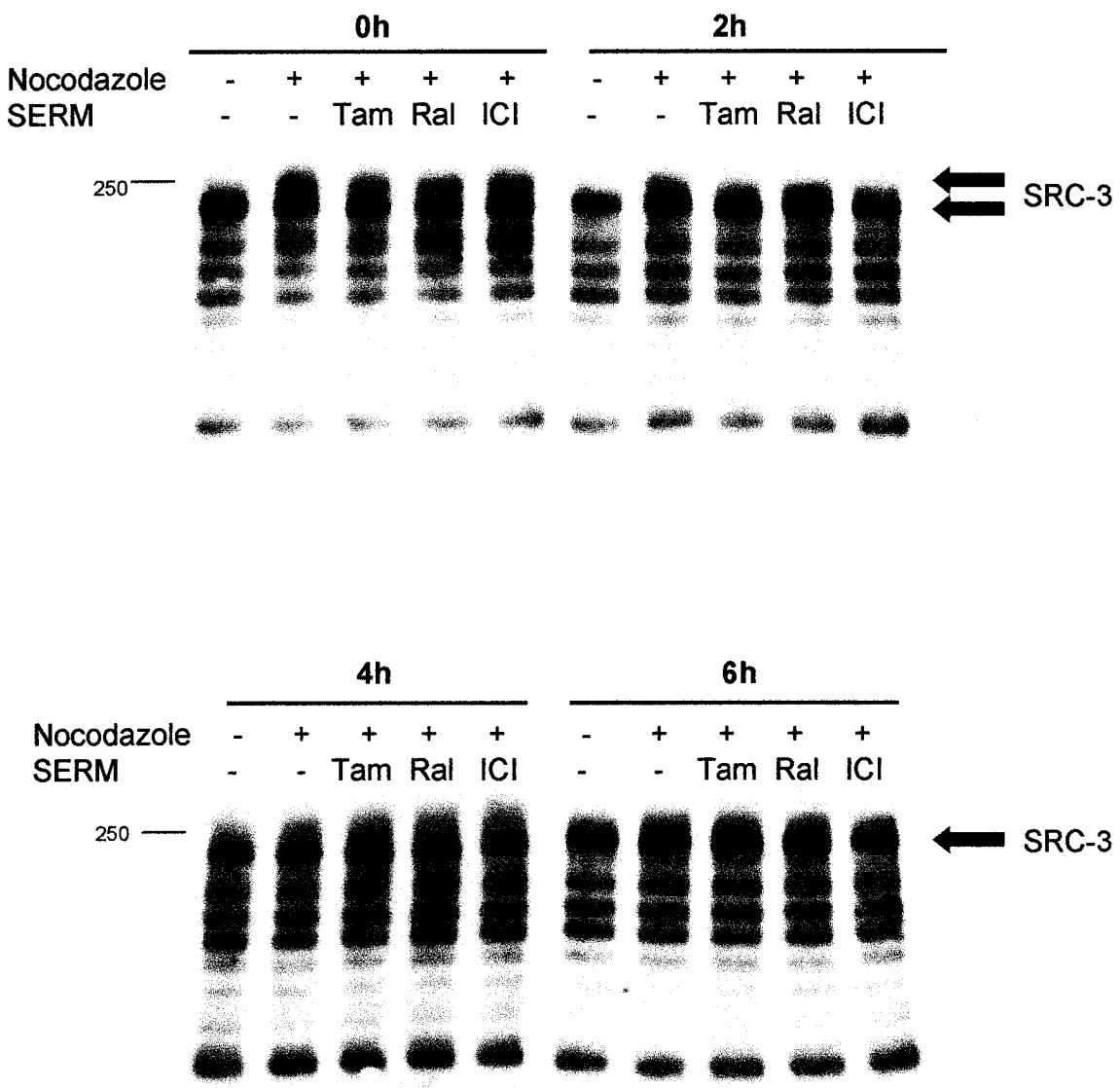
0h
2h
Nocodazole - + + + + - + + + +
SERM - - Tam Ral ICI - - Tam Ral ICI
250
SRC-3
4h
6h
Nocodazole - + + + + - + + + +
SERM - - Tam Ral ICI - - Tam Ral ICI
250
SRC-3

DISCUSSION

Summary

It has been shown that SRC-3 activity is regulated by post-translational modifications such as phosphorylation and ubiquitination, and by subcellular compartmentalization (Font de Mora *et al*, 2000; Wu *et al*, 2002; Yan *et al*, 2003; Wu *et al*, 2004; Qutob *et al*, 2002). Additionally, it has been suggested that SRC-3 plays a role in promotion of S phase transit as an E2F coactivator (Louie *et al*, 2004). However, to our knowledge, no one has established the cell cycle-dependent regulation of SRC-3. Our initial findings suggested that SRC-3 is stabilized during interphase and modified during late G2/M of the cell cycle. Thus, we postulated that SRC-3 is differentially regulated during the cell cycle and could play a role in normal cell cycle events. In the present study, we report that SRC-3 protein is indeed regulated during mitosis in a Cdk1-, proteasome- and partial MAPK-dependent manner. Furthermore, aberrant SRC-3 expression results in decreased cellular growth rates, abnormal cell morphology, deregulated cell cycle progression and loss of DNA content. Collectively, our results suggest that SRC-3 plays a crucial role in normal cell cycle progression, and that deregulated SRC-3 expression has catastrophic effects on cellular viability.

SRC-3 PROTEIN IS DYNAMICALLY REGULATED THROUGHOUT THE CELL CYCLE

Modification of SRC-3 in mitotic cells

We have studied the regulation of SRC-3 protein expression throughout the cell cycle. Our most commonly used system for Western blot analysis was a highly porous SDS gel containing glycerol (Doucet *et al*, 1990). Originally designed to preserve the enzymatic activity of proteins following electrophoresis, the glycerol gel helps maintain the native structure of proteins. Consequently, the apparent molecular weight of proteins resolved in this gel reflects both their secondary and tertiary structures, and their molecular weight. The SRC-3 band that we detected in this gel appeared slightly larger than the predicted 160 kDa size quoted in the literature, with an apparent molecular weight of approximately 200 kDa. This gel system also allowed us to visualize the modified form of SRC-3, which was not readily identifiable in the regular Laemmli SDS gel (data not shown). Since the Laemmli gel denatures proteins more completely than the glycerol gel, this finding suggests that the observed shift in SRC-3 molecular weight was at least partially due to a conformational change triggered by modification.

Our data demonstrates that SRC-3 protein is stabilized as MCF-7 cells progress through G2, and is modified in G2/M. Immunocytochemical analysis of cells arrested in mitosis clearly showed that SRC-3 protein expression was increased in these cells compared to those arrested in late G1 (figure 3.1). Western blot analysis of synchronized MCF-7 cells showed a transient modification of SRC-3 in mitosis (figure 3.2). Additionally, a transient decrease in SRC-3 protein expression followed modification,

suggesting that SRC-3 is degraded as cells end and/or exit mitosis. To support this hypothesis, there was also an increase in the number and amount of lower molecular weight immunoreactive species following SRC-3 disappearance, suggesting that these species represented partially degraded forms of SRC-3. Moreover, the proteasome inhibitor MG132 stabilized both the modified and regular forms of SRC-3 following mitotic release in both MCF-7 and MCF-10A cells, and decreased the number and amount of lower molecular weight species present in these samples (figure 3.5A). Taken together, the results suggest that SRC-3 is degraded in a proteasome-dependent manner following modification in mitosis.

Since proteins are targeted to the proteasome by ubiquitination, we hypothesized that SRC-3 was ubiquitinated in mitosis. In order to directly show this ubiquitination, we attempted to immunoprecipitate SRC-3 conjugated to ubiquitin molecules. We used several different immunoprecipitations in synchronous and asynchronous cells to accomplish this task, including immunoprecipitating endogenous SRC-3; exogenous SRC-3; exogenous SRC-3 in ubiquitin-cotransfected cells; exogenous SRC-3 in MG132-treated cells; and coimmunoprecipitating SRC-3 with ubiquitin or anti-His_6 antibodies in His_6-ubiquitin-transfected cells. In general, we were unable to immunoprecipitate ubiquitinated SRC-3 with SRC-3-specific antibodies. However, this was not unexpected since it is often difficult to detect ubiquitinated proteins *in vivo* due to the rapid activity of DUBs and the proteasome (Sheaff *et al*, 2000). For instance, Mizrahi and Moore (2000) showed that ubiquitinated endogenous Pap1, the poly(A) polymerase of *S. cerevisiae*, could not be detected with Pap1 antibody. Additionally, ubiquitinated forms of exogenous Pap1 could only be detected with HA antibodies following cotransfection with

HA-tagged ubiquitin, and not a Pap1 antibody. The authors postulated that the ubiquitinated Pap1 species were not abundant and therefore could not be detected by a Pap1-specific antibody. However, multiple HA-tagged ubiquitin adducts were present on each Pap1 molecule, resulting in a significantly amplified signal detectable by HA-specific antibodies. Similarly, we were able to detect ubiquitinated SRC-3 species using an anti-His_6 antibody in SRC-3- and His_6-ubiquitin-cotransfected cells (figure 3.5B).

It is also possible that we were unable to detect ubiquitinated SRC-3 because the ubiquitin molecules interfered with the ability of the SRC-3-specific antibody to recognize its epitope. Since the glycerol gel partially retains the native structure of proteins, it is possible that the epitope was hidden from the antibody due to the conformation of the protein following ubiquitination. In order to examine this possibility, the immunoprecipitates should be resolved on a Laemmli gel which more completely denatures proteins.

Because we consistently observed numerous discrete low molecular weight immunoreactive SRC-3 species following SRC-3 disappearance, we thought it was possible that caspase(s) might be responsible for SRC-3 degradation. Caspases cleave proteins at specific cysteinyl aspartate recognition sites, resulting in the production of discrete protein fragments. In addition to their role in apoptosis, caspases also function in cellular proliferation and differentiation (reviewed in Schwerk and Schulze-Osthoff, 2003). For example, caspases target several cell cycle inhibitors including Wee1, a protein kinase that mediates the inhibitory phosphorylation of Cdk1. Cleavage of Wee1 inhibits its activity, ultimately leading to cell cycle progression.

When cells were released from nocodazole arrest in the presence of Z-VAD, a general caspase inhibitor, there was no change in the number or amount of lower molecular weight species observed compared to control cells (figure 3.5C). Additionally, Z-VAD treatment alone had no effect on SRC-3 stability or the number and intensity of the lower molecular weight species. In contrast, proteasome inhibition both stabilized SRC-3 and reduced the intensity and number of low molecular weight immunoreactive species following release from nocodazole arrest (figure 3.5A). Thus, it appears that caspases are not involved in SRC-3 degradation during mitotic exit. Nevertheless, it would be interesting to confirm these results in serum-deprived cells by treating them with Z-VAD or MG132 as they become quiescent, to determine if SRC-3 can also be stabilized under these conditions.

It is noteworthy that Yan *et al* (2003) have shown that SRC-3 is ubiquitinated in COS-7 cells predominantly via the aid of the conjugating enzymes UBC2, UBC3, UBC4 and UBC5. In addition, SRC-3 sequence analysis revealed that it contains a potential PEST site, a polypeptide sequence associated with promotion of protein turnover, between amino acids 647–674 (Rechsteiner, 1990). The most logical candidate for ubiquitination of SRC-3 is the APC, since it targets proteins for degradation as cells exit mitosis (Murray, 2004). Our analysis of the SRC-3 protein sequence did not reveal any destruction or KEN boxes, the recognition sites associated with APC-mediated-degradation. However, this deficiency does not exclude SRC-3 as an APC substrate, since it is possible that additional, hitherto unknown APC recognition sites exist. For example, a new consensus sequence called the A box was recently described for the mitotic kinase Aurora-A (Littlepage and Ruderman, 2002). In order to examine the

possible contribution of APC in SRC-3 ubiquitination, an *in vitro* ubiquitination assay with [^{35}S]methionine-labelled SRC-3 in the presence of ubiquitin, E1 and APC could be performed (described in Yan *et al*, 2003). Conversely, another possible contributor to SRC-3 ubiquitination is hHR6A, the human homologue of UBC2, which is most active in G2/M of the cell cycle (Sarcevic *et al*., 2002). Since UBC2 has the ability to ubiquitinate SRC-3, it may also be a possible candidate for SRC-3 ubiquitination in mitosis.

Since all our experiments were performed in estrogenic conditions, we wondered whether estrogen was playing a role in the degradation of SRC-3 following mitosis, and consequently, if ER-antagonists could stabilize SRC-3 protein. We tested this theory by releasing MCF-7 cells from nocodazole-induced mitotic arrest in the presence of the ER antagonists tamoxifen, raloxifene or ICI 182,780. The modified form of SRC-3 was not stabilized by ER inhibition, suggesting that SRC-3 degradation occurs independently of ER activity (figure 3.15). Consistent with this result, we observed the mitotic regulation of SRC-3 protein in the hormone-independent COS-7 cell line (data not shown). Thus, it is unlikely that E2 signalling is involved in the cell cycle-dependent degradation of SRC-3.

Subcellular localization of SRC-3 during the cell cycle

In order to further examine the cell cycle-dependent regulation of SRC-3, we analyzed its localization throughout the cell cycle. We found that endogenous SRC-3 protein undergoes cyclical nuclear/cytoplasmic shuttling. Using immunocytochemistry, we showed that SRC-3 was predominantly localized in the nucleus throughout interphase and was dissociated from DNA during mitosis (figure 3.4). The change is localization

occurred at the onset of prophase, when SRC-3 expression became increasingly punctate and began to appear in the cytoplasm. By mid prophase, it was predominantly cytoplasmic with a significant fraction of protein localized in a punctate, circular pattern around the nucleus. This finding raises the possibility that SRC-3 associates with, and is exported by, a nuclear pore complex at the onset of prophase. Consistent with this notion, Qutob *et al* (2002) showed that SRC-3 can be transported in a CRM-1/exportin1 receptor-dependent manner, and that it contains a nuclear localization signal and a nuclear export signal. CRM-1 mediates the rapid transport of many regulatory proteins to the cytoplasm such as kinases and cell cycle proteins, as well as the SRC family member SRC-1 (Amazit *et al*, 2003). Thus, it is possible that SRC-3 is exported from the nucleus during prophase in a CRM-1-dependent manner.

Conversely, it is possible that SRC-3 was not transported to the cytoplasm at the onset of prophase but rather diffused out of the nucleus following NE disassembly. However, this scenario is unlikely since the NE does not fragment until late prophase/prometaphase (Georgatos *et al*, 1997) and SRC-3 was detected in the cytoplasm during early and mid prophase. In order to control for this possibility, the cells should be co-stained with a NE marker such as lamin A, whose release into the cytoplasm does not occur until NE breakdown in late prophase/prometaphase.

SRC-3 protein remained dissociated from DNA throughout the remainder of mitosis and cytokinesis. Strikingly, when the cytoplasm had been partitioned between the daughter cells but DNA was still in the process of decondensing, SRC-3 very rapidly accumulated in the nucleus, suggesting that a transport mechanism was involved. This hypothesis is supported by the timing of import, which coincides with sealing of the NE

in late telophase and assembly of the integral nucleoporin gp210, which leads to the onset of nucleoporin complex function and the rapid, active, nucleocytoplasmic transport of proteins (Buendia *et al*, 2001).

Qutob *et al* (2002) also observed differential compartmentalization of SRC-3 in HeLa cells using a p/CIP antibody. However, their results are contradictory to ours. They found that SRC-3 protein is predominantly localized and then exclusively localized in the cytoplasm during G1 and S respectively. During late G2 and before chromosome condensation and NE breakdown, they observed a rapid nuclear accumulation of this protein, which was subsequently redistributed to the cytoplasm during mitosis. It is noteworthy that in their study, they also examined the expression of SRC-3 in other asynchronous cell lines and found that it was predominantly localized in the nucleus of MCF-7 cells, contrary to HeLa cells. This finding suggests that SRC-3 protein localization may be dependent on the specific cell line or tissue. It is also possible that the human SRC-3 protein undergoes species-specific conformational changes throughout the cell cycle that cannot be recognized by an antibody for the mouse homologue p/CIP. In our study, we also observed the expression of SRC-3 throughout the cell cycle of ZR-75-1 (ER positive) and SK-Br-3 (ER negative) breast cancer cells, as well as COS-7 cells, and found similar protein distribution to MCF-7 cells. Thus, in the cell lines we examined, SRC-3 subcellular localization was similarly regulated.

Intracellular trafficking and compartmentalization are commonly used mechanisms of protein regulation. Since different cellular compartments contain unique complements of proteins, and specific protein functions are dependent on the presence and/or activity of upstream and downstream regulators, binding partners and inhibitory

proteins, a single molecule can have numerous functions depending on its localization within the cell. For example, Moore *et al* (2003) showed that cyclin B1 has the ability to induce DNA replication in frog egg extracts. However, it does not do so *in vivo* because it is secluded in the cytoplasm during the S phase. Similarly, SRC-3 may be secluded from the nucleus during mitosis to prevent it from activating or inhibiting specific protein functions during mitosis; conversely, it may be actively involved in mitosis by mediating the activity of cytoplasmic proteins. Consistent with the former hypothesis, SRC-3 is modified then degraded as cells progress through and exit mitosis, suggesting that its activity must be attenuated during this phase.

Role of Cdk1 and MAPK in SRC-3 modification

Post-translational modifications such as phosphorylation are often necessary to trigger a change in protein activity or status. For example, many proteins are phosphorylated prior to ubiquitination or subcellular transport. In this study, we found that modification of SRC-3 in mitosis occurs in a MAPK- and Cdk1-dependent manner (figures 3.7 and 3.8). We were more interested in the involvement of Cdk1 than MAPK since Cdk1 plays such an integral role in mitotic regulation. Additionally, MAPK has been implicated in the activation of SRC-3 (Font de Mora and Brown, 2000), which appears to contradict the attenuation of SRC-3 activity by degradation that we observed in mitosis. However, MAPK does play a role in G2/M transition and assembly of the mitotic spindle (Wright *et al*, 1999; Roberts *et al*, 2002; Horne and Guadagno, 2003), so it is possible that both MAPK and Cdk1 contribute to the mitotic regulation of SRC-3,

either directly or via cross-talk between pathways. This possibility requires further examination and is beyond the scope of this study.

Consistent with the involvement of Cdk1 in SRC-3 modification, we found that these proteins interact in MCF-7 cells (figure 3.9). Interestingly, Cdk1 is imported into the nucleus at the onset of prophase, while SRC-3 is exported out of the nucleus during early to mid prophase. This presents the possibility that following nuclear import, Cdk1 is involved in triggering the modification and subsequent degradation and/or transport of SRC-3.

It was surprising that the interaction between SRC-3 and Cdk1 appeared to be constitutive since we found that SRC-3 is predominantly localized in the nucleus during interphase, whereas Cdk1 is localized in the cytoplasm during this time (Porter and Donoghue, 2003). This apparent contradiction could be due to post-lysis interaction endured during the immunoprecipitation, which occurs between proteins with mutual high affinities. In order to confirm this result, fluorescence resonance energy transfer (FRET) studies could be performed in synchronized cells. FRET measures the interaction between two proteins genetically fused to two different fluorophores, a donor and an acceptor. When the donor fluorophore is excited by electromagnetic energy of a specific wavelength, it absorbs and then reemits the energy at a different wavelength. However, when the donor fluorophore is in close proximity to the acceptor fluorophore (i.e. when the two proteins are interacting), the acceptor fluorophore absorbs the energy emitted by the donor fluorophore and reemits it at its own specific wavelength. Thus, the interaction between two proteins can be accurately examined. It would also be important to determine the activation state of the coimmunoprecipitated Cdk1 to better understand the

role of this kinase in SRC-3 modification and/or activity. The activation state could be determined by immunoblotting with phospho-Cdk1 antibodies specific for residues Thr^{14} and Tyr^{15}, which are phosphorylated on inactive Cdk1, and Thr^{161}, which is phosphorylated on active Cdk1 (Shah *et al*, 2003).

Proteins phosphorylated by Cdk1 generally have a consensus site defined as (K/R)(S/T)P(R/P/K)(R/K/H) where S/T is the phosphorylated residue (figure 4.1A) (Murray, 2004). P directs the phosphorylation on the (S/T) site and is thus crucial to the consensus sequence. Previous studies have shown that Cdk1 is least sensitive to substitutions at the -1 position (with respect to S/T), fairly sensitive to substitutions at +2 and most sensitive to substitutions at +3 (Holmes and Solomon, 1996). Analysis of the SRC-3 sequence (accession number Q9EPU2) revealed five potential Cdk1 consensus sites, of which one (S867) is a reported bonafide phosphorylation site (figure 4.1B) (Wu *et al*, 2004). S867 is phosphorylated by p38 and JNK kinases but not ERK, PKA, CK1 and IKK. Phosphorylation at this site increases the ability of SRC-3 to interact with the HAT CBP, while phosphorylation-defective SRC-3 mutants are less able to interact with CBP. It would be interesting to determine if the S867-specific antibody developed by this group recognizes the modified form of SRC-3. However, it is also important to determine if the other SRC-3 residues are phosphorylated by Cdk1 by performing *in vitro* kinase assays with truncated SRC-3 proteins, followed by mutational analyses of the specific residues of interest. Once the phosphorylation sites are determined, a mutated and tagged SRC-3 protein could be transfected into MCF-7 cells to determine the effect on mitotic modification of SRC-3.

Figure 4.1. Potential Cdk1 phosphorylation sites in SRC-3.

(A) The typical Cdk1 recognition sequence. Cdk1 phosphorylates the Ser/Thr residue at position 0 in a proline-directed manner. **(B)** SRC-3 protein sequence (accession number Q9EPU2). All Ser/Thr-Pro residues are highlighted in red. Each site was individually analyzed to assess its potential as a Cdk1 recognition site. Five potential sites (highlighted in blue) were found. Previously identified phosphorylation sites are highlighted in green (Wu *et al*, 2004).

A

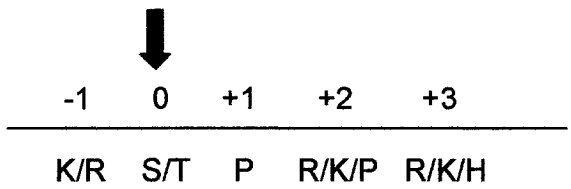

B

1 msglgenldp lasdsrkrkl pcd**pgqglt** csgekrrreq eskyieelae lisanlsdid
61 nfnvkpdkca ilketvrqir qikeqgktis ndddvqkadv sstgqgvidk dslgpllqa
121 ldgflfvvnr dgnivfvsen vtqylqykqe dlvntsvyni lheedrkdfl knlpkstvng
181 vswtnetqrq kshtfncrml mktphdiled ina**spe**mrqr yetmqcfals qprammeege
241 dlqscmicva rrittgertf psnpesfitr hdlsgkvvni dtnslrssmr pgfediirrc
301 iqrffslndg qswsqkrhyq eaylnghaet pvyrfsladg tivtaqtksk lfrnpvtndr
361 hgfvsthflq reqngyrpnp npvgqgirpp magcnssvgg msm**sp**nqglq mpssraygla
421 dpsttgqmsg aryggssnia s**ltpgpgmqs** pssyqnnnyg lnm**sspphgs** pglapnqqni
481 mi**sprnrgsp** k**i**ashq**fspv** agvh**spmass** gntgnhsfss sslsalqais egvgtsllst
541 l**sspgpk**ldn **sp**nmnitqps kvsnqdsk**sp** lgfycdqnpv essmcqsnsr dhlsdkeske
601 ssvegaenqr gpleskghkk llqlltcssd drghssltn**s pl**dssckess vsvt**sp**sgvs
661 sstsggvsst snmhgsllqe khrilhkllq ngn**spa**evak itaeatgkdt ssitscgdgn
721 vvkqeq**lspk kk**ennallry lldrddpsda lskelqpqve gvdnkmsqct sstipsssqe
781 kdpkiktets eegsgdldnl dailgdltss dfynnsissn gshlgtkqqv fqgtnslglk
841 ssqsvqsirp pynrav**sld**s **pvsvgs**s**ppv k**nisafpmlp kqpmlggnpr mmdsqenygs
901 smggpnrnvt vtq**tp**ssgdw glpnskagrm epmnsnsmgr pggdyntslp rpalggsipt
961 lplrsnsipg arpvlqqqqq mlqmrpgeip mgmganpygq aaasnqlgsw pdgmlsmeqv
1021 shgtqnrpll rnsldd**l**vgp psnlegqsde ralldqlhtl lsntdatgle eidralgipe
1081 lvnqgqalep kqdafqgqea avmmdqkagl ygqtypaqgp pmqggfhlqg q**sp**sfnsmmn
1141 qmnqqgnfpl qgmhpranim rprtn**tp**kql rmqlqqrlqg qqflnqsrqa lelkmenpta
1201 ggaavmrpmm qpqvssqqgf lnaqmvaqrs rellshhfrq qrvammmqqq qqqqqqqqqq
1261 qqqqqqqqqq qqqqqqtqaf **spp**pnvta**sp** smdgllagpt mpqappqqfp yqpnygmgqq
1321 pdpafgrvs**s pp**nammssrm gpsqnpmmqh pqaasiyqss emkgwpsgnl arnssfsqqq
1381 fahqgnpavy smvhmngssg hmgqmnmnpm pmsgmpmgpd qkyc

One of the most significant difficulties we encountered in our studies was the relative inability to immunoprecipitate SRC-3. Consequently, we were unable to directly determine the identity or identities of the mitotic SRC-3 modification. The results from our degradation studies suggest that this form of SRC-3 is either a ubiquitinated species or a species that signals for ubiquitination and subsequent degradation. If the latter case is correct, we could be detecting a phosphorylated form of SRC-3 which acts as the necessary signal for degradation. In order to examine the identity of the modified form, we attempted an *in vivo* metabolic labelling reaction with [^{32}P]orthophosphate to determine if SRC-3 is preferentially phosphorylated in mitosis. However, we were unable to recover full-length SRC-3 (data not shown). We were also unable to immunoprecipitate sufficient SRC-3 to directly demonstrate Cdk1-mediated phosphorylation in an *in vitro* kinase assay. Thus, it would be useful to attempt the kinase assay with *in vitro* translated SRC-3 to avoid the need for immunoprecipitation.

Another significant limitation of our study was our inability to determine the exact timing of SRC-3 modification. The nocodazole studies suggest that it occurs prior to metaphase since there was a considerable accumulation of the modified form in metaphase-arrested cells. If this is the case, modification may trigger nuclear export, protein degradation, or a combination of both, which ultimately leads to the attenuation of SRC-3 activity. SRC-3 modification may also induce conformational changes that trigger allosteric interactions with a different set of proteins that sequester SRC-3 or inhibit its activity. Alternatively, the thymidine studies suggest that SRC-3 is modified at the end of mitosis/the beginning of G1. In this case, SRC-3 modification may trigger the nuclear import or the cytoplasmic degradation of this protein, or a combination of both.

In order to better elucidate the timing of SRC-3 modification, the phosphorylation status of Cdk1 and expression level of cyclin B1 could be coordinately determined.

Implications of SRC-3 degradation during mitosis

Our novel observation that SRC-3 is modified and then degraded during mitosis in a Cdk1-, MAPK- and proteasome-dependent manner, coupled with our findings that SRC-3 is exported from the nucleus during prophase and excluded from DNA for the remainder of mitosis, suggest that SRC-3 activity must be attenuated for normal mitotic progression to occur. An appealing candidate pathway that may be regulated through SRC-3 during mitosis is the PI3K/Akt/mTOR pathway. This pathway plays a crucial role in the regulation of ribosome biogenesis, which has been estimated to demand as much as 80% of a cell's energy (reviewed in Fingar and Blenis, 2004). During mitosis, the activity of S6K1, one of the most downstream effectors of this pathway, is inhibited by Cdk1-mediated phosphorylation (Shah *et al*, 2003). Presumably, inhibition allows the cell to reserve energy for the high demands of mitosis. It has been shown that SRC-3 overexpression enhances the activity of this pathway, while RNAi-mediated SRC-3 downregulation decreases protein synthesis (Zhou *et al*, 2003). We hypothesize that SRC-3 must also be inhibited, possibly in a Cdk1-dependent manner, in order to more effectively attenuate the activity of S6K1 during mitosis (figure 4.2). In support of this hypothesis, several of the stable SRC-3-overexpressing clones harboured overactive S6K1 (see below). Additionally, SRC-3 was degraded when cells were deprived of serum (figure 3.6), consistent with attenuated mTOR-mediated translation in quiescence.

Figure 4.2. Proposed model of SRC-3 inactivation in mitosis.

During interphase, the PI3K/Akt/mTOR pathway actively stimulates protein synthesis via S6K1. In mitosis, Cdk1 phosphorylates and inactivates S6K1 in order to preserve energy for mitotic events. Cdk1 might also phosphorylate SRC-3, triggering its ubiquitination and degradation. In this way, the cell more effectively attenuates protein synthesis and reserves energy for the high demands of mitosis.

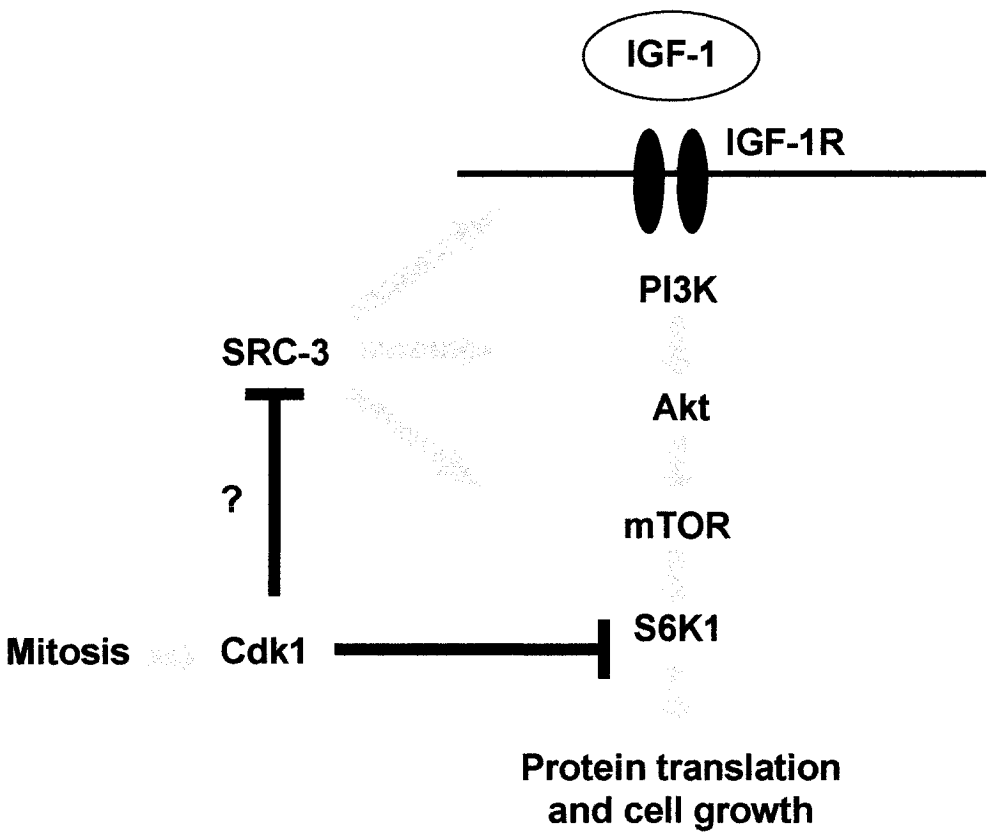
IGF-1
IGF-1R
PI3K
SRC-3
Akt
?
mTOR
Mitosis
Cdk1
S6K1
Protein translation
and cell growth

SRC-3 DEREGULATION DISRUPTS CELL CYCLE PROGRESSION AND DNA CONTENT

SRC-3 overexpression in MCF-7 cells reduces growth and alters cell cycle dynamics

In order to examine the effect of disrupted SRC-3 expression on cellular function, we established stable SRC-3 overexpressing clones. Despite the reported oncogenic activity of SRC-3, this process was challenging. We attempted to establish SRC-3 stable clones in several cell lines, including MCF-7, HeLa and COS-7. However, only the MCF-7 cells survived the expansion process, albeit on a limited basis. Although these stable clones originally expressed high levels of SRC-3 protein, they lost their ability to overexpress it after five to six passages, even while maintained in puromycin-supplemented media (figure 3.11D). Consistent with our results, Zhou *et al* (2003) reported that they were unable to establish SRC-3 overexpressing clones in several unidentified cell lines. Moreover, Chen *et al* (personal communication) were unable to detect exogenous SRC-3 using a SRC-3-specific or FLAG-tag antibody. These results suggest that continued high levels of SRC-3 may decrease or inhibit cellular proliferation, and/or may be toxic to cells. In support of this notion, the stable clones grew at a distinctly slower rate that their control counterparts (figure 3.11B and C).

It is noteworthy that in the literature, the cell lines that were able to stably overexpress SRC-3 were defective in p53 (T-47D and MDA-MB-436 cells) (Anzick *et al*, 2003; Louie *et al*, 2004). This observation presents the interesting possibility that cells must have a significant defect in cell cycle arrest in order to support high levels of SRC-3 protein. We showed that SRC-3 overexpression increases the proportion of MCF-7 cells

containing a >2N<4N DNA content (see explanation below), suggesting that an S phase block may have been activated. If SRC-3 overexpressing cells are unable to arrest in the cell cycle due to a p53 mutation, they could continue cycling despite replication errors or altered mitosis, leading to the rapid acquisition of oncogenic mutations. This notion would explain the dichotomy between the toxicity of SRC-3 in p53 positive MCF-7 cells, and the oncogenicity of this gene in p53 mutant cells. It would be worthwhile to test this hypothesis by depleting p53 in MCF-7 cells with human papillomavirus E6 and then determining the effect of SRC-3 overexpression.

Previous reports have shown that SRC-3-overexpressing clones have a large size cell phenotype with abundant cytoplasm (Anzick *et al*, 2003; Zhou *et al*, 2003). We noticed similar phenotypic changes in the slower-growing colonies. The most commonly observed phenotypic alterations included large, flat cells with abundant cytoplasm and large nuclei, or spindly cells with dendrite-like processes (figure 3.13). Additionally, several clones were multinucleated. Zhou *et al* (2003) showed that increased activity of the PI3K/Akt/mTOR pathway accounted for the increased cell size observed in SRC-3 overexpressing cells. Although we detected increased S6K1 activity in many of our clones, which is indicative of mTOR activity, it was not correlated with high SRC-3 expression (figure 3.12). This result suggests that the increase in cell size that we observed in MCF-7 cells was not due to S6K1 overactivity. Alternatively, since SRC-3 overexpression disrupts cell cycle progression, it is possible that the cells expressing the highest levels of SRC-3 were actually arrested in the cell cycle. Consequently, S6K1 activity would not be elevated in these cells.

Because of the flattened shape and extensive cytoplasm present in the SRC-3 stable clones, which are characteristics commonly observed in senescent cells (Dimri *et al*, 1995), we questioned whether SRC-3 overexpression might induce senescence. Since replicative senescence is a state of irreversible arrested growth and proliferation, it would explain the apparent decrease in growth rate observed in the clones. However, SA-ß-gal staining revealed that SRC-3 overexpressing cells were not senescent (data not shown). It is noteworthy that this assay was performed on cells that had been passaged several times. Since SRC-3 overexpression is quickly lost in stably transfected cells (figure 3.11), it is possible that the apparent negative result was due to loss of SRC-3 overexpression following various passages. It would be worthwhile to repeat this assay in freshly transfected SRC-3 stable clones.

Quiescent and G1 somatic cells contain a diploid complement of DNA, consisting of 2 sets of 23 homologous chromosomes (2N), each inherited from a parental set. In contrast, G2/M cells, which have undergone genome duplication in preparation for cell division, contain 4 sets of 23 homologous chromatids (4N). Between these groups lie the S phase cells that are in the midst of DNA replication. Consequently, they have a >2N<4N DNA content. Flow cytometry is a form of analysis that measures the DNA content of a population of cells to determine the proportion of those cells present in a given phase of the cell cycle. It also measures the mean 2N and 4N peak DNA contents, which indicate the total amount of DNA contained in the 46 chromosomes or 92 duplicated chromatids.

Changes in DNA content can be interpreted in several different ways. For example, an increase in the >2N<4N population may be due to an increased proportion of

replicating cells (an increased S phase population); an S phase arrest due to checkpoint activation; or nascent aneuploidy, if there is no evidence of a corresponding diploid peak for the aneuploid cells. Similarly, an increase in the 4N population may be interpreted as an increase in the proportion of cells undergoing mitosis; a G2/M phase arrest due to checkpoint activation; or nascent polyploidy. Lastly, deviation of the mean 2N or 4N peak DNA contents relative to controls may be due to aneuploidy in the population.

In our study, we investigated the cell cycle effects of both SRC-3 overexpression and depletion. SRC-3 depletion resulted in a prolonged G1 phase and shortened G2/M phases (figure 3.11). This result was not unexpected since SRC-3 coactivates the ER and also recruits it to the cyclin D1 promoter during G1, effectively promoting G1 progression (Planas-Silva *et al*, 2001). SRC-3 has also been implicated in the promotion of G1/S transition by coactivating the E2F transcription factors (Louie *et al*, 2004). Thus, SRC-3 depletion likely decreases the growth-promoting activities of these proteins, resulting in an accumulation of cells in G1. It is also possible that SRC-3 depletion is necessary for proper mitotic exit in MCF-7 cells, and consequently, premature depletion increases the rate of mitotic exit. These possibilities are not mutually exclusive. Interestingly, SRC-3 depletion did not affect the ability of cells to arrest in or re-enter the cell cycle following treatment with exogenous agents such as thymidine and nocodazole, suggesting that it does not play a direct role in cell cycle arrest.

In contrast to the depletion studies, the few clones we obtained that stably overexpressed SRC-3 provided information about the longer-term effects of constitutive SRC-3 overactivity. Strikingly, SRC-3 transfected clones had significantly altered cell cycle phase distributions, reflected in the proportion of cells with greater than 2N DNA

content (figure 3.14A). Clones S5 and M3, which expressed high levels of SRC-3, had a consistent decrease in the mean peak G1 and G2 DNA contents compared to control clones and SRC-3 clones no longer expressing high levels of this protein (figure 3.14C). Moreover, these clones had dramatically altered >2N<4N DNA contents. As detailed above, these results can be interpreted in several ways. The leftward shift in mean peak DNA content suggests that the clones had experienced a net loss in DNA, which may be attributed to aneuploidy. In contrast, the disruption in the >2N<4N phase distributions may represent an S-phase block, an increase in the number of proliferating cells, or nascent aneuploidy. For example, clone S5 had an accumulation of cells in early S phase, suggesting that the S phase checkpoint had been activated. Clone M2, on the other hand, is more difficult to interpret, since the merger of the S and M phases may be due to a combination of all the factors mentioned above.

As a coactivator, SRC-3 potentiates the activity of many transcription factors throughout the cell cycle. SRC-3 has repeatedly been described as a promiscuous protein that is involved in many signalling pathways, including but not limited to, HER2/neu, NFκB and PI3K/Akt/mTOR (Goel and Janknecht, 2004; Werbajh *et al*, 2000; Wu *et al*, 2002; Wang *et al*, 2000; Zhou *et al*, 2003). The possibility for cross talk and synergy between these pathways exists. SRC-3 is also involved in cell cycle progression by increasing the expression and activity of cell cycle regulators, including the E2F family of transcription factors and several cyclins. (Louie *et al*, 2004). It is noteworthy that overexpression of several checkpoint and cell cycle proteins has been implicated in the promotion of aneuploidy. For example, overactive cyclin B1 and cyclin E contribute to chromosomal instability leading to aneuploidy (Sarafan-Vasseur *et al*, 2002; Ekholm-

Reed *et al*, 2004; Kawamura *et al*, 2004). Thus, it is possible that the DNA loss we observed in the SRC-3 overexpressing clones was at least partially due to aneuploidy caused by cyclin B1 and E overactivity. It will be important to establish the activity of these proteins in SRC-3 overexpressing cells. Moreover, BrdU labelling experiments should be performed to distinguish between S phase accumulation and aneuploidy.

Proposed model of dual SRC-3 roles in growth arrest and oncogenesis

Based on previous studies showing that SRC-3 is involved in the promotion of cell cycle progression via the stimulation of ER activity; the coactivation of E2F; the overexpression of cyclins E, A and B, and Cdk2; and the activation of the PI3K/Akt/mTOR pathway; coupled with our results showing that SRC-3 protein levels and localization are dynamically regulated throughout the cell cycle; and SRC-3 overexpression results in cells with abnormal DNA contents and cell cycles, we hypothesize that SRC-3 protein activity must remain tightly regulated for normal cell cycle progression to occur. Deviation from this highly regulated state results in the inappropriate activation of a multitude of signalling pathways that promote growth, DNA and protein synthesis, ultimately leading to deregulation of the cell cycle, altered mitosis and aneuploidy. In cells with functional checkpoints, this aberrant activity leads to apoptosis and/or senescence (figure 4.3). In support of this hypothesis, SRC-3 overexpression was toxic to MCF-7 cells, which are p53 positive, and resulted in decreased growth rates in those that survived. Additionally, the surviving clones showed increased >2N<4N DNA contents and loss of DNA, suggesting that many of the cells were arrested at the S or early G2/M checkpoints and/or were aneuploid.

Figure 4.3. Proposed model of dual SRC-3 roles in growth arrest and oncogenesis. SRC-3 overexpression activates a multitude of signalling pathways that promote growth, cell cycle progression and protein synthesis. This aberrant activity leads to altered mitosis and DNA loss. In the presence of functional tumour suppressors, such as p53, cells can arrest in response to this aberrant activity. However, in the absence of functional tumour suppressors, the cells are not able to respond, resulting in the acquisition of oncogenic mutations and possible malignancy (see text for details).

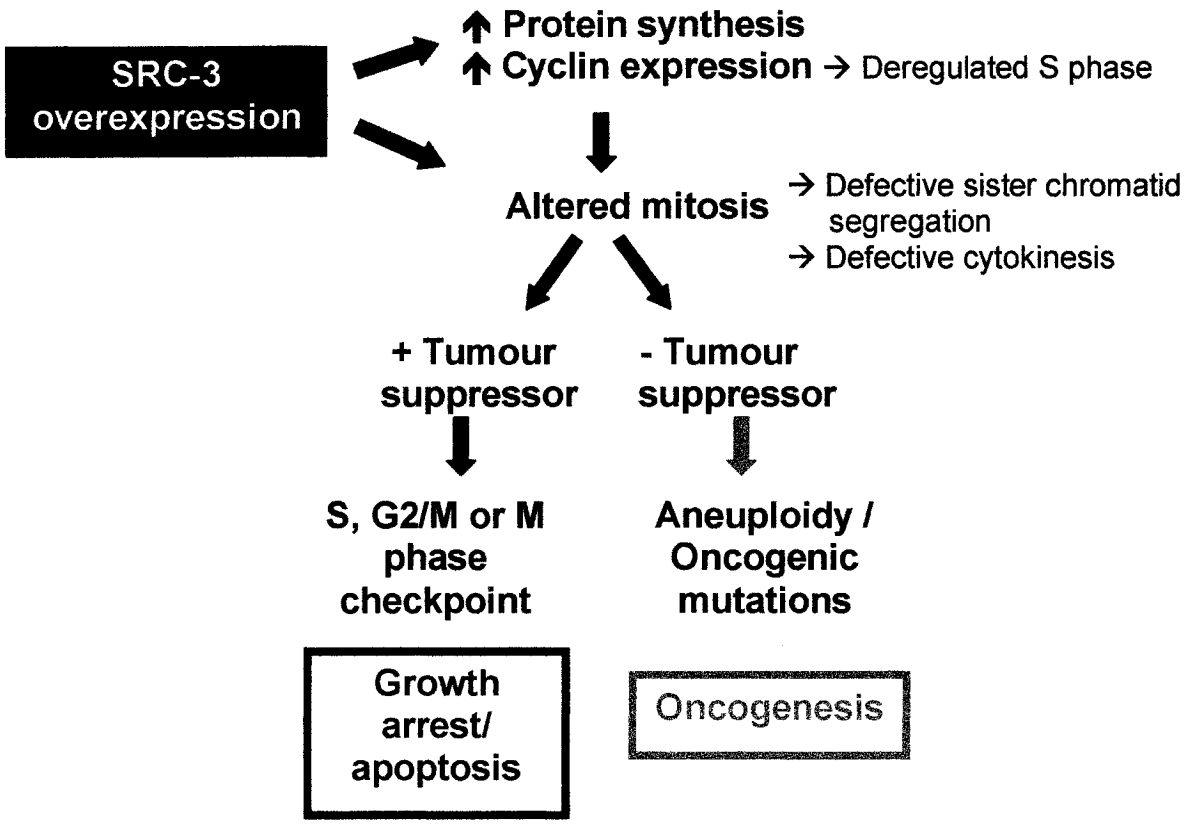
SRC-3 overexpression
↑ Protein synthesis
↑ Cyclin expression → Deregulated S phase
Altered mitosis
→ Defective sister chromatid segregation
→ Defective cytokinesis
+ Tumour suppressor
- Tumour suppressor
S, G2/M or M phase checkpoint
Aneuploidy / Oncogenic mutations
Growth arrest/ apoptosis
Oncogenesis

We also hypothesize that despite their deregulated cell cycles, a small number of cells evade the checkpoint arrests. This evasion may lead to altered mitosis, characterized by defective cytokinesis and/or inappropriate segregation of chromosomes at the metaphase plate. The latter phenomenon, referred to as mitotic slippage, results in cell cycle arrest in G1. However, if a cell escapes arrest in G1, due to a mutant tumour suppressor such as p53, it will undergo multipolar mitosis, leading to apoptosis or aneuploidy (figure 4.3) (Storchova and Pellman, 2004). Once chromosomal instability is established, the cell will continuously and rapidly acquire a series of other mutations that could give rise to an increasingly malignant cell. This progression may account for the oncogenic ability of SRC-3 reported in the literature. In support of this theory, many of the cells that survived SRC-3 transfection had a decreased DNA peak content and aberrant cell cycles, suggesting that they represented an aneuploid population. Additionally, one of the most obvious characteristics of a polyploid cell is an increase in cell size (Storchova and Pellman, 2004), which was observed in our stable cell lines. Furthermore, several SRC-3 transfectants were multinucleated, which may be an indication of aberrant mitosis and consequent aneuploidy. Finally, researchers were able to establish SRC-3 overexpressing clones in the T-47D breast cancer cell line, which harbours a mutant p53 (Louie *et al*, 2004). This finding suggests that mutant p53, and the consequent inability to block cell cycle progression in response to DNA damage, may be a key factor in influencing the oncogenic capacity of SRC-3. Consistent with this notion, SRC-3 overexpression in breast cancers has been correlated with positivity for mutant p53 (Bouras *et al*, 2001).

REFERENCES

Abal M, Andreu JM, Barasoain I. (2003). Taxanes: Microtubule and Centrosome Targets, and Cell Cycle Dependent Mechanisms of Action. Current Cancer Research. 3, 193-203.

Adams J. (2003). The proteasome: structure, function, and role in the cell. Cancer Treat Rev. 29 Suppl 1, 3-9.

Amazit L, Alj Y, Tyagi RK, Chauchereau A, Loosfelt H, Pichon C, Pantel J, Foulon-Guinchard E, Leclerc P, Milgrom E, Guiochon-Mantel A. (2003). Subcellular localization and mechanisms of nucleocytoplasmic trafficking of steroid receptor coactivator-1. J Biol Chem. 278, 32195-203.

Anzick SL, Azorsa DO, Simons SS Jr, Meltzer PS. (2003). Phenotypic alterations in breast cancer cells overexpressing the nuclear receptor co-activator AIB1. BMC Cancer. 3, 22.

Anzick SL, Kononen J, Walker RL, Azorsa DO, Tanner MM, Guan XY, Sauter G, Kallioniemi OP, Trent JM, Meltzer PS. (1997). AIB1, a steroid receptor coactivator amplified in breast and ovarian cancer. Science. 277, 965-8.

Bautista S, Valles H, Walker RL, Anzick S, Zeillinger R, Meltzer P, Theillet C. (1998). In breast cancer, amplification of the steroid receptor coactivator gene AIB1 is correlated with estrogen and progesterone receptor positivity. Clin Cancer Res. 4, 2925-9.

Bharadwaj R, Yu H. (2004). The spindle checkpoint, aneuploidy, and cancer. Oncogene. 23, 2016-27.

Bouras T, Southey MC, Venter DJ. (2001). Overexpression of the steroid receptor coactivator AIB1 in breast cancer correlates with the absence of estrogen and progesterone receptors and positivity for p53 and HER2/neu. Cancer Res. 61, 903-7.

Brown K, Chen Y, Underhill TM, Mymryk JS, Torchia J. (2003). The coactivator p/CIP/SRC-3 facilitates retinoic acid receptor signaling via recruitment of GCN5. Biol Chem. 278, 39402-12.

Buendia B, Courvalin JC, Collas P. (2001). Dynamics of the nuclear envelope at mitosis and during apoptosis. Cell Mol Life Sci. 58, 1781-9.

Cailleau R, Young R, Olive M, Reeves WJ Jr. (1974). Breast tumor cell lines from pleural effusions. J Natl Cancer Inst. 53, 661-74.

Chen D, Ma H, Hong H, Koh SS, Huang SM, Schurter BT, Aswad DW, Stallcup MR. (1999). Regulation of transcription by a protein methyltransferase. Science. 284, 2174-7.

Chen H, Lin RJ, Schiltz RL, Chakravarti D, Nash A, Nagy L, Privalsky ML, Nakatani Y, Evans RM. (1997). Nuclear receptor coactivator ACTR is a novel histone acetyltransferase and forms a multimeric activation complex with P/CAF and CBP/p300. Cell. 90, 569-80.

Chen YJ, Lin SC, Kao T, Chang CS, Hong PS, Shieh TM, Chang KW. (2004). Genome-wide profiling of oral squamous cell carcinoma. J Pathol. 204, 326-332.

Ciechanover A, Heller H, Katz-Etzion R, Hershko A. (1981). Activation of the heat-stable polypeptide of the ATP-dependent proteolytic system. Proc Natl Acad Sci U S A. 78, 761-5.

Dimri GP, Lee X, Basile G, Acosta M, Scott G, Roskelley C, Medrano EE, Linskens M, Rubelj I, Pereira-Smith O. (1995). A biomarker that identifies senescent human cells in culture and in aging skin in vivo. Proc Natl Acad Sci U S A. 92, 9363-7.

Dinter A, Berger EG. (1998). Golgi-disturbing agents. Histochem Cell Biol. 109, 571-90.

Doucet JP, Murphy BJ, Tuana BS. (1990). Modification of a discontinuous and highly porous sodium dodecyl sulfate-polyacrylamide gel system for minigel electrophoresis. Anal Biochem. 190, 209-11.

Eastman A. (2004). Cell cycle checkpoints and their impact on anticancer therapeutic strategies. J Cell Biochem. 91, 223-31.

Ekholm-Reed S, Mendez J, Tedesco D, Zetterberg A, Stillman B, Reed SI. (2004). Deregulation of cyclin E in human cells interferes with prereplication complex assembly. J Cell Biol. 165, 789-800.

Engel LW, Young NA, Tralka TS, Lippman ME, O'Brien SJ, Joyce MJ. (1978). Establishment and characterization of three new continuous cell lines derived from human breast carcinomas. Cancer Res. 38, 3352-3364.

Fingar DC, Blenis J. (2004). Target of rapamycin (TOR): an integrator of nutrient and growth factor signals and coordinator of cell growth and cell cycle progression. Oncogene. 23, 3151-71.

Font de Mora J, Brown M. (2000). AIB1 is a conduit for kinase-mediated growth factor signaling to the estrogen receptor. Mol Cell Biol. 20, 5041-7.

Ford HL, Pardee AB. (1999). Cancer and the cell cycle. J Cell Biochem. Suppl 32-33, 166-172.

Furukawa Y, Iwase S, Kikuchi J, Terui Y, Nakamura M, Yamada H, Kano Y, Matsuda M. (2000). Phosphorylation of Bcl-2 protein by CDC2 kinase during G2/M phases and its role in cell cycle regulation. J Biol Chem. 275, 21661-7.

Georgatos SD, Pyrpasopoulou A, Theodoropoulos PA. (1997). Nuclear envelope breakdown in mammalian cells involves stepwise lamina disassembly and microtubule-drive deformation of the nuclear membrane. J Cell Sci. 110, 2129-40.

Ghadimi BM, Schrock E, Walker RL, Wangsa D, Jauho A, Meltzer PS, Ried T. (1999). Specific chromosomal aberrations and amplification of the AIB1 nuclear receptor coactivator gene in pancreatic carcinomas. Am J Pathol. 154, 525-36.

Gluzman Y. (1981). SV40-transformed simian cells support the replication of early SV40 mutants. Cell. 23, 175-82.

Gnanapragasam VJ, Leung HY, Pulimood AS, Neal DE, Robson CN. (2001). Expression of RAC 3, a steroid hormone receptor co-activator in prostate cancer. Br J Cancer. 85, 1928-36.

Goel A, Janknecht R. (2004). Concerted activation of ETS protein ER81 by p160 coactivators, the acetyltransferase p300 and the receptor tyrosine kinase HER2/Neu. J Biol Chem. 279, 14909-16.

Gonczy P. (2002). Nuclear envelope: torn apart at mitosis. Curr Biol. 12, R242-4.

Gregoli PA, Bondurant MC. (1999). Function of caspases in regulating apoptosis caused by erythropoietin deprivation in erythroid progenitors. J Cell Physiol. 178, 133-43.

Hegde AN, DiAntonio A. (2002). Ubiquitin and the synapse. Nat Rev Neurosci. 3, 854-61.

Henke RT, Haddad BR, Kim SE, Rone JD, Mani A, Jessup JM, Wellstein A, Maitra A, Riegel AT. (2004). Overexpression of the nuclear receptor coactivator AIB1 (SRC-3) during progression of pancreatic adenocarcinoma. Clin Cancer Res.10, 6134-42.

Holmes JK, Solomon MJ. (1996). A predictive scale for evaluating cyclin-dependent kinase substrates. A comparison of p34cdc2 and p33cdk2. J Biol Chem. 271, 25240-6.

Horne MM, Guadagno TM. (2003). A requirement for MAP kinase in the assembly and maintenance of the mitotic spindle. J Cell Biol. 161, 1021-8.

Huang ZJ, Edery I, Rosbash M. (1993). PAS is a dimerization domain common to Drosophila period and several transcription factors. Nature. 364, 259-62.

Hutchins JR, Clarke PR. (2004). Many fingers on the mitotic trigger: post-translational regulation of the Cdc25C phosphatase. Cell Cycle. 3, 41-5.

Kawamura K, Izumi H, Ma Z, Ikeda R, Moriyama M, Tanaka T, Nojima T, Levin LS, Fujikawa-Yamamoto K, Suzuki K, Fukasawa K. (2004). Induction of centrosome

amplification and chromosome instability in human bladder cancer cells by p53 mutation and cyclin E overexpression. Cancer Res. 64, 4800-9.

King RW, Deshaies RJ, Peters JM, Kirshner MW. (1996). How proteolysis drives the cell cycle. Science. 274, 1652-9.

Kitagawa, M, Okabe, T, Ogino, H., Matsumoto, H., Suzuki-Takahashi, I., Kokubo, T, Higashi, H, Saitoh, S, Taya, Y, Yasuda, H, *et al.* (1993). Butyrolactone I, a selective inhibitor of cdk2 and cdc2 kinase. Oncogene. 8, 2425-32.

Kong EH, Pike AC, Hubbard RE. (2003). Structure and mechanism of the oestrogen receptor. Biochem Soc Trans. 31, 56-9.

Laemmli, UK (1970). Cleavage of structural proteins during the assembly of the head of bacteriophage T4. Nature. 227, 680-5.

Lauritsen KJ, List HJ, Reiter R, Wellstein A, Riegel AT. (2002). A role for TGF-beta in estrogen and retinoid mediated regulation of the nuclear receptor coactivator AIB1 in MCF-7 breast cancer cells. Oncogene. 21, 7147-55.

Lee DH, Goldberg AL. (1998). Proteasome inhibitors: valuable new tools for cell biologists. Trends Cell Biol. 8, 397-403.

Lee SK, Kim HJ, Kim JW, Lee JW. (1999). Steroid receptor coactivator-1 and its family members differentially regulate transactivation by the tumor suppressor protein p53. Mol Endocrinol. 13, 1924-33.

Li H, Chen JD. (1998). The receptor-associated coactivator 3 activates transcription through CREB-binding protein recruitment and autoregulation. J Biol Chem. 273, 5948-54.

Li H, Gomes PJ, Chen JD. (1997). RAC3, a steroid/nuclear receptor-associated coactivator that is related to SRC-1 and TIF2. Proc Natl Acad Sci U S A. 94, 8479–8484.

List HJ, Lauritsen KJ, Reiter R, Powers C, Wellstein A, Riegel AT. (2001a). Ribozyme targeting demonstrates that the nuclear receptor coactivator AIB1 is a rate-limiting factor for estrogen-dependent growth of human MCF-7 breast cancer cells. J Biol Chem. 276, 23763-8.

List HJ, Reiter R, Singh B, Wellstein A, Riegel AT. (2001b). Expression of the nuclear coactivator AIB1 in normal and malignant breast tissue. Breast Cancer Res Treat. 68, 21-8.

Littlepage LE, Ruderman JV. (2002). Identification of a new APC/C recognition domain, the A box, which is required for the Cdh1-dependent destruction of the kinase Aurora-A during mitotic exit. Genes Dev. 16, 2274-85.

Lonard DM, Tsai SY, O'Malley BW. (2004). Selective estrogen receptor modulators 4-hydroxytamoxifen and raloxifene impact the stability and function of SRC-1 and SRC-3 coactivator proteins. Mol Cell Biol. 24, 14-24.

Louie MC, Yang HQ, Ma AH, Xu W, Zou JX, Kung HJ, Chen HW. (2003). Androgen-induced recruitment of RNA polymerase II to a nuclear receptor-p160 coactivator complex. Proc Natl Acad Sci U S A. 100, 2226-30.

Louie MC, Zou JX, Rabinovich A, Chen HW. (2004). ACTR/AIB1 functions as an E2F1 coactivator to promote breast cancer cell proliferation and antiestrogen resistance. Mol Cell Biol. 24, 5157-71.

Macgregor JI, Jordan VC. (1998). Basic guide to the mechanisms of antiestrogen action. Pharmacological Reviews. 50, 151-196.

McGowan CH. (2002). Checking in on Cds1 (Chk2): A checkpoint kinase and tumor suppressor. Bioessays. 24, 502-11.

McKenna NJ, O'Malley BW. (2002). Minireview: nuclear receptor coactivators- an update. Endocrinology. 143, 2461-5.

Meraldi P, Honda R, Nigg EA. (2002). Aurora-A overexpression reveals tetraploidization as a major route to centrosome amplification in p53-/- cells. EMBO J. 21, 483-92.

Millward TA, Zolnierowicz S, Hemmings BA. (1999). Regulation of protein kinase cascades by protein phosphatase 2A. Trends Biochem Sci. 24, 186-91.

Mizrahi N, Moore C. (2000). Posttranslational phosphorylation and ubiquitination of the Saccharomyces cerevisiae Poly(A) polymerase at the S/G(2) stage of the cell cycle. Mol Cell Biol. 20, 2794-802.

Moore JD, Kirk JA, Hunt T. (2003). Unmasking the S-phase-promoting potential of cyclin B1. Science. 300, 987-90.

Murphy LC, Simon SL, Parkes A, Leygue E, Dotzlaw H, Snell L, Troup S, Adeyinka A, Watson PH. (2000). Altered expression of estrogen receptor coregulators during human breast tumorigenesis. Cancer Res. 60, 6266-71.

Murray AW. (2004). Recycling the cell cycle: cyclins revisited. Cell. 116, 221-34.

Osborne CK, Bardou V, Hopp TA, Chamness GC, Hilsenbeck SG, Fuqua SA, Wong J, Allred DC, Clark GM, Schiff R. (2003). Role of the estrogen receptor coactivator AIB1 (SRC-3) and HER-2/neu in tamoxifen resistance in breast cancer. J Natl Cancer Inst. 95, 353-61.

Peters JM. (2002). The anaphase-promoting complex: proteolysis in mitosis and beyond. Mol Cell. 9, 931-43.

Planas-Silva MD, Shang Y, Donaher JL, Brown M, Weinberg RA. (2001). AIB1 enhances estrogen-dependent induction of cyclin D1 expression. Cancer Res. 61, 3858-62.

Porter LA, Donoghue DJ. (2003). Cyclin B1 and CDK1: nuclear localization and upstream regulators. Prog Cell Cycle Res. 5, 335-47.

Putti T, Abd El-Rehim D, Rakha E, Paish C, Lee A, Pinder S, Ellis I. (2005). Estrogen receptor-negative breast carcinomas: a review of morphology and immunophenotypical analysis. Modern Pathology. 18, 26-35.

Qutob MS, Bhattacharjee RN, Pollari E, Yee SP, Torchia J. (2002). Microtubule-dependent subcellular redistribution of the transcriptional coactivator p/CIP. Mol Cell Biol. 22, 6611-26.

Rechsteiner M. (1990). PEST sequences are signals for rapid intracellular proteolysis Semin Cell Biol. 1, 433-40.

Roberts EC, Shapiro PS, Nahreini TS, Pages G, Pouyssegur J, Ahn NG. (2002). Distinct cell cycle timing requirements for extracellular signal-regulated kinase and phosphoinositide 3-kinase signaling pathways in somatic cell mitosis. Mol Cell Biol. 22, 7226-41.

Sakakura C, Hagiwara A, Yasuoka R, Fujita Y, Nakanishi M, Masuda K, Kimura A, Nakamura Y, Inazawa J, Abe T, Yamagishi H. (2000). Amplification and over-expression of the AIB1 nuclear receptor co-activator gene in primary gastric cancers. Int J Cancer. 89, 217-23.

Sarafan-Vasseur N, Lamy A, Bourguignon J, Pessot FL, Hieter P, Sesboue R, Bastard C, Frebourg T, Flaman JM. (2002). Overexpression of B-type cyclins alters chromosomal segregation. Oncogene. 21, 2051-7.

Sarcevic B, Mawson A, Baker RT, Sutherland RL. (2002). Regulation of the ubiquitin-conjugating enzyme hHR6A by CDK-mediated phosphorylation. EMBO J. 21, 2009-18.

Schwerk C, Schulze-Osthoff K. (2003). Non-apoptotic functions of caspases in cellular proliferation and differentiation. Biochem Pharmacol. 66, 1453-8.

Shah OJ, Ghosh S, Hunter T. (2003). Mitotic regulation of ribosomal S6 kinase 1 involves Ser/Thr, Pro phosphorylation of consensus and non-consensus sites by Cdc2. J Biol Chem. 278, 16433-42.

Sheaff RJ, Singer JD, Swanger J, Smitherman M, Roberts JM, Clurman BE. (2000). Proteasomal turnover of p21Cip1 does not require p21Cip1 ubiquitination. Mol Cell. 5, 403-10.

Shibata A, Hayashi Y, Imai T, Funahashi H, Nakao A, Seo H. (2001). Somatic gene alteration of AIB1 gene in patients with breast cancer. Endocr J. 48, 199-204.

Sjogren K, Liu JL, Blad K, Skrtic S, Vidal O, Wallenius V, LeRoith D, Tornell J, Isaksson OG, Jansson JO, Ohlsson C. (1999). Liver-derived insulin-like growth factor I (IGF-I) is the principal source of IGF-I in blood but is not required for postnatal body growth in mice. Proc Natl Acad Sci U S A. 96, 7088-92.

Smits VAJ, Medema RH. (2001). Checking out the G2/M transition. Biochim Biophys Acta. 1519, 1-12.

Soule HD, Vazguez J, Long A, Albert S, Brennan M. (1973). A human cell line from a pleural effusion derived from a breast carcinoma. J Natl Cancer Inst. 51, 1409-16.

Spector DL, Goldman RD, Leinwand LA. 1998. Synchronization of Cell Populations, p. 14.4-14.13. *In* Cells. A Laboratory Manual. Volume 1. Cold Spring Harbor Laboratory Press, USA.

Suen CS, Berrodin TJ, Mastroeni R, Cheskis BJ, Lyttle CR, Frail DE. (1998). A transcriptional coactivator, steroid receptor coactivator-3, selectively augments steroid receptor transcriptional activity. J Biol Chem. 273, 27645-53.

Storchova Z, Pellman D. (2004). From polyploidy to aneuploidy, genome instability and cancer. Nat Rev Mol Cell Biol. 5, 45-54.

Tait L, Soule HD, Russo J. (1990). Ultrastructural and immunocytochemical characterization of an immortalized human breast epithelial cell line, MCF-10. Cancer Res. 50, 6087-94.

Takizawa CG, Morgan DO. (2000). Control of mitosis by changes in the subcellular location of cyclin-B1-Cdk1 and Cdc25C. Curr Opin Cell Biol. 12, 658-65.

Tan JA, Hall SH, Petrusz P, French FS. (2000). Thyroid receptor activator molecule, TRAM-1, is an androgen receptor coactivator. Endocrinology. 141, 3440-50.

Tanner MM, Grenman S, Koul A, Johannsson O, Meltzer P, Pejovic T, Borg A, Isola JJ. (2000). Frequent amplification of chromosomal region 20q12-q13 in ovarian cancer. Clin Cancer Res. 6, 1833-9.

Torchia J, Rose DW, Inostroza J, Kamei Y, Westin S, Glass CK, Rosenfeld MG. (1997). The transcriptional co-activator p/CIP binds CBP and mediates nuclear-receptor function. Nature. 387, 677-84.

Torres-Arzayus MI, De Mora JF, Yuan J, Vazquez F, Bronson R, Rue M, Sellers WR, Brown M. (2004). High tumor incidence and activation of the PI3K/AKT pathway in transgenic mice define AIB1 as an oncogene. Cancer Cell. 6, 263-74.

Vahabi, M. (2003). Breast cancer screening methods: a review of the evidence. Health Care for Women International. 24, 773–793.

Wang Y, Wu MC, Sham JS, Zhang W, Wu WQ, Guan XY. (2002). Prognostic significance of c-myc and AIB1 amplification in hepatocellular carcinoma. A broad survey using high-throughput tissue microarray. Cancer. 95, 2346-52.

Wang Z, Rose DW, Hermanson O, Liu F, Herman T, Wu W, Szeto D, Gleiberman A, Krones A, Pratt K, Rosenfeld R, Glass CK, Rosenfeld MG. (2000). Regulation of somatic growth by the p160 coactivator p/CIP. Proc Natl Acad Sci U S A. 97, 13549-54.

Werbajh S, Nojek I, Lanz R, Costas MA. (2000). RAC-3 is a NF-kappa B coactivator. FEBS Lett. 485, 195-9.

Wilkinson KD. (2000). Ubiquitination and deubiquitination: targeting of proteins for degradation by the proteasome. Semin Cell Dev Biol. 11, 141-8.

Wright JH, Munar E, Jameson DR, Andreassen PR, Margolis RL, Seger R, Krebs EG. (1999). Mitogen-activated protein kinase kinase activity is required for the G(2)/M transition of the cell cycle in mammalian fibroblasts. Proc Natl Acad Sci U S A. 96, 11335-40.

Wu RC, Qin J, Yi P, Wong J, Tsai SY, Tsai MJ, O'Malley BW. (2004). Selective phosphorylations of the SRC-3/AIB1 coactivator integrate genomic responses to multiple cellular signaling pathways. Mol Cell. 15, 937-49.

Wu RC, Qin J, Hashimoto Y, Wong J, Xu J, Tsai SY, Tsai MJ, O'Malley BW. (2002). Regulation of SRC-3 (pCIP/ACTR/AIB-1/RAC-3/TRAM-1) Coactivator activity by I kappa B kinase. Mol Cell Biol. 22, 3549-61.

Xu J, Liao L, Ning G, Yoshida-Komiya H, Deng C, O'Malley BW. (2000). The steroid receptor coactivator SRC-3 (p/CIP/RAC3/AIB1/ACTR/TRAM-1) is required for normal growth, puberty, female reproductive function, and mammary gland development. Proc Natl Acad Sci U S A. 97, 6379-84.

Yan F, Gao X, Lonard DM, Nawaz Z. (2003). Specific ubiquitin-conjugating enzymes promote degradation of specific nuclear receptor. Mol Endocrinol. 17, 1315-31.

Zhao C, Yasui K, Lee CJ, Kurioka H, Hosokawa Y, Oka T, Inazawa J. (2003). Elevated expression levels of NCOA3, TOP1, and TFAP2C in breast tumors as predictors of poor prognosis. Cancer. 98, 18-23.

Zhou G, Hashimoto Y, Kwak I, Tsai SY, Tsai MJ. (2003). Role of the steroid receptor coactivator SRC-3 in cell growth. Mol Cell Biol. 23, 7742-55.

Zieve GW, Turnbull D, Mullins JM, McIntosh JR. (1980). Production of large numbers of mitotic mammalian cells by use of the reversible microtubule inhibitor nocodazole. Nocodazole accumulated mitotic cells. Exp Cell Res. 126, 397-405.